2007-03-13

Regulation of Cell Polarization and Map Kinase Signaling in the Saccharomyces Cerevisiae Pheromone Response Pathway: a Dissertation

Shelly Catherine Strickfaden
University of Massachusetts Medical School

REGULATION OF CELL POLARIZATION AND MAP KINASE SIGNALING IN THE *Saccharomyces cerevisiae* PHEROMONE RESPONSE PATHWAY

A Dissertation Presented

By

SHELLY CATHERINE STRICKFADEN

Submitted to the Faculty of the

University of Massachusetts Medical School of Biomedical Sciences, Worcester in partial fulfillment of the requirements for the degree of

DOCTOR OF PHILOSOPHY

MARCH 13, 2007

INTERDISCIPLINARY GRADUATE PROGRAM

COPYRIGHT INFORMATION

Portions of this dissertation have appeared in separate publications:

Strickfaden, S.C., Winters, M.J., Ben-Ari, G., Lamson, R.E., Tyers, M., and Pryciak, P.M. (2007) A mechanism for cell-cycle regulation of MAP kinase signaling in a yeast differentiation pathway. Cell 128: 519-531.

Strickfaden, S.C., Pryciak, P.M. (2007) Qualitatively different roles for two Gα-Gβ interfaces in cell polarity control by a yeast heterotrimeric G protein. Manuscript in preparation.

REGULATION OF CELL POLARIZATION AND MAP KINASE SIGNALING IN THE *Saccharomyces cerevisiae* PHEROMONE RESPONSE PATHWAY

A Dissertation presented by

SHELLY CATHERINE STRICKFADEN

Approved as to style and content by:

Dannel McCollum, Ph.D., Chairman of Committee

Nick Rhind, Ph.D., Member of Committee

David Lambright, Ph.D., Member of Committee

Duane Jenness, Ph.D., Member of Committee

Daniel Lew, Ph.D., Member of Committee

Peter Pryciak, Ph.D., Thesis Advisor

Anthony Carruthers, Ph.D.,
Dean of the Graduate School of Biomedical Sciences

Interdisciplinary Graduate Program

March 13, 2007

ACKNOWLEDGEMENTS

I would like to thank Peter Pryciak for being a great mentor. His encouragement, support and guidance have helped me develop as a scientist. Also, thank you to all the members of the Pryciak lab for your support and making this an interesting and great place to work (chicken). Thanks to the Biotech IV community for providing a helpful friendly environment. I would also like to thank my committee members for their advice and support during my thesis work.

Also, thank you so much to all of my friends. I appreciate all the great times we have had and hope for many more. I am also very grateful for your support and willingness to listen and help over the years. Thanks to Kiran, Satoe and Jess for providing feedback on my thesis.

Finally, thank you to my family and Joe. Your support, encouragement and understanding have been greatly appreciated. A special thanks to my little brother Will for providing me with some perspective and to my brother Carl for taking the time to try and figure out what it is I do. Joe- thank you for putting up with me through it all, I couldn't have done this without you.

ABSTRACT

Exposure to external stimuli promotes a variety of cellular responses including changes in morphology, gene expression and cell division status. These responses are promoted by signaling pathways composed of modules that are conserved from lower to higher eukaryotes. In *Saccharomyces cerevisiae* response to the external stimuli provided by mating pheromone is governed by the pheromone response pathway. This pathway is composed of a G protein coupled receptor/heterotrimeric G protein (Gαβγ) module and a MAP kinase cascade. Activation of this pathway allows the heterotrimeric G protein βγ dimer (Gβγ) to recruit polarity proteins to promote changes in cell morphology and to activate signaling through the MAP kinase cascade. Here we investigate the regulation of these pheromone-induced responses.

We first examine how an asymmetric polarization response is generated. Normally, a gradient of pheromone serves as a spatial cue for formation of a polarized mating projection, but cells can still polarize when pheromone is present uniformly. Here we show that an intact receptor/Gαβγ module is required for polarization in response to both a gradient and uniform concentration of pheromone. Further investigation into regulation of Gβγ by Gα revealed that the two interaction interfaces between Gα and Gβ have qualitatively different roles. Our results suggest that one interface controls signaling whereas the other governs coupling to the receptor. Overall our results indicate that communication between the receptor and Gαβγ is required for proper polarization.

We then examine how G1 CDKs regulate MAP kinase signaling. Response to pheromone is restricted to the G1 stage of the cell cycle. Once cells commit to a round of division they become refractory to mating pheromone until that round of division is complete. One contributor to this specificity involves inhibition of signaling through the MAP kinase cascade by G1 CDKs, but it was not known how this occurs. Here, we show that the MAP kinase cascade scaffold Ste5 is the target of this inhibition. Cln/CDKs inhibit signaling by phosphorylating sites surrounding a small membrane-binding domain in Ste5, thereby disrupting the membrane localization of Ste5. Furthermore, we found that disrupting this regulation allows cells to arrest at an aberrant non-G1 position. Our findings define a mechanism and a physiological benefit for restricting pheromone-induced signaling to G1.

This thesis describes findings related to generation of an asymmetric polarization response, heterotrimeric G protein function, and coordination of differentiation signaling with cell division status. Lessons learned here might be applicable to the regulation of polarization and differentiation responses in other systems as the signaling modules are conserved.

TABLE OF CONTENTS

LIST OF FIGURES

CHAPTER I

CHAPTER II

CHAPTER III

CHAPTER IV

LIST OF TABLES

CHAPTER I

GENERAL INTRODUCTION

Cellular responses to external stimuli are mediated by signal transduction networks composed of signaling modules that are conserved between higher and lower eukaryotes. Common signaling modules include G protein coupled receptors (GPCRs) and their associated heterotrimeric G proteins and mitogen-activated protein (MAP) kinase cascades (Neer, 1995; Robinson and Cobb, 1997; Dohlman and Thorner, 2001; Qi and Elion, 2005). These modules regulate a variety of cellular responses including changes in morphology, gene expression and cell division status.

In the budding yeast *Saccharomyces cerevisiae*, a signaling pathway composed of a GPCR/heterotrimeric G protein module and a MAP kinase cascade mediates response to the external stimuli provided by mating pheromones (Dohlman and Thorner, 2001). This mating reaction stimulates cells to arrest the cell cycle in the G1 phase, induce expression of pheromone-responsive genes, and undergo polarized morphogenesis. Because the signaling modules used in the yeast pheromone response pathway are conserved in higher eukaryotes and because of its tractable genetics, *S. cerevisiae* is a good model system to use to investigate how cellular responses to external stimuli are regulated. Here the yeast pheromone response pathway was used to study i) how cells generate an asymmetric morphological response to pheromone and ii) how pheromone response is restricted to the G1 stage of the cell cycle.

S. cerevisiae pheromone response pathway

In *S. cerevisiae*, the two haploid cell types (**a** or α) secrete cell type-specific mating pheromones (**a** factor or α factor, respectively), which serve as chemoattractants that stimulate mating responses in cells of the opposite mating type (Figure 1-1) (Elion, 2000; Dohlman and Thorner, 2001). Each pheromone binds to a cell type specific GPCR that couples to a common heterotrimeric G protein (Gαβγ, composed of Gα, Gβ and Gγ subunits). Binding of pheromone to the receptor catalyzes exchange of GTP for GDP on the Gα subunit, causing dissociation of Gα-GTP from the Gβγ dimer. Once released from the inhibitory Gα subunit, Gβγ can trigger signaling through a MAP kinase cascade, which involves membrane recruitment of the scaffold protein Ste5, leading to activation of the Ste5-associated kinases, Ste11 (MAPKKK), Ste7 (MAPKK) and Fus3 (MAPK). Signaling though this MAP kinase cascade results in the transcription of mating specific genes and cell cycle arrest in the G1 stage of the cell cycle. Gβγ also recruits proteins necessary for the formation of an elongated mating projection (Figure 1-2). This projection will grow toward its partner cell until the two cells meet and fuse to form a diploid zygote (Figure 1-1).

Figure 1-1 *S. cerevisiae* mating reaction

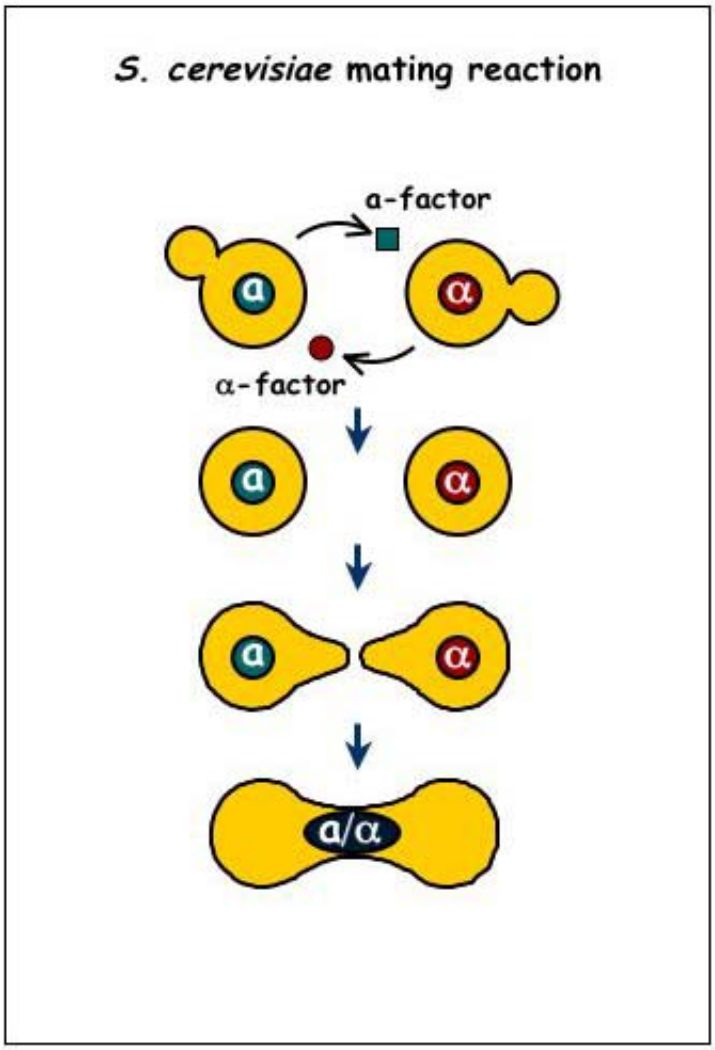

Figure 1-1. *S. cerevisiae* mating reaction

Exposure to mating pheromones secreted by a haploid cell of the opposite mating type stimulates mating responses, which include arrest in the G1 stage of the cell cycle and formation of an elongated mating projection. This projection is oriented toward the mating partner and will grow toward the partner until the projections meet and fuse to yield a diploid zygote.

Figure 1-2. The pheromone response pathway

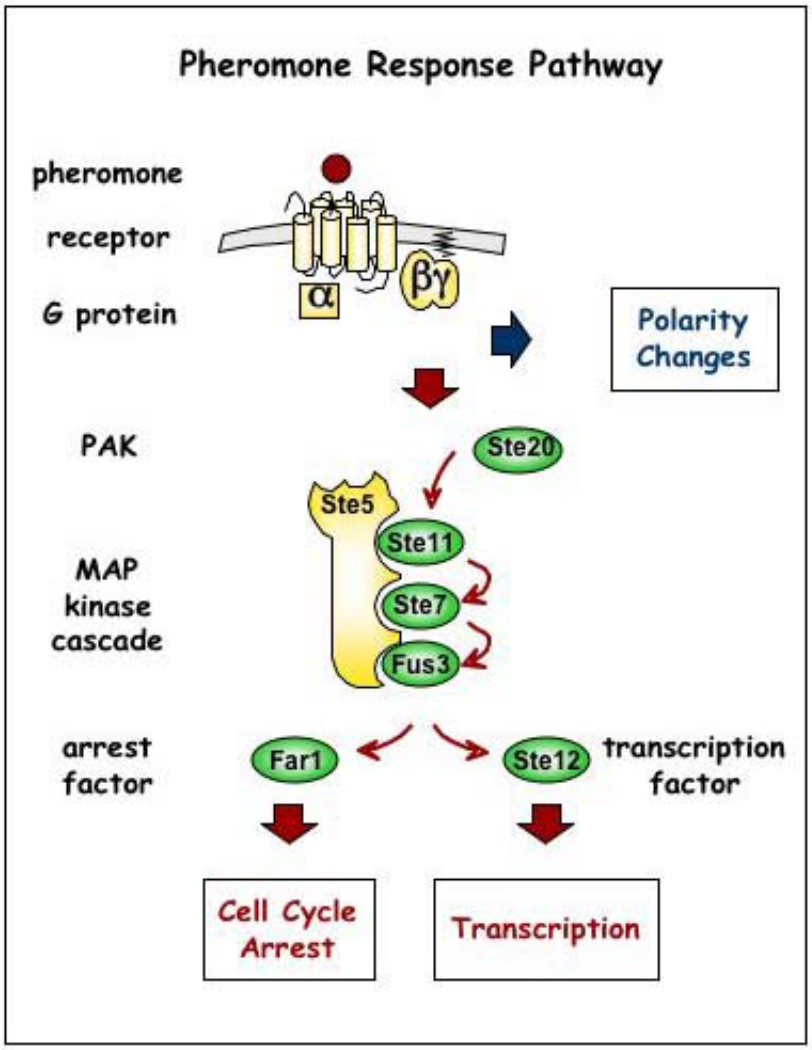

Figure 1-2. The pheromone response pathway

The mating reaction is mediated by the pheromone response pathway. Binding of pheromone to its G protein coupled receptor activates the pathway by catalyzing the exchange of GTP for GDP on the Gα subunit of the associated heterotrimeric G protein. This results in dissociation of Gα from the Gβγ dimer. Gα and Gβγ remain at the plasma membrane due to lipid modifications on the Gα subunit (not shown) and Gγ subunit (squiggled line). Once free from Gα inhibition, Gβγ triggers signaling through the MAP kinase cascade by recruiting Ste5 and its associated kinases to the plasma membrane thus brining the MAPKKK Ste11 into proximity of its activator Ste20. This activates the phosphorelay system whereby Ste11 phosphorylates and activates the MAPKK Ste7, Ste7 then phosphorylates and activates the MAPK Fus3. Fus3 then activates the downstream targets Far1 and Ste12 leading to cell cycle arrest and the transcription of mating genes, respectively.

Free Gβγ also promotes polarity changes by recruiting the proteins necessary for the formation of a polarized mating projection.

KEY PLAYERS IN THE PHEROMONE RESPONSE PATHWAY:

GPCR/Gαβγ module

GPCRs mediate response to a wide variety of external stimuli including hormones, neurotransmitters, odorants and light (Pierce et al., 2002). These receptors are composed of 7 transmembrane helices connected via extracellular and intracellular loops with the intracellular loops serving as the G protein-binding domain (Bourne, 1997; Hamm, 2001; Pierce et al., 2002). In the yeast pheromone response pathway, the G protein coupled receptors mediate response to mating pheromone. Ste2 is the receptor for α factor, and Ste3 is the receptor for **a** factor. These proteins are not similar at the sequence level but have similar structural features. Both are serpentine receptors with seven α-helical membrane-spanning regions that have extracellular N-termini and intracellular C termini (Jenness et al., 1983; Burkholder and Hartwell, 1985; Nakayama et al., 1985; Hagen et al., 1986; Blumer et al., 1988). The receptors are cell type specific, but they both couple to the same signaling pathway to promote pheromone response (Bender and Sprague, 1986; Nakayama et al., 1987).

G protein coupled receptors interact with heterotrimeric G proteins (Gαβγ), composed of Gα, Gβ and Gγ subunits (Neer, 1995). The Gα subunit is a GTPase that can bind GDP or GTP. In the absence of stimulus, Gα is bound to GDP and associates with the Gβγ dimer. In this state Gαβγ is inactive. Gαβγ is activated when ligand binds to its receptor. The receptor then catalyzes the exchange of GTP for GDP on the Gα subunit causing dissociation of Gα-GTP from the Gβγ dimer (Neer, 1995; Bourne, 1997;

Sprang, 1997). Once dissociated, Gα and/or Gβγ activate downstream effectors to promote a variety of cellular responses (Gutkind, 2000; Neves et al., 2002).

In yeast, a heterotrimeric G protein composed of the subunits, Gpa1 (Gα) (Dietzel and Kurjan, 1987; Miyajima et al., 1987), Ste4 (Gβ) and Ste18 (Gγ) (Whiteway et al., 1989), regulates the pheromone response pathway. In this pathway Gβγ activates the downstream responses, with Gα serving to inhibit Gβγ activity. This was demonstrated by experiments showing that loss of Gpa1 causes constitutive pathway activation (Dietzel and Kurjan, 1987; Miyajima et al., 1987), whereas loss of Ste4 or Ste18 eliminates pheromone response and can suppress the constitutive activation caused by the loss of Gpa1 (Nakayama et al., 1988; Blinder et al., 1989; Whiteway et al., 1989). In addition, overexpression of Ste4 itself can activate pathway signaling but required Ste18 to do so, further demonstrating Gβγ's role in activating pathway effectors (Cole et al., 1990; Nomoto et al., 1990; Whiteway et al., 1990). Gβγ activates pathway responses in two ways: it regulates the proteins that control cell polarity and it triggers MAP kinase cascade signaling (Figure 1-2) (Butty et al., 1998; Nern and Arkowitz, 1998; Pryciak and Huntress, 1998; Mahanty et al., 1999; Nern and Arkowitz, 1999; Winters et al., 2005).

Lipid modification of the Gα and Gγ subunits

A feature common to heterotrimeric G proteins is lipid modification on the Gα and Gγ subunits. The Gα subunit is myristoylated and/or palmitoylated at its N terminus, while the Gγ subunit is prenylated at its C terminus (Wedegaertner et al., 1995). The Gβ

and Gγ subunits are tightly associated and function as a single unit (Neer, 1995), thus lipid modification on Gγ regulates the Gβγ dimer. In yeast, the Gα subunit (Gpa1) is myristoylated and palmitoylated (Stone et al., 1991; Song and Dohlman, 1996; Manahan et al., 2000) and the Gγ subunit (Ste18) is both prenylated and palmitoylated (Hirschman and Jenness, 1999; Manahan et al., 2000). These lipid modifications serve to anchor the proteins to the plasma membrane and are important for their function (Wedegaertner et al., 1995; Chen and Manning, 2001). Mutations that disrupt lipid modification of Gpa1 disrupt its targeting to the plasma membrane and result in activation of the pathway (Stone et al., 1991; Song and Dohlman, 1996; Song et al., 1996; Manahan et al., 2000). Also, mutations that disrupt lipid modification of Ste18 disrupt signaling, as these modifications are required to maintain Gβγ at the plasma membrane after receptor activation (Hirschman and Jenness, 1999; Manahan et al., 2000).

MAP kinase cascade and scaffold protein

MAP kinase cascade

MAPK cascades are composed of three protein kinases that act in a series. The MAP kinase kinase kinase (MAPKKK) is a serine/threonine kinase that phosphorylates and activates the dual specificity MAP kinase kinase (MAPKK). Once activated the MAPKK then activates the MAP kinase (MAPK) by phosphorylating it on a threonine and tyrosine residue (T-X-Y motif) in the activation loop of the conserved kinase domain (Gustin et al., 1998). The MAPK then phosphorylates various effectors on serine or

threonine residues in the consensus PXS/TP sequence to regulate cellular activities (Robinson and Cobb, 1997; Johnson and Lapadat, 2002; Qi and Elion, 2005).

The yeast pheromone response pathway consists of a MAPK cascade composed of the MAPKKK Ste11, MAPKK Ste7, the MAPK Fus3 and an associated scaffold protein, Ste5 (Figure 1-2). A variety of biochemical and genetic experiments have established the order of these components (Dohlman and Thorner, 2001; Bardwell, 2005). In response to pheromone, Gβγ triggers membrane recruitment of Ste5 thus bringing Ste11 into proximity of its membrane-localized activator Ste20 (Pryciak and Huntress, 1998; Mahanty et al., 1999; van Drogen et al., 2000). Ste20, a member of the PAK (p21-activated kinase) family of kinases, is localized to the membrane and activated via interaction with the membrane-bound Rho-family GTPase Cdc42. Ste5 also brings Ste7 and Fus3 to the plasma membrane and thus Ste5 provides an activation platform for the MAPK cascade (van Drogen et al., 2001). After activation by Ste20, Ste11 activates Ste7, and then Ste7 activates Fus3. Fus3 is the primary MAPK kinase in this pathway, but in cells lacking Fus3 another MAPK, Kss1 can mediate pathway responses (Madhani et al., 1997; Madhani and Fink, 1998). Once activated Fus3 phosphorylates downstream targets that include the cell cycle arrest factor Far1 and the transcription factor Ste12, which mediates transcriptional induction of mating genes (Dohlman and Thorner, 2001; Bardwell, 2005).

MAPK cascade scaffold protein, Ste5

Ste5 is a scaffold protein for the yeast MAPK cascade (Choi et al., 1994; Kranz et al., 1994; Marcus et al., 1994; Printen and Sprague, 1994). Since the discovery of Ste5, mammalian scaffold proteins have also been identified. These scaffold proteins are not similar to Ste5 or each other at the sequence level, but are instead functionally similar (Whitmarsh and Davis, 1998; Burack and Shaw, 2000; Morrison and Davis, 2003). Scaffold proteins are thought to facilitate signaling by bringing the associated kinases into close proximity of one another and to promote pathway specificity by preventing cross-talk between the associated kinases with other MAPK cascades (Elion, 2001; Harris et al., 2001; Morrison and Davis, 2003; Park et al., 2003). Scaffolds can also serve as adaptors by targeting the kinase cascade to a subcellular location.

An important step in activation of the mating pathway is the plasma membrane recruitment of Ste5 by the pheromone-activated Gβγ dimer (Figure 1-3A) (Pryciak and Huntress, 1998; Mahanty et al., 1999; van Drogen et al., 2001; Winters et al., 2005). Ste5 binds to Ste4 and mutations that disrupt this interaction disrupt Gβγ mediated signaling (Whiteway et al., 1995; Inouye et al., 1997; Feng et al., 1998). In addition, artificial targeting of Ste5 to the plasma membrane causes constitutive signaling further demonstrating the functional significance of this recruitment (Pryciak and Huntress, 1998). Membrane recruitment of Ste5 serves two roles: (1) it promotes activation of Ste11 by its membrane-localized activator, Ste20 (Pryciak and Huntress, 1998; van Drogen et al., 2000); and (2) it amplifies signal transmission from active Ste11 through the remainder of the kinase cascade (Lamson et al., 2006).

Recently, work from our lab has shown that although Gβγ is the usual trigger for Ste5 recruitment to the plasma membrane, it is not sufficient. Instead, Ste5 also binds directly to membranes, and the cooperative effect of these two weak interactions (Ste5-Gβγ and Ste5-membrane) controls membrane recruitment (Figure 1-3B) (Winters et al., 2005). The Ste5-membrane interaction requires an N-terminal "PM" (plasma membrane) domain, a short basic-rich amphipathic α-helix that binds acidic phospholipid membranes, and which can also target Ste5 to the nucleus when not engaged at the plasma membrane. Gain-of-function mutations in the PM domain cause increased membrane affinity, allowing Ste5 to localize to the plasma membrane and activate signaling even without Gβγ (Winters et al., 2005).

In the yeast pheromone response pathway, two cellular responses triggered by Gβγ are: (i) formation of a polarized mating projection and (ii) activation of MAP kinase cascade signaling which leads to cell cycle arrest.

Figure 1-3. Pathway activation involves recruitment of the MAPK cascade scaffold protein Ste5 to the plasma membrane

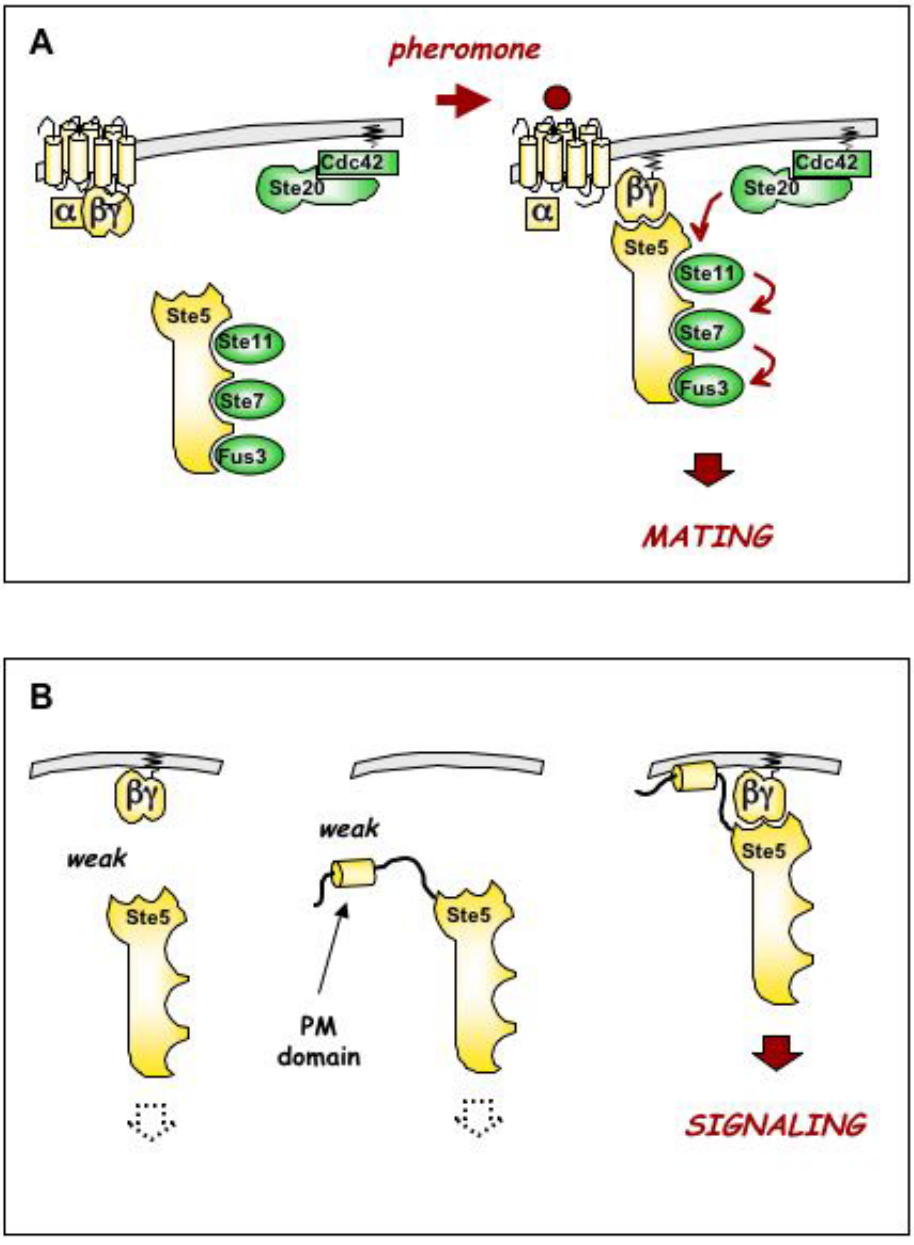

Figure 1-3. Pathway activation involves recruitment of the MAPK cascade scaffold protein Ste5 to the plasma membrane

(A) Plasma membrane recruitment of Ste5 by the pheromone-activated Gβγ dimer is an important step in activation of the pheromone response pathway. This recruitment results in the assembly of a membrane-bound signaling complex that allows signal to proceed through the MAPK kinase cascade.

(B) Although Gβγ triggers membrane recruitment of Ste5, the Gβγ/Ste5 interaction is not sufficient to bring Ste5 to the membrane. Rather, it acts synergistically with a separate Ste5/membrane interaction, which is itself too weak to act on its own. The Ste5/membrane interaction is mediated by the plasma membrane (PM) domain which is depicted here as a cylinder in the N-terminus of Ste5.

CELLULAR POLARIZATION

The ability to polarize is important for the development and function of many eukaryotic cells. Cellular polarization involves the asymmetric distribution of intracellular materials in a way that is directed toward instructional cues that are themselves localized. These cues may be internal or external to the cell. For example, internal cues provided by the localization of polarity establishment proteins govern the asymmetric cell divisions that occur in *Drosophila* neuroblasts or *Caenorhabditis elegans* zygotes (Knoblich, 2001; Cowan and Hyman, 2004; Wodarz, 2005). Whereas, external cues govern chemotaxis in *Dictyostelium discoideum* and mammalian neutrophils, such that a gradient of chemoattractant from a localized source stimulates cell polarization and directed cell movement along the gradient (Iijima et al., 2002; Bagorda et al., 2006; Franca-Koh et al., 2006).

Polarization in *S. cerevisiae*

S. cerevisiae polarizes in response to both internal and external polarity cues. Polarization is controlled by the polarity establishment proteins, Cdc24 and Cdc42 (Madden and Snyder, 1998; Pruyne and Bretscher, 2000b; Etienne-Manneville, 2004). Cdc24 is the guanine nucleotide exchange factor (GEF) for the Rho family GTPase Cdc42. It activates Cdc42 by promoting exchange of GTP for GDP. Once activated Cdc42 interacts with downstream effectors to organize the actin cytoskeleton, which in turn guides secretion to promote polarized cell growth (Pruyne and Bretscher, 2000a; Pruyne and Bretscher, 2000b). A key step in polarization of the actin cytoskeleton is the

recruitment and local activation of Cdc42 at growth sites (Pruyne and Bretscher, 2000b; Pruyne et al., 2004). This recruitment occurs in response to internal or external polarity establishment cues. During vegetative growth internal cues determine the site of polarization, whereas external cues govern polarization during mating.

Use of internal polarity cues during budding

S. cerevisiae can exist as haploid or diploid cells and these cells reproduce vegetatively by budding (Figure 1-4A). Polarized growth during budding occurs at specific sites that are determined by internal polarity cues. Haploid cells bud in an axial fashion in which the next bud is formed adjacent to the previous bud site, while diploid cells bud in a bipolar fashion in which the bud is formed at one of the poles of the cell (Madden and Snyder, 1998; Chant, 1999). These patterns of division are controlled by the bud site selection proteins, which serve as internal landmarks for polarity establishment. There are three classes of bud site selection proteins: (i) those specifically involved in marking the site for axial budding, (ii) those involved in bipolar budding, and (iii) general bud site selection proteins which are required for both axial and bipolar budding (Madden and Snyder, 1998; Chant, 1999; Casamayor and Snyder, 2002).

The general bud site selection proteins consist of the Ras-related GTPase Rsr1 (also known as Bud1), its GEF Bud5 and its GTPase activating protein (GAP) Bud2 (Bender and Pringle, 1989; Chant et al., 1991; Chant and Herskowitz, 1991; Park et al., 1993). Localized activation of Rsr1 at the bud site allows the recruitment of the polarity establishment proteins Cdc24 and Cdc42 to the bud site (Chant, 1999; Pruyne et al.,

2004). This is thought to promote localized activation of Cdc42 thereby allowing bud formation. Although the general bud site selection proteins are important for both budding patterns their loss does not inhibit budding, but rather results in a random budding pattern (Figure 1-4A) (Madden and Snyder, 1998; Chant, 1999; Casamayor and Snyder, 2002).

Use of external polarity cues during mating

Polarization in response to a gradient of pheromone

In response to a gradient of pheromone emitted from a mating partner, a cell will form a polarized mating projection that is oriented toward the partner (Figure 1-4B). Thus, unlike bud formation, which uses predetermined sites to guide polarization, a mating projection can form at any point on the cell surface (Madden and Snyder, 1992). The mating projection will grow toward its partner, following the pheromone gradient, in a process known as chemotropism (Arkowitz, 1999). This ability to respond directionally was demonstrated by the formation and growth of a mating projection along an artificial pheromone gradient (Segall, 1993). In addition, this was also shown by discrimination assays, which measure the cell's ability to find a partner and mate when exposed to a mixture of potential partners that did or did not produce pheromone. It was found that cells preferentially mated with pheromone producing partners (Jackson and Hartwell, 1990b; Jackson and Hartwell, 1990a). The ability to coordinate the direction of cell growth with the location of the external signal implies that the initial sensing of chemoattractant and at least some of the subsequent intracellular signal transduction

events do not occur uniformly within the cell but instead occur in an asymmetric, spatially-restricted manner.

Prior studies indicated that the receptor and heterotrimeric G protein are involved in detecting the directional information provided by the pheromone gradient as cells lacking these components are compromised in their ability to discriminating between pheromone producing and pheromoneless cells (Jackson et al., 1991; Schrick et al., 1997). This suggested that the receptor, the Gα subunit, or the Gβγ dimer might interact with the proteins involved in polarity establishment. To this end, it has been found that Gβγ interacts the polarity proteins Far1 and Cdc24 (Butty et al., 1998; Nern and Arkowitz, 1998; Nern and Arkowitz, 1999).

Far1 is an adaptor protein that binds both Gβγ and Cdc24 (Butty et al., 1998; Nern and Arkowitz, 1999). In the G1 phase of the cell cycle Far1 localizes to the nucleus via its nuclear localization signal (NLS) (Blondel et al., 1999) and sequesters Cdc24 in the nucleus (Toenjes et al., 1999; Nern and Arkowitz, 2000b; Shimada et al., 2000). In the absence of pheromone, Cln/CDKs phosphorylate Far1 thereby triggering its degradation (McKinney et al., 1993; Henchoz et al., 1997). This releases Cdc24 (Nern and Arkowitz, 2000b; Shimada et al., 2000) and allows it to be recruited to the bud site to promote bud formation. However, in response to pheromone the Far1/Cdc24 complex is exported from the nucleus (Blondel et al., 1999; Nern and Arkowitz, 2000b). Far1 then targets Cdc24 to Gβγ (Nern and Arkowitz, 2000b; Shimada et al., 2000). Cells expressing mutant forms of either Far1 or Cdc24 that cannot bind Gβγ are defective in orienting their growth toward a mating partner (Figure 1-4B) (Butty et al., 1998; Nern and Arkowitz,

1998). Hence, communication between Gβγ and Far1/Cdc24 is thought to direct Cdc42 activity to the proper site to establish the mating projection along the gradient of pheromone. However, it is not known how Gβγ activity is spatially regulated to promote the formation of an asymmetric projection in the direction of the pheromone signal.

Figure 1-4. Polarized growth during budding and mating

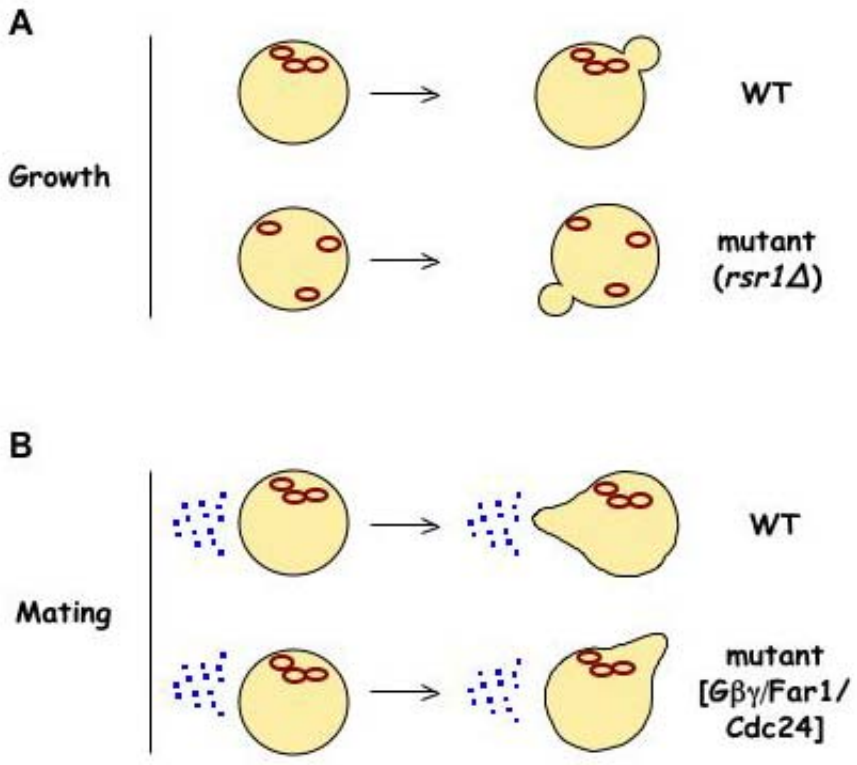

Figure 1-4. Polarized growth during budding and mating

(A) *S. cerevisiae* reproduce vegetatively by budding. Haploid cells bud in an axial fashion in which the next bud is formed adjacent to the previous bud site. This budding pattern can be visualized by examining the bud scars, which are remnants from cell separation (depicted here as red rings). During axial budding the scars form a continuous chain (Chant, 1999). Disrupting the general bud site selection machinery, for instance by loss of Rsr1 (*rsr1*Δ), causes the cell to bud randomly, which is depicted here by the randomly localized scars.

(B) Upon exposure to a gradient of mating pheromone cells reorient their growth away from the bud site and form a polarized mating projection toward the source of pheromone. This chemotropic response involves communication between Gβγ, Far1 and Cdc24. If this complex is disrupted, for instance by mutations in any one of these proteins, cells can no longer reorient their growth in response to pheromone. They will instead form a mating projection using the bud site selection proteins as a spatial cue, which leads to formation of a mating projection at the bud site.

Polarization in response to a uniform concentration of pheromone

For chemotactic cells (*Dictyostelium* and neutrophils) and chemotropic cells (yeast), a gradient of chemoattractant normally serves as a spatial cue for the direction of polarization. However, these cells will still polarize when exposed to a uniform concentration of chemoattractant, implying the existence of "symmetry breaking" mechanisms that can generate asymmetric responses to symmetric signals (Sohrmann and Peter, 2003; Wedlich-Soldner and Li, 2003). Symmetry breaking is thought to involve an initial asymmetry that arises through stochastic variation, which is then amplified to provide an axis of polarization (Kirschner et al., 2000; Wedlich-Soldner and Li, 2003).

In yeast, prior work indicated that there are two ways in which a cell can polarize when pheromone is provided uniformly rather than as a gradient. We will refer to them as "default" and "*de novo"* polarization (Figure 1-5). Default polarization uses pre-existing polarity information provided by the bud site selection proteins as a spatial cue, resulting in the formation of a mating projection at the presumptive bud site (Madden and Snyder, 1992; Dorer et al., 1995; Nern and Arkowitz, 1999). This default polarization is independent of Far1-Cdc24 communication but is dependent on bud site selection proteins. In cells lacking these default sites (such as in *rsr1*Δ mutants where the budding pattern is disrupted), *de novo* polarization occurs at random positions that bear no relationship to previous polarization sites. This *de novo* polarization is independent of bud site selection proteins but requires binding between Far1 and Cdc24 (Nern and Arkowitz, 1999). Thus, interactions that are required for asymmetric response to a gradient of pheromone are also required for generating asymmetry *de novo* in response to

a uniform field of pheromone. However, it is not known how the symmetry provided by the uniform stimulus is broken or how a polarization site is established and maintained.

Figure 1-5. Yeast can polarize by two different means when pheromone is provided uniformly

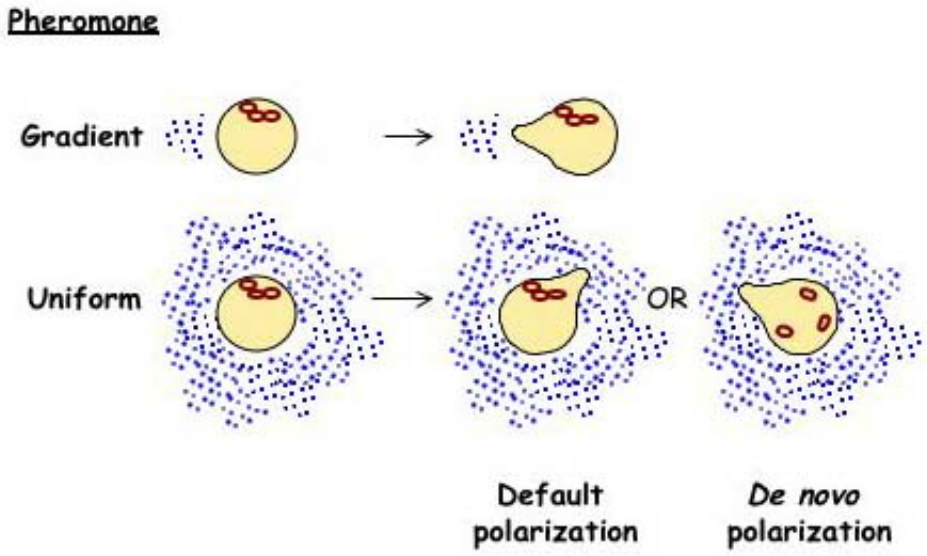

Figure 1-5. Yeast can polarize by two different means when pheromone is provided uniformly

A gradient of pheromone normally serves as a spatial cue for polarization. However, in a uniform concentration of pheromone this spatial cue is lacking, but cells can still polarize. This polarization occurs by default or *de novo* processes. Default polarization uses the bud site selection proteins as a spatial cue for polarization and the projection is formed at the bud site. This is indicated here by the formation of a projection next to the bud scars. Cells can still polarize when these default sites are lacking, for instance in *rsr1*Δ cells. This *de novo* projection formation occurs at random locations and requires binding between Far1 and Cdc24.

INDUCTION OF CELL CYCLE ARREST

In the G1 stage of the cell cycle, yeast cells can respond to the external stimulus, mating pheromone (Figure 1-6). However, in the absence of pheromone, once cells have reached the proper size and have enough nutrients to support division, they will pass Start and enter the division cycle (Cross, 1995). Start marks the transition from G1 to S phase and is the point at which the cell becomes committed to finishing the division cycle. Once cells have passed Start they become refractory to pheromone arrest, a property that was used to define Start as a unique point of commitment to a new round of division (Hartwell et al., 1974). Mammalian cells also must pass a similar commitment point, termed the restriction point, before beginning S phase (Blagosklonny and Pardee, 2002).

Cyclin/CDK activities

The cell cycle is driven by cyclin dependent kinases (CDKs). These kinases, which are conserved from higher to lower eukaryotes, are activated by association with cyclin subunits. The yeast cell cycle is driven by the CDK Cdc28, which associates with nine different cyclin subunits to promote various cell cycle transitions. There are three G1 cyclins (Clns), Cln1-Cln3, and six B-type cyclins (Clbs), Clb1-Clb6 (Cross, 1995; Nasmyth, 1996). The Clb family of cyclins regulates DNA replication and mitosis; Clb5 and Clb6 promote DNA replication, Clb3 and Clb4 play a role in the formation of mitotic spindles, and Clb1 and Clb2 promote nuclear division and the switch to isotopic bud growth in the G2 stage of the cell cycle (Nasmyth, 1996; Bloom and Cross, 2007).

The G1 cyclins promote passage though Start. Deletion of all three G1 cyclins causes cells to arrest in G1, however any one of the three is sufficient to promote proliferation (Richardson et al., 1989; Cross, 1990). Despite this redundancy, the three G1 cyclins have different properties. Expression of *CLN1* and *CLN2* is periodic during the cell cycle and reaches maximum levels during late G1, whereas *CLN3* expression is less variable throughout the cell cycle (Wittenberg et al., 1990; Tyers et al., 1993). Furthermore, Cln3 is thought to play a different role in promoting Start than Cln1 and Cln2. Cln3 activates the transcription of genes that are necessary for the progression from G1 to S phase, including *CLN1* and *CLN2* and the B-type cyclins *CLB5* and *CLB6* (Tyers et al., 1993; Dirick et al., 1995; Stuart and Wittenberg, 1995). Whereas Cln1 and Cln2 regulate other Start related events including i) bud emergence, ii) spindle pole body (SPB) duplication and iii) proteolysis of the cyclin B-CDK inhibitor, Sic1 (Nasmyth, 1996; Bloom and Cross, 2007). In addition, the Cln1/2 CDK complexes also play a role in restricting pheromone response to the G1 stage of the cell cycle (Oehlen and Cross, 1994; Wassmann and Ammerer, 1997).

G1 specificity of cell cycle arrest

One contributor to the G1 specificity of pheromone arrest involves mutual antagonism between CDKs and Far1 (Figure 1-7A). Far1, in addition to its role in promoting cell polarity (above), is also a CDK inhibitor (Chang and Herskowitz, 1990). Pheromone signaling in G1 cells allows the MAPK Fus3 to phosphorylate and activate Far1 (Chang and Herskowitz, 1992; Peter et al., 1993; Breitkreutz et al., 2001). Once

activated Far1 associates with the G1 cyclin/CDK complexes and inhibits their activity by an unresolved mechanism (Tyers and Futcher, 1993; Peter and Herskowitz, 1994; Gartner et al., 1998; Jeoung et al., 1998). Conversely, Far1 expression and stability are regulated by the cell cycle. Accumulation of Far1 protein is restricted to the G1 stage of the cell cycle and as cells pass Start, Cln/CDKs phosphorylate Far1, targeting it for ubiquitin-mediated degradation (McKinney et al., 1993; Henchoz et al., 1997).

In addition, other mechanisms may play an equally critical role in restricting pheromone arrest to G1, but they are poorly understood. In particular, the activity of the pheromone response pathway is regulated by the cell cycle. It has been shown that the basal and pheromone induced transcription of mating genes (e.g. *FUS1*) fluctuates during the cell cycle. In synchronized cultures transcription levels of *FUS1* are high in early G1, decreased in late G1 and S phase, and high again later in the cell cycle. Conversely, the transcript levels of the G1 cyclins *CLN1* and *CLN2* were low in early G1, high in late G1 and S phase, and then fell again (Oehlen and Cross, 1994; Wassmann and Ammerer, 1997). Thus the transcription of mating genes is minimized during periods of maximum G1 cyclin expression.

Furthermore, it was found that overexpression of Cln2 could inhibit pheromone induced signaling through the mating pathway, and this repression required Cdc28 kinase activity (Figure 1-7B) (Oehlen and Cross, 1994; Wassmann and Ammerer, 1997). Overexpression of Cln1 had a similar effect but required deletion of Far1 as well. These effects were specific to Cln2 and Cln1, as overexpression of Cln3 did not inhibit signaling (Oehlen and Cross, 1994). These results demonstrated that G1 CDKs actively

inhibit signal transduction though the mating pathway MAP kinase cascade. This results in a period from Start through S phase in which cells are unresponsive to pheromone.

While G1 CDK inhibition of pheromone signaling has been recognized for many years, the target and mechanism have remained elusive (Figure 1-7B). Previous studies suggested that the inhibited step of the signaling pathway lay somewhere between the heterotrimeric G protein βγ dimer (Gβγ) and the first kinase of the MAP kinase cascade, the MAPKKK Ste11 (Wassmann and Ammerer, 1997; Oehlen and Cross, 1998). Indeed, Cln2/CDK can phosphorylate the PAK-family kinase Ste20 (Oehlen and Cross, 1998; Wu et al., 1998), but removing CDK sites in Ste20 had no effect on the ability of Cln/CDK to inhibit pheromone signaling (Oda et al., 1999), thus failing to confirm Ste20 as a relevant target.

Figure 1-6. Mating is restricted to the G1 stage of the cell cycle

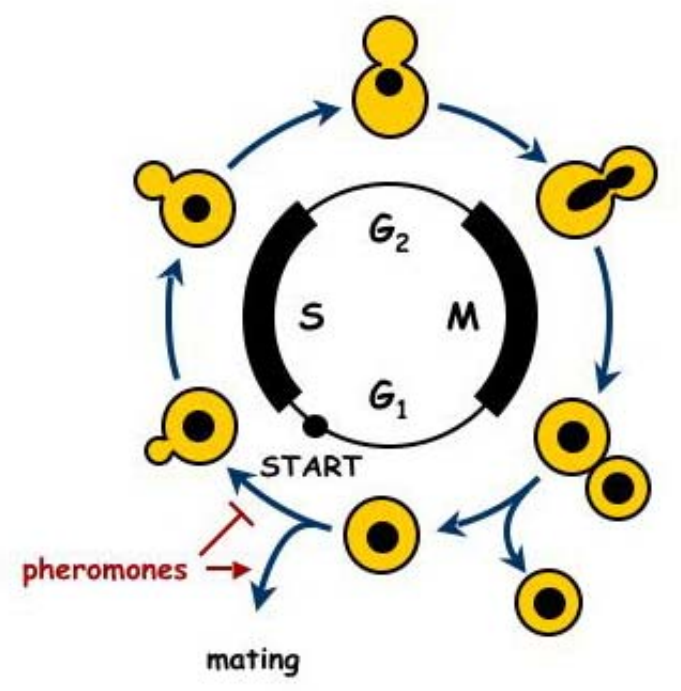

Figure 1-6. Mating is restricted to the G1 stage of the cell cycle

Exposure to mating pheromones during the G1 stage of the cell cycle causes cell cycle arrest and prevents passage though Start. However, once cells pass Start and commit to another round of division, they become resistant to pheromone until that round of division is complete at which time they become sensitive to pheromone again.

Figure 1-7. Mutual antagonism between the cell cycle and the pheromone response pathway contributes to the G1 specificity of cell cycle arrest

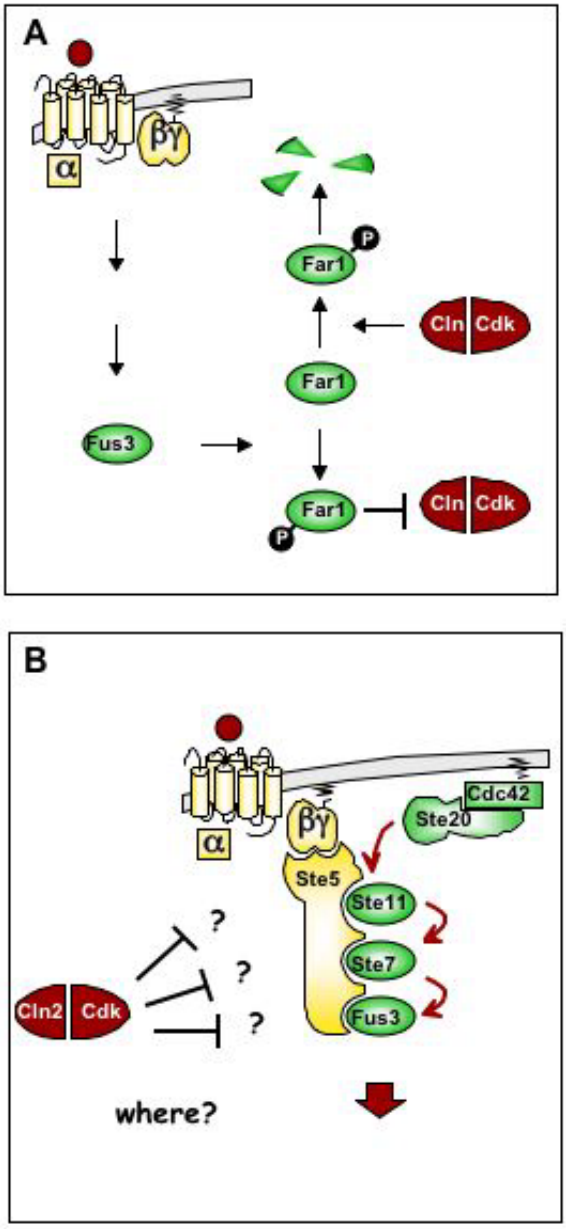

Figure 1-7. Mutual antagonism between the cell cycle and the pheromone response pathway contributes to the G1 specificity of cell cycle arrest

(A) In response to pheromone, the CDK inhibitor Far1 is phosphorylated and activated by Fus3. This allows Far1 to inhibit the G1 cyclin/CDK complexes and promote cell cycle arrest. Conversely, as cells pass Start the Cln/CDKs phosphorylate Far1, thereby triggering its degradation.

(B) Cln2/CDK also plays a role in restricting pheromone response to G1 by inhibiting signal transduction through the mating pathway MAPK cascade. However, the target and mechanism of this inhibition was unknown.

GOAL OF THIS WORK

The goal of this work was to examine how cellular responses to external stimuli are regulated. To accomplish this I used the yeast pheromone response pathway to examine how cells generate an asymmetric polarization response and how pheromone response is restricted to G1. First, how Gβγ activity was regulated to generate an axis of polarization in response a gradient (chemotropism) or uniform concentration (*de novo* polarization) of pheromone was investigated (Chapter II). Second, how G1 CDKs inhibit signal transduction through the mating pathway MAPK cascade was determined (Chapter III).

CHAPTER II

QUALITATIVELY DIFFERENT ROLES FOR TWO Gα-Gβ INTERFACES IN CELL POLARITY CONTROL BY A YEAST HETEROTRIMERIC G PROTEIN

Figure 2-1, Figure 2-3 D, and Figures 2-5 B and C were contributed by Dr. Peter Pryciak. Rachel Lamson provided technical assistance.

Summary

In the pheromone response pathway, the heterotrimeric G protein Gβγ dimer activates MAP kinase cascade signaling and also recruits polarity proteins to induce a polarized mating projection. Here, by activating the MAP kinase pathway independent of Gβγ, we studied the polarity role of Gβγ in isolation from its signaling role. We show that, in addition to Gβγ, the Gα subunit and the receptor are required for following pheromone gradients (chemotropism) and for establishing a persistent polarity axis in the absence of pheromone gradients (*de novo* polarization). To explore regulation of Gβγ by Gα, we mutated Gβ residues in two structurally-distinct Gα-Gβ binding interfaces, resulting in two phenotypic categories: mutations in the N-terminal interface strongly disrupted chemotropism and *de novo* polarization, whereas mutations in the switch interface did not. Incorporation of these mutations into a Gβ-Gα fusion protein, which forces the subunits to remain associated, revealed that dissociation of the switch interface regulates signaling, whereas the N-terminal interface may govern receptor-Gαβγ coupling. In addition, we found that chemotropism and *de novo* polarization require GTP hydrolysis by Gα, suggesting that receptor-guided polarization involves Gα cycling between GDP and GTP bound states. Overall, our results suggest that continuous communication between the receptor and Gαβγ is important for proper cell polarization, and that the Gαβγ heterotrimer may be able to function in a partially-dissociated state, tethered by the N-terminal interface.

Introduction Chapter II

Polarized growth involves choosing a direction for polarization and then reorienting the cytoskeleton in the chosen direction. The direction for polarization can be established in response to internal or external polarity cues. *S. cerevisiae* polarize in response to both internal cues (for budding) and external cues (for mating) (Chant, 1999). In response to the external polarity cue, mating pheromone, yeast will form a polarized mating projection. Normally, a gradient of pheromone emitted from a mating partner serves as a spatial cue to direct polarization and the cell will form a mating projection that grows along the gradient in a process termed chemotropism (Segall, 1993). However, yeast can also polarize when pheromone is provided uniformly. This occurs in two ways: default and *de novo* polarization (Madden and Snyder, 1992; Dorer et al., 1995; Nern and Arkowitz, 1999).

This morphological response is mediated by the pheromone response pathway, which is activated when pheromone binds to its receptor. This binding triggers dissociation of a heterotrimeric G protein (Gαβγ) into Gα-GTP and Gβγ. Once freed from Gα inhibition, the Gβγ dimer then triggers signaling through the MAP kinase cascade and also recruits the polarity proteins to establish a polarized mating projection (Butty et al., 1998; Nern and Arkowitz, 1998; Pryciak and Huntress, 1998; Mahanty et al., 1999; Nern and Arkowitz, 1999; Winters et al., 2005).

To better understand how external signals couple to intracellular factors to generate an asymmetric response, we studied the regulation of Gβγ activity in response to

a gradient or uniform field of pheromone. Here we show that, in addition to Gβγ, the receptor and Gα subunit are required not only to sense pheromone gradients during chemotropism but also for *de novo* polarization in response to a uniform field of pheromone. To further investigate this requirement, we used a series of mutations in Gβ (Ste4) to disrupt regulation of Gβγ by Gα. Gβγ interacts with Gα through two distinct structural regions, the N-terminal interface and the switch interface (Wall et al., 1995; Lambright et al., 1996). We found that these mutations cause qualitatively different phenotypes depending on which Gα-Gβ interaction interface is disrupted. Our results suggest that the switch interface controls signaling, while the N-terminal interface governs coupling between Gαβγ and the receptor.

Results Chapter II

Separating the polarity role of Gβγ from its signaling role

The Gβγ dimer normally performs two roles in the mating pathway: it activates MAP kinase cascade signaling and it regulates proteins that control cell polarity (Butty et al., 1998; Nern and Arkowitz, 1998; Pryciak and Huntress, 1998; Mahanty et al., 1999; Nern and Arkowitz, 1999; Winters et al., 2005). Our goal in this work was to study the polarity role of the receptor-Gαβγ module in isolation from its role in activating the MAP kinase cascade. Therefore, we used a variety of methods to activate signaling independent of pheromone and Gβγ, and then studied how perturbing Gαβγ function affects chemotropism and cell polarization. This strategy is an extension of one used previously in which overexpression of the transcription factor Ste12 was used to study the mating role of various MAP kinase pathway components while bypassing their role in transcriptional induction (Schrick et al., 1997). Here, we used several newer reagents, including membrane-targeted versions of Ste5 (Ste5ΔN-CTM and Ste5ΔN-Sec22), which can promote robust MAP kinase cascade signaling, wild-type levels of mating, and normal polarized morphogenesis (Pryciak and Huntress, 1998; Harris et al., 2001). To ensure that communication between Gβγ and Ste5 was severed, these reagents used a truncated form of Ste5 that lacks the Gβγ-binding site (Ste5ΔN), and all assays were performed in *ste5*Δ strains. For comparison, we also used a constitutively-active form of Ste11 (Ste11ΔN) (Pryciak and Huntress, 1998) and overexpressed Ste12 (Dolan and Fields, 1990; Schrick et al., 1997). When signaling output was measured by induction of

a transcriptional reporter construct (*FUS1-lacZ*), we found that some bypass methods activated signaling more strongly than others, but all were independent of Ste4 (Gβ) and pheromone (Figure 2-1A, right).

We then used these signaling bypass methods to address the role of Gβγ in chemotropic mating. Chemotropism was monitored using a "pheromone confusion" assay (Dorer et al., 1995; Nern and Arkowitz, 1998), in which mating success is compared in the absence vs. presence of excess exogenously-added pheromone (α factor), which obscures natural pheromone gradients emanating from partner cells. Chemotropically-proficient cells can use pheromone gradients to locate mating partners, and thus mate with higher efficiency when pheromone gradients are left intact (- α factor) than when gradients are obscured (+ α factor); cells defective at chemotropism are insensitive to the presence or absence of pheromone gradients and thus mate at the lower efficiency under either condition. Unlike earlier measures of "mating partner discrimination" (Jackson and Hartwell, 1990b; Jackson and Hartwell, 1990a), chemotropic proficiency in the pheromone confusion assay requires both Far1 and Far1-Cdc24 binding (Dorer et al., 1995; Valtz et al., 1995; Nern and Arkowitz, 1998) and accurately reflects the ability of cells to establish a new polarization axis along pheromone gradients (Valtz et al., 1995; Nern and Arkowitz, 1998). Using this assay, we found that cells expressing Ste4 (*ste5Δ*) were proficient at chemotropism, whereas those lacking Ste4 (*ste5Δ ste4Δ*) were defective (Figure 2-1A, left). Among the different bypass methods, the membrane-targeted Ste5 reagents clearly promoted the most efficient mating. Nevertheless, a consistent behavior was observed regardless of the

bypass method or the absolute signaling level: namely, removal of Ste4 or addition of excess pheromone disrupted chemotropic mating without altering MAP kinase pathway signaling.

Gβγ activates MAP kinase cascade signaling via interactions with Ste5 and Ste20 (Whiteway et al., 1995; Inouye et al., 1997; Feng et al., 1998; Leeuw et al., 1998; Pryciak and Huntress, 1998; Mahanty et al., 1999; Winters et al., 2005). To unequivocally determine whether these interactions are dispensable for the chemotropic role of Gβγ, we performed quantitative assays of chemotropic mating in *ste5*Δ and *ste5*Δ *ste20*Δ backgrounds, using activated Ste11 (Ste11ΔN) or excess Ste12 to induce signaling or transcription. Indeed, cells lacking Ste5 or both Ste5 and Ste20 remained proficient at chemotropism, because mating efficiency was higher (by 10- to 1000-fold) when gradients were left intact (- α factor) than when they were obscured (+ α factor), whereas strains lacking Ste4 (*ste5*Δ *ste4*Δ and *ste5*Δ *ste4*Δ *ste20*Δ) were defective at chemotropism (Figure 2-1B). Thus, the chemotropism role of Gβγ does not require it to interact with Ste5 or Ste20. These findings provided a framework from which to further probe the chemotropism and polarity functions of the receptor-Gαβγ module without concern for their effects on MAP kinase pathway signaling.

The pheromone receptor and all three Gαβγ subunits are required for chemotropism

The ability of Gβγ to mediate chemotropism without regulating MAP kinase cascade signaling is consistent with the fact that Gβγ directly interacts with polarity

proteins via Far1 (Butty et al., 1998; Nern and Arkowitz, 1998; Nern and Arkowitz, 1999). However, because chemotropism is a directional phenomenon, it would be logical that Gβγ-Far1 binding could help guide polarization in the proper direction only if Gβγ was activated in a spatially asymmetric manner, congruent with the pheromone gradient. Since Gβγ activation is regulated by the receptor and Gα subunit, we directly compared the requirement for the receptor and all three G protein subunits in chemotropic mating assays. As above, MAP kinase signaling and/or transcription was activated independent of Gβγ, so that genetic perturbation of the receptor-Gαβγ module would affect only chemotropism. Despite approximately equal signaling levels (Figure 2-1D), the cells with an intact receptor-Gαβγ module could use pheromone gradients to increase their mating success, whereas cells lacking the receptor (*ste5Δ ste2Δ*) or any one of the G-protein subunits (*ste5Δ gpa1Δ*, *ste5Δ ste4Δ*, or *ste5Δ ste18Δ*) could not (Figure 2-1C). Microscopic analysis confirmed that the intact receptor-Gαβγ module allowed cells to locate and fuse with mating partners, as judged by the formation of dumbbell shaped diploid zygotes (Figure 2-1E), although the mating-defective cells could still form polarized mating projections (Figure 2-1E). Therefore, under these conditions the receptor-Gαβγ module is not required for polarization *per se*, but for properly guiding cell polarization toward a mating partner. Note that these findings are consistent with the expectation that polarization in the "correct" direction (i.e., toward the source of pheromone) should require spatial regulation of Gβγ activity, and so they do not necessarily imply that the receptor and/or Gα perform separate polarization functions.

Figure 2-1

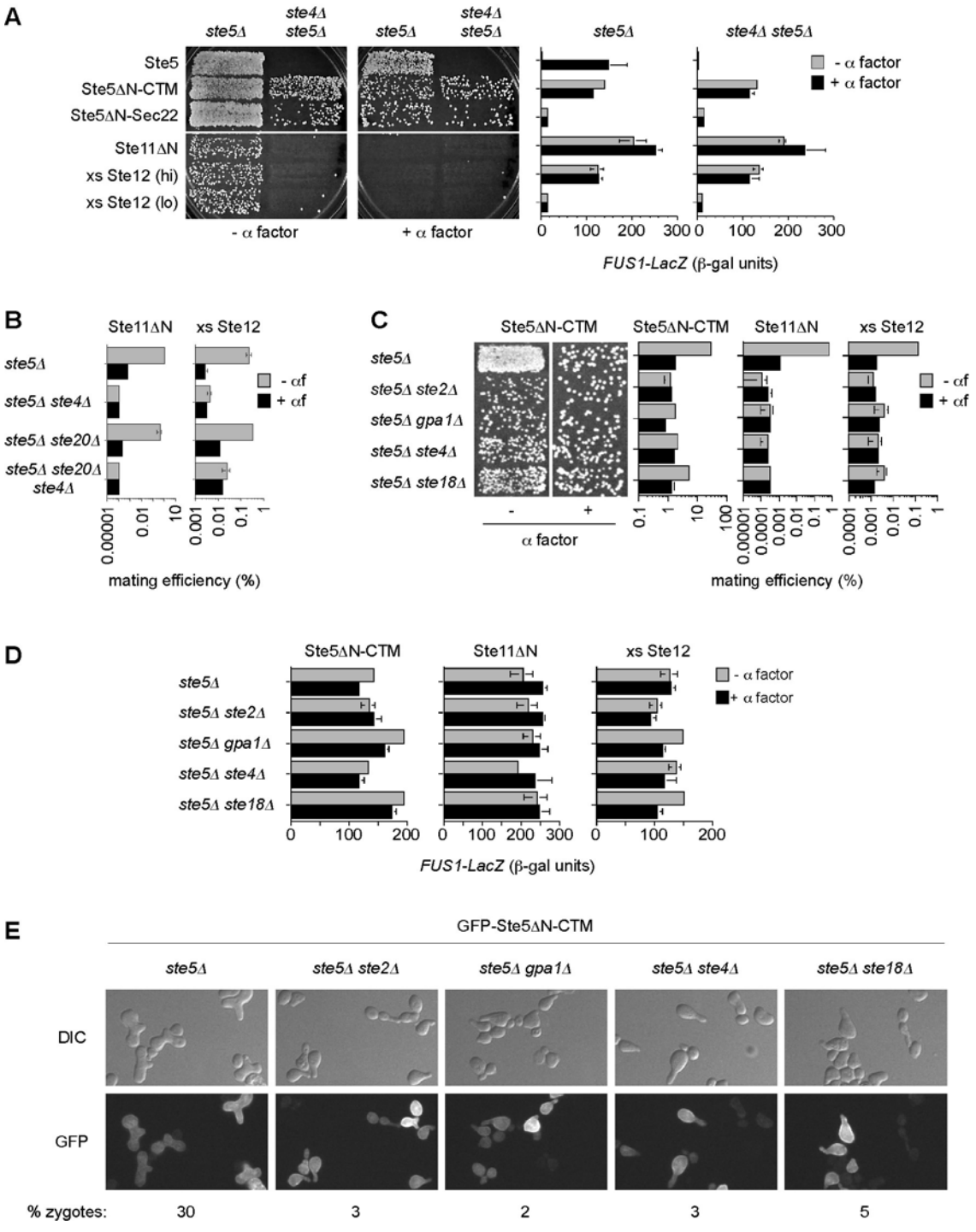
A
ste5Δ
ste4Δ ste5Δ
Ste5
Ste5ΔN-CTM
Ste5ΔN-Sec22
Ste11ΔN
xs Ste12 (hi)
xs Ste12 (lo)
- α factor
+ α factor
FUS1-LacZ (β-gal units)
B
Ste11ΔN
xs Ste12
ste5Δ
ste5Δ ste4Δ
ste5Δ ste20Δ
ste5Δ ste20Δ ste4Δ
- αf
+ αf
mating efficiency (%)
C
Ste5ΔN-CTM
Ste11ΔN
xs Ste12
ste5Δ ste2Δ
ste5Δ gpa1Δ
ste5Δ ste4Δ
ste5Δ ste18Δ
α factor
D
E
GFP-Ste5ΔN-CTM
DIC
GFP
% zygotes: 30 3 2 3 5

Figure 2-1. Chemotropism role of Gαβγ and receptor is separate from signaling

(A) Chemotropism requires Ste4 even when its signaling role is bypassed. Strains PPY858 (*ste5*Δ) and PPY886 (*ste5*Δ *ste4*Δ) harbored galactose-inducible forms of Ste5 (pPP452), Ste5ΔN-CTM (pPP513), Ste5ΔN-Sec22 (pPP524), Ste11ΔN (pPP575), or Ste12 (pPP741 or pPP271). Chemotropic proficiency (left) was assessed by patch matings performed in the absence (-) or presence (+) of exogenous α factor. The mating results using the Ste5 derivatives show the more-dilute 2° replica, whereas the others show the 1° replica (see Appendix A Materials and Methods Chapter II). Results were similar in both **a** and α cells, and in both W303 and 381G strain backgrounds (P.M. Pryciak, personal communication). Transcriptional activation of *FUS1-lacZ* (right) is shown for the same strains and plasmids after galactose induction for 4 hours ± 10 μM α factor. Bars, mean ± SD (n=3). To emphasize that transcription levels were not the primary determinant of mating efficiency, results are shown using Ste12 overexpression constructs that yield high (hi) or low (lo) levels of transcriptional induction (due to different vector contexts).

(B) Interaction with Ste5 and Ste20 is not required for the chemotropism role of Ste4. Quantitative matings were performed ± exogenous α factor. Strains PPY861, PPY867, PPY863, PPY842 harbored either galactose-inducible Ste11ΔN (pRD-STE11-H3) or Ste12 (pNC252). Bars, mean ± SD (n=2).

(C) An intact receptor-Gαβγ module is required for chemotropism. Signaling was activated by galactose-inducible constructs (pPP513, pPP575, pPP741) in the indicated strains (PPY858, PPY979, PPY978, PPY886 and PPY989). Chemotropism was monitored by patch or quantitative mating assays in the absence (-) or presence (+) of α factor. Bars, mean ± SD (n=2-4).

(D) Transcriptional activation of *FUS1-lacZ* by the same strains and constructs as in panel C after galactose induction for 4 hours ± 10μM α factor. Bars, mean ± SD (n=3).

(E) Zygote formation. Strains from panel C, harboring galactose-inducible GFP-Ste5ΔN-CTM (pPP513), were mated with PT2α partner cells for 5.5 hours. Representative fields of DIC and fluorescence (GFP) images are shown. 500 cells were counted for each mixture and the percent of zygotes was determined.

Free Gβγ is insufficient for *de novo* polarization

In order to study the polarity function of the receptor-Gαβγ module in a setting where cells do not have to detect the direction of a localized stimulus, we assayed *de novo* polarization in response to a uniform field of pheromone. Polarization was restricted to the *de novo* pathway by using *rsr1*Δ mutant strains, in which the default pathway is inactivated (Nern and Arkowitz, 1999). First, we tested if pheromone had a role in *de novo* polarization beyond activating the MAP kinase cascade. Pathway signaling was activated independent of pheromone and Gβγ by expressing either Ste5ΔN-CTM (P_{GAL1}-*STE5*Δ*N-CTM*) or an activated form of Ste11 (Ste11ΔN) fused to Ste7 (P_{GAL1}-*STE11*Δ*N-STE7*), which permits normal mating morphology by reducing cross-activation of other (non-mating) pathways (Harris et al., 2001). Unlike treatment with pheromone, pathway activation by Ste5ΔN-CTM or Ste11ΔN-Ste7 could not trigger *de novo* polarization (i.e., in *rsr1*Δ cells), despite being able to trigger default polarization (i.e., in *RSR1* cells) (Figure 2-2A). This inability to induce *de novo* polarization was not due to interference from excess MAP kinase pathway signaling, as cells harboring these pathway activators (*ste5*Δ + P_{GAL1}-*STE5*Δ*N-CTM* or P_{GAL1}-*STE11*Δ*N-STE7*) could undergo *de novo* polarization when pheromone was added (Figure 2-2B). Importantly, we also found that *de novo* polarization requires Gβγ activity, as cells lacking the Gβ subunit (*ste4Δ ste5Δ* + P_{GAL1}-*STE11ΔN-STE7*) did not polarize even when pheromone was added (Figure 2-2B). Notably, however, communication between Gβγ and Ste5 was not required, because pheromone could stimulate polarization in cells lacking Ste5 (*ste5Δ* + P_{GAL1}-*STE11ΔN-STE7*) (Figure 2-2B). These results show that, as with chemotropism,

the ability of pheromone and Gβγ to regulate *de novo* polarization is separable from any regulatory effects on the MAP kinase cascade.

Because *de novo* polarization does not require cells to sense the direction from which pheromone emanates, and because Gβγ interacts with the polarity proteins Far1 and Cdc24, (Butty et al., 1998; Nern and Arkowitz, 1998; Nern and Arkowitz, 1999), it seemed possible that Gβγ alone would be sufficient to promote *de novo* polarization, with pheromone serving only to generate free Gβγ by dissociating the Gαβγ heterotrimer. To test this view, Gβγ was activated without using pheromone, by deletion of *GPA1* or by over-expression of *STE4* (P_{GAL1}-*STE4*) (Dietzel and Kurjan, 1987; Miyajima et al., 1987; Cole et al., 1990; Nomoto et al., 1990; Whiteway et al., 1990). To avoid persistent growth arrest due to constitutive MAP kinase pathway signaling, *GPA1* was deleted in a *ste5*Δ strain harboring P_{GAL1}-*STE11*Δ*N*-*STE7* (Figure 2-2B) or in a *ste4*Δ strain harboring P_{GAL1}-*STE4* (Figure 2-2C). Remarkably, although each method of Gβγ activation (i.e., *gpa1*Δ or P_{GAL1}-*STE4*) could induce cell cycle arrest and cell polarization by the default pathway (i.e., in *RSR1* cells), neither method could induce *de novo* polarization (i.e., in *rsr1*Δ cells) (Figure 2-2B and 2-2C). Furthermore, the ability of pheromone to trigger *de novo* polarization was actually eliminated by the *gpa1*Δ mutation (Figures 2-2B and 2-2C, right columns), and thus requires Gα in addition to Gβγ. Therefore, while Gβγ can directly communicate with polarization proteins, free Gβγ is not sufficient for *de novo* polarization. This deficiency might reflect a separate role for ligand-bound receptors or GTP-loaded Gα. Alternatively, it might indicate that ligand-bound receptors and Gα can

promote an asymmetric distribution of Gβγ activity even when external pheromone is distributed uniformly.

Figure 2-2

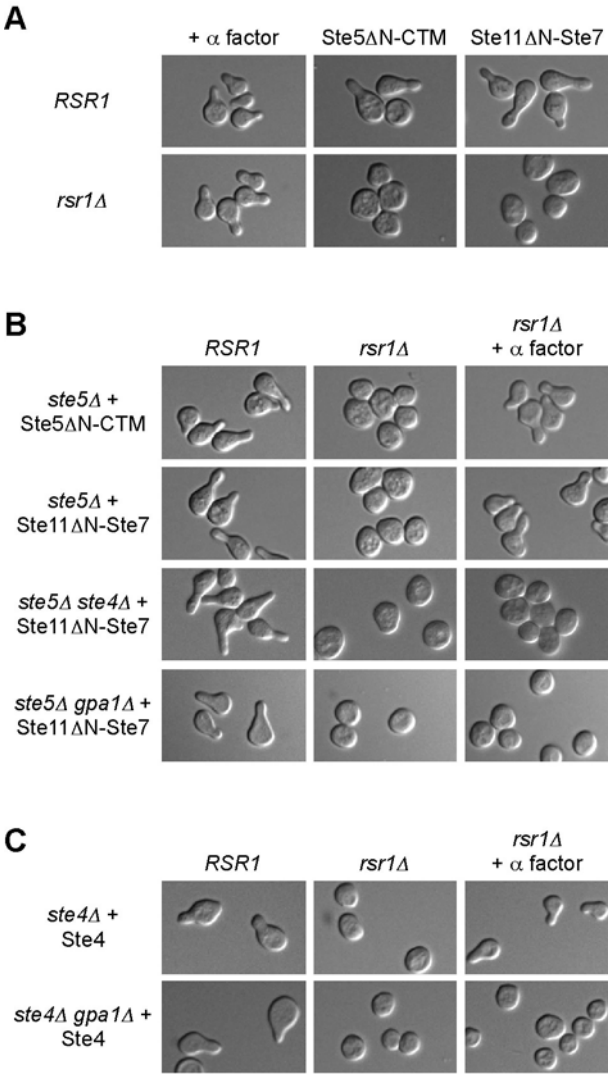
A
+ α factor
Ste5ΔN-CTM
Ste11ΔN-Ste7
RSR1
rsr1Δ
B
RSR1
rsr1Δ
rsr1Δ
+ α factor
ste5Δ +
Ste5ΔN-CTM
ste5Δ +
Ste11ΔN-Ste7
ste5Δ ste4Δ +
Ste11ΔN-Ste7
ste5Δ gpa1Δ +
Ste11ΔN-Ste7
C
RSR1
rsr1Δ
rsr1Δ
+ α factor
ste4Δ +
Ste4
ste4Δ gpa1Δ +
Ste4

Figure 2-2. *De novo* polarization requires pheromone and Gα, in addition to Gβγ

(A) Polarization was examined in *RSR1* or *rsr1*Δ cells, after signaling was activated by pheromone (10μM α factor) (strains PPY398 and PPY1259) or by galactose induction of P_{GAL1}-*STE5*Δ*N-CTM* (strains PPY1303 and PPY1306) or P_{GAL1}-*STE11*Δ*N-STE7* (strains PPY1309 and PPY1312).

(B) Pheromone, Ste4 and Gpa1 are required for *de novo* polarization. The indicated *rsr1*Δ strains harboring P_{GAL1}-*STE5*Δ*N-CTM* or P_{GAL1}-*STE11*Δ*N-STE7* (strains PPY1307, PPY1313, PPY1314, PPY1952) were examined after induction with galactose ± 10μM α factor. Congenic *RSR1* strains (PPY1304, PPY1310, PPY1311, PPY1951) show that the galactose-inducible constructs can activate polarization by the default pathway.

(C) Free Gβγ is not sufficient for *de novo* polarization. Strains PPY794 (*ste4*Δ *RSR1*), PPY1228 (*ste4*Δ *gpa1*Δ *RSR1*), PPY1248 (*ste4*Δ *rsr1*Δ) and PPY1380 (*ste4*Δ *gpa1*Δ *rsr1*Δ) harboring P_{GAL1}-*STE4* (pGT-STE4) were induced with galactose ± 10μM α factor.

Gβ mutants reveal different roles for the two Gα-Gβ interfaces

To further investigate the requirement for the intact receptor-Gαβγ module in chemotropism and *de novo* polarization, we used a series of Gβ mutants to disrupt regulation of Gβγ by the Gα subunit. Crystal structures of mammalian Gαβγ heterotrimers reveal two contact surfaces between Gα and Gβ, termed the "switch interface" and the "N-terminal interface" (Wall et al., 1995; Lambright et al., 1996). The switch (Sw) interface involves a region of Gα that undergoes a conformational switch upon GTP binding, whereas the N-terminal (Nt) interface involves an N-terminal helix of Gα that protrudes away from the remainder of the globular GTPase domain (Figure 2-3A). The Gα and Gβ residues contacting one another in each interface are conserved between mammalian and yeast counterparts (Lambright et al., 1996; Sondek et al., 1996); in Gβ these include 16 residues. Here, we studied a series of Gβ (*STE4*) mutations that collectively affect all residues predicted to contact Gα. Briefly, these mutations derive from four sources: (i) a screen for Ste4 mutants that are competent to signal but show mating defects (in which multiple isolates at K126 were found); (ii) a screen for Ste4 mutants that show disrupted binding to Gpa1 but retain normal binding to Ste18 and Ste5; (iii) a previously described mutation in the Sw interface at Ste4 residues W136 L138 (Whiteway et al., 1994); and (iv) site-directed mutagenesis of Ste4 residues that were predicted to be Gα contact points but were not uncovered in unbiased screens (and which showed the weakest Gα-binding defects, explaining why they were not uncovered in screens).

Co-immunoprecipitation and two-hybrid assays showed that mutations in either interface disrupt Gpa1-Ste4 binding without affecting binding to Far1 (Figure 2-3D). Furthermore, as expected for mutants released from repression by Gpa1, these Ste4 mutants cause constitutively-active MAP kinase pathway signaling (Figure 2-3B), and they trigger default polarization in *RSR1* cells (Figure 2-3C). We focused most of our subsequent studies on the four Gβ mutants that were most defective for binding Gpa1, which include two in the Nt interface (L117R and K126E) and two in the Sw interface (W136R/L138F and L154R/N156K; hereafter termed "WL/RF" and "LN/RK", respectively).

Despite behaving similarly in binding, signaling, and default polarization assays the two classes of mutants (Nt interface versus Sw interface) showed opposing chemotropism phenotypes. Mutations in the Nt interface disrupted chemotropism, as they caused low levels of mating whether pheromone gradients were intact (- α factor) or obscured (+ α factor) (Figure 2-3D). This phenotype is consistent with disrupted interaction between Gpa1 and Ste4. Surprisingly, however, the Sw interface mutants were chemotropism-proficient (Figure 2-3D), even though by signaling and binding criteria they appeared to be as strongly dissociated from Gpa1 as the Nt interface mutants. Even when multiple Sw interface mutations were combined--i.e. W136R, L138F, L154R and N156K ("WL/RF+LN/RK")--chemotropism remained intact (Figure 2-3D). Consistent with these findings, the Ste4 mutants also segregated into two phenotypic classes in *de novo* polarization assays, in which the Sw interface mutants remained competent while the Nt interface mutants were defective (Figure 2-3E).

Notably, although the Sw interface mutants could mediate *de novo* polarization, they still required the addition of pheromone, as with wild-type Ste4. This finding indicates that there is an additional pheromone dependent step that can occur with the Sw interface mutants, despite their strong dissociation from Gpa1 in binding and signaling assays. This raised the possibility that the Sw interface mutants can maintain a weak interaction between Gα and Gβ at the Nt interface and thus remain in regulatory communication with the pheromone receptor. This scenario, and others, was addressed by further experiments described below.

Figure 2-3

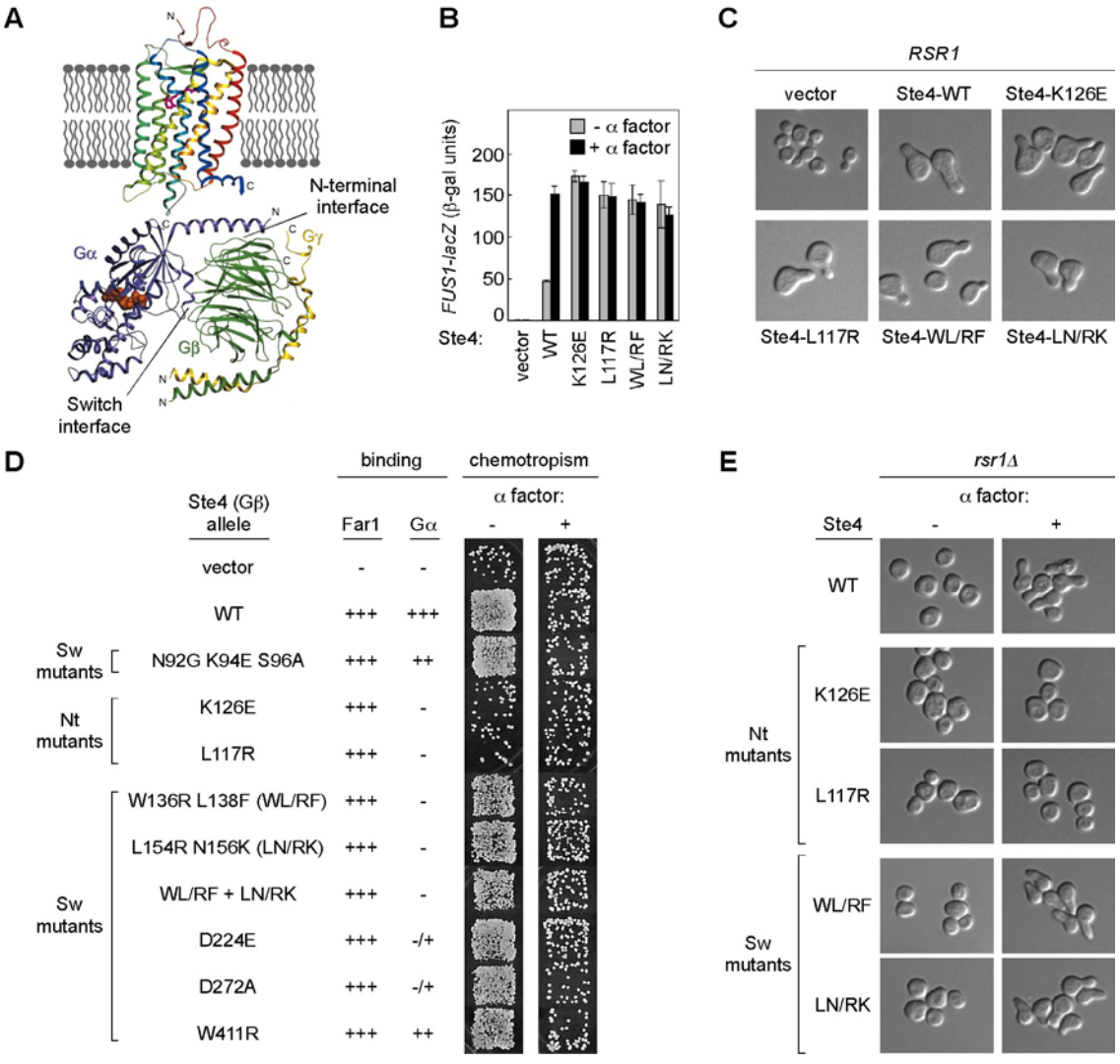
A
N-terminal interface
Switch interface
Gα
Gβ
Gγ
B
- α factor
+ α factor
FUS1-lacZ (β-gal units)
200
150
100
50
0
Ste4:
vector
WT
K126E
L117R
WL/RF
LN/RK
C
RSR1
vector
Ste4-WT
Ste4-K126E
Ste4-L117R
Ste4-WL/RF
Ste4-LN/RK
D
binding
chemotropism
α factor:
Ste4 (Gβ) allele
Far1
Gα
-
+
vector - -
WT +++ +++
Sw mutants
N92G K94E S96A +++ ++
Nt mutants
K126E +++ -
L117R +++ -
Sw mutants
W136R L138F (WL/RF) +++ -
L154R N156K (LN/RK) +++ -
WL/RF + LN/RK +++ -
D224E +++ -/+
D272A +++ -/+
W411R +++ ++
E
rsr1Δ
α factor:
Ste4
-
+
WT
Nt mutants
K126E
L117R
Sw mutants
WL/RF
LN/RK

Figure 2-3. Phenotypic consequences of Ste4 mutations that disrupt interaction between Gβ (Ste4) and Gα (Gpa1)

(A) Model for orientation of the G protein coupled receptor rhodopsin, the heterotrimeric G protein transducin, and the membrane. Adapted from (Hamm, 2001). The N-terminal and Switch interfaces are indicated.

(B) Constitutively-active signaling by Ste4 mutants. To avoid persistent growth arrest, the Ste4 derivatives were expressed from the native *STE4* promoter (see Table A-2) in *ste4*Δ *ste7*Δ cells (PPY1662) harboring P_{GAL1}-*STE7* (pPP2773). Cells were treated with galactose ± 10μM α factor and *FUS1-lacZ* activation was measured. Bars, mean ± SD (n=4).

(C) Ste4 mutants trigger default polarization. *ste4*Δ cells (PPY794) expressing the indicated Ste4 variants from the *GAL1* promoter were examined after galactose induction.

(D) Ste4 Nt interface and Sw interface mutants behave similarly in binding assays but show opposing chemotropism phenotypes. (Left) Ste4 mutants were tested for binding to Far1 and Gpa1 by co-immunoprecipitation and two-hybrid analysis. Results are summarized (P.M. Pryciak, personal communication). (Right) Chemotropism proficiency was assessed by patch mating assays performed in the absence (-) or presence (+) of exogenous α factor. PPY867 (*ste4*Δ *ste5*Δ) harbored P_{GAL1}-*STE5*Δ*N-SEC22* (pPP524) and a *STE4* construct, from top to bottom: pGAD424, pPP268, pPP969, pPP2865, pPP2866, pPP266, pPP966, pPP968, pPP2867, pPP2868, pPP971.

(E) The two classes of Ste4 mutants (Nt interface vs. Sw interface) also show differences in *de novo* polarization proficiency. *ste4*Δ *rsr1*Δ cells (PPY1248) expressing Ste4 variants as in panel C were examined for polarization proficiency after induction with galactose ± 10μM α factor.

Compensatory mutation in Gα suppresses Nt interface mutant phenotype

First, we wanted to determine if the stronger phenotype of the Nt mutants was truly a consequence of disrupted interaction between Gβ and Gα, rather than between Gβ and some other protein involved in cell polarity. Binding assays (Figure 2-3D) showed that the Ste4 mutants could still bind the polarity protein Far1, but in principle we could not rule out effects on binding to other, unknown partners. Therefore, we attempted to restore Gα-Gβ binding via a compensatory mutation in Gpa1. One of the Nt interface mutations (Ste4-K126E) involves a residue that, based on mammalian Gαβγ structures, is expected to form an ion pair between Lys126 in Ste4 and Glu28 in Gpa1 (Figure 2-4A). The Ste4 mutation changes Lys126 to Glu (K126E), thereby reversing the charge. To make a compensatory charge-reversal mutation in Gpa1, we changed Glu28 to Lys (E28K). This Gpa1-E28K mutation, but not a control mutation (Gpa1-E28A), was able to restore a measurable binding interaction with Ste4-K126E (Figure 2-4B), although not to wild-type levels. Also, the Gpa1 E28K and E28A mutations each reduced binding to wild-type Ste4, though by a mild degree that was most noticeable when Ste4 was expressed at lower levels from a weak promoter (Figure 2-4B). It was not entirely surprising that Gpa1-E28K only partially restored binding to Ste4-K126E and that Ste4-K126E caused a stronger binding defect than Gpa1-E28K, because the mammalian Gβ residue homologous to Ste4 K126 contacts Gα not only through this ion pair but also though hydrogen bonding and van der Waals interactions (Lambright et al., 1996). Nevertheless, these binding effects were enough to confer informative phenotypes in mating assays.

Indeed, the chemotropism defect of the Ste4-K126E mutant was at least partially suppressed by the Gpa1-E28K mutant, as mating of cells harboring Ste4-K126E was more efficient when co-expressed with Gpa1-E28K than with Gpa1-WT (Figure 2-4C and 2-4D). Although mating was not restored to wild-type levels, this result was consistent with the incomplete restoration of Gpa1-Ste4 binding. In addition, the observed suppression was allele-specific, as Gpa1-E28A did not suppress Ste4-K126E, and neither Gpa1-E28K nor Gpa1-E28A could suppress the other Nt mutant, Ste4-L117R. Furthermore, although the Gpa1-E28K mutation improved mating by Ste4-K126E, it reduced mating by Ste4-WL/RF and Ste4-LN/RK, such that these Sw mutants were actually more defective than Ste4-K126E in cells expressing Gpa1-E28K (Figure 2-4C). This finding makes it highly unlikely that the phenotypic differences between Ste4 Nt and Sw mutations can be explained by their different impact on binding between Gβγ and an unknown factor. Instead, the pattern of allele-specific suppression and enhancement found with the Gpa1-E28K mutation supports a special role for Gα-Gβ binding via the Nt interface in chemotropism and cell polarization, and suggests that this interface can remain functional when the Sw interface is dissociated by mutation. Because the Gpa1-E28K mutant is sensitized to disruption of the Sw interface, an intact Sw interface may help maintain Gα-Gβ association when the Nt interface is mildly disrupted.

Figure 2-4

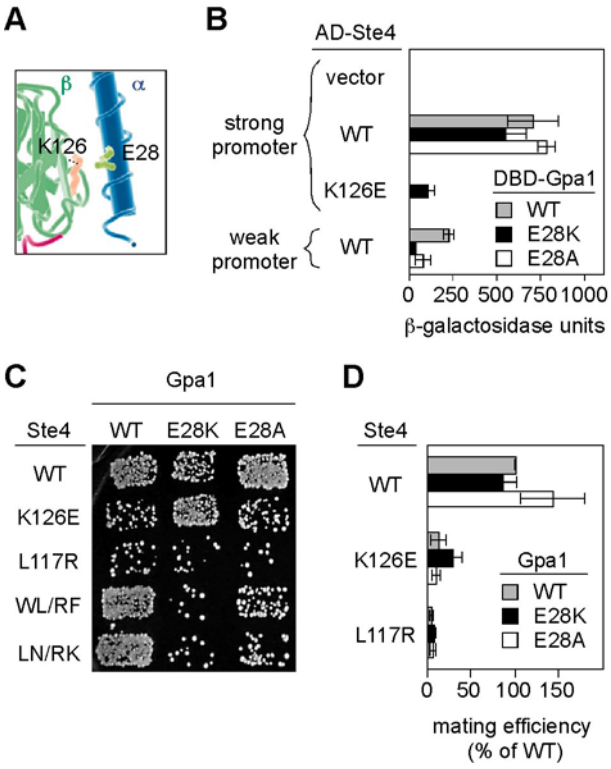
A
β
α
K126
E28
B
AD-Ste4
vector
strong promoter
WT
K126E
weak promoter
WT
DBD-Gpa1
WT
E28K
E28A
0 250 500 750 1000
β-galactosidase units
C
Gpa1
Ste4
WT
E28K
E28A
WT
K126E
L117R
WL/RF
LN/RK
D
Ste4
WT
K126E
L117R
Gpa1
WT
E28K
E28A
0 50 100 150
mating efficiency
(% of WT)

Figure 2-4. Allele specific suppression of chemotropism defect of Nt interface mutant

(A) Residues in the Nt interface. Ste4 (Gβ)-K126 contacts Gpa1 (Gα)-E28.

(B) Two-hybrid analysis showing that the Gpa1-E28K mutation partially restores interaction with Ste4-K126E. DNA binding domain (DBD) fusions to Gpa1 derivatives (pPP247, pPP1502, pPP1505) were co-expressed in PPY762 with AD-Ste4 fusions under control of either a strong or weak promoter (pGADXP, pGADXP-STE4, pPP1121, or pPP249). Bars, mean ± SD (n=3).

(C) Gpa1-E28K partially suppresses the chemotropism defect of Ste4-K126E. Patch mating assay of *ste4*Δ *gpa1*Δ *ste5*Δ cells (PPY1230) harboring P_{GAL1}-*STE5*Δ*N*-*SEC22* (pPP524) and the indicated combination of *GPA1* (YCpGPA1, pPP1501, pPP1503) and P_{GAL1}-*STE4* constructs (pGT-STE4, pPP1233, pPP1229, pPP1228, pPP1209).

(D) Quantitative mating assay of cells carrying constructs as in panel C except that the Ste4 derivatives were expressed from the native *STE4* promoter, and the mating partner was PPY258. Bars, mating efficiency expressed relative to that of the wild type Ste4 and Gpa1 combination (mean ± SD, n=3).

Differences between Nt interface and Sw interface mutants are not due to altered interaction between Gpa1 and Fus3

Next, we considered the possibility that an intact Nt interface was required to properly position the N-terminal helix of Gα for interactions with other proteins, such as pheromone receptor molecules or possible downstream targets of Gα. Relevant to the latter possibility, Gpa1 can interact with the MAPK Fus3 via a MAPK docking motif in the N-terminal α-helix of Gpa1 (Metodiev et al., 2002). Mutations in this docking motif (Gpa1-K21E R22E, herein referred to as Gpa1-EE) disrupt Fus3 binding and reduce mating (Metodiev et al., 2002). This raised the possibility that an intact Nt interface is required mainly to allow proper interaction between the Gpa1 N-terminus and Fus3. To test this notion we used the Gpa1-EE mutant to disrupt interaction between Gpa1 and Fus3, and then asked if the Nt and Sw mutations in Ste4 still showed any phenotypic differences. We found that the Gpa1-EE mutant did not disrupt the chemotropic proficiency of wild-type Ste4 or the Sw interface mutants, whereas the Nt interface mutants were still defective (Figure 2-5A). We also tested the Ste4 mutants in cells lacking Fus3 (*ste4*Δ *fus3*Δ). Here, mating by the Sw interface mutants was not as efficient as that of wild type Ste4, but it was still more efficient than that of the Nt interface mutants (Figure 2-5A). Thus, both approaches suggest that the role of the Nt interface, and the different behavior of the Nt vs. Sw mutants, cannot be explained by indirect effects on the Gpa1-Fus3 interaction.

It is notable that we did not detect a strong mating or chemotropism defect for the Gpa1-EE mutant alone, suggesting that the Gpa1-Fus3 interaction may not be required

for chemotropism. To address this issue further, we compared the roles of Fus3 and Far1 in chemotropism, using the pheromone confusion assay (Figure 2-5B). Loss of either Far1 or Fus3 caused a mating defect, but a much greater defect occurred when both Fus3 and Far1 were absent, indicating that although both proteins are required for maximum mating efficiency, each protein can still function in the absence of the other (Figure 2-5B). Moreover, an important distinction between the roles of Fus3 and Far1 was apparent: the *fus3*Δ cells were proficient at chemotropism (i.e., they were sensitive to the loss of pheromone gradients), whereas the *far1*Δ cells were defective (Figure 2-5B). To rule out the possibility that chemotropic proficiency in *fus3*Δ cells reflects redundancy between Fus3 and Kss1, we performed quantitative mating assays using *fus3*Δ *kss1*Δ cells (in which sterility was suppressed by P_{GAL1}-*STE12*). Despite low overall mating efficiency, the *fus3*Δ *kss1*Δ cells could still use pheromone gradients, and this behavior required Far1 (Figure 2-5C). The simplest overall interpretation is that detecting gradients and using gradient information to locate mating partners does not require Fus3, whereas morphogenesis and successful fusion with a partner may require Fus3 functions that are distinct from gradient sensing *per se*.

Figure 2-5

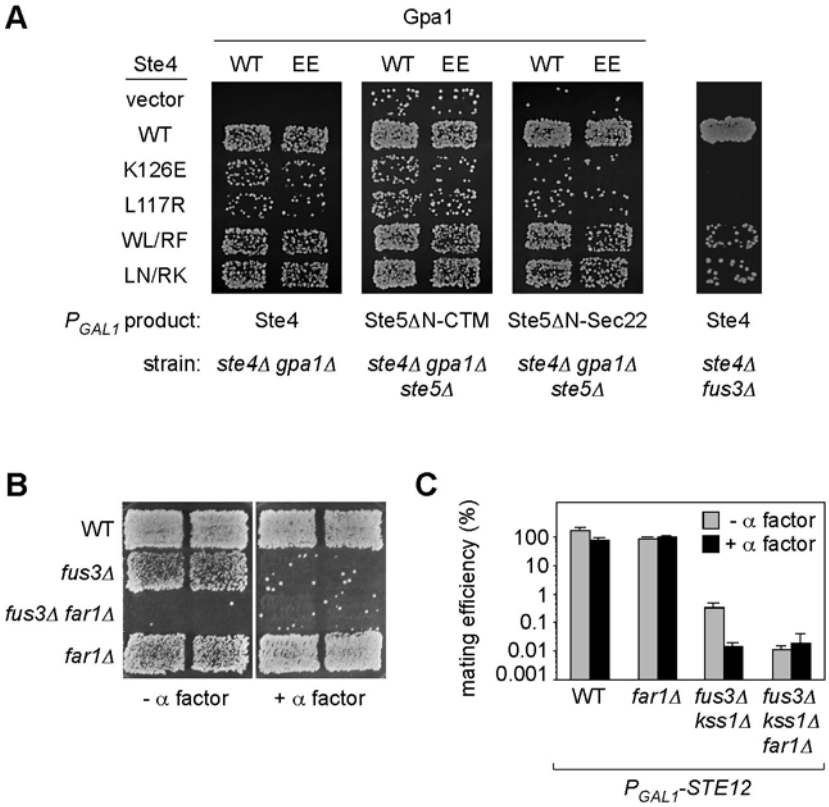
A
Gpa1
Ste4
WT EE WT EE WT EE
vector
WT
K126E
L117R
WL/RF
LN/RK
P_{GAL1} product:
Ste4
Ste5ΔN-CTM
Ste5ΔN-Sec22
Ste4
strain:
ste4Δ gpa1Δ
ste4Δ gpa1Δ ste5Δ
ste4Δ gpa1Δ ste5Δ
ste4Δ fus3Δ
B
WT
fus3Δ
fus3Δ far1Δ
far1Δ
- α factor
+ α factor
C
mating efficiency (%)
100
10
1
0.1
0.01
0.001
- α factor
+ α factor
WT
far1Δ
fus3Δ kss1Δ
fus3Δ kss1Δ far1Δ
P_{GAL1}-STE12

Figure 2-5. Qualitative differences between Ste4 mutants are not due to altered interaction between Gpa1 and Fus3

(A) The Ste4 Nt interface and Sw interface mutants still show differences in chemotropic proficiency when interaction between Gpa1 and Fus3 is disrupted by the Gpa1-EE mutations. Patch mating assays were performed using: (left) strain PPY1228 (*ste4*Δ *gpa1*Δ) harboring the indicated Gpa1 derivatives (pPP2711 or pPP2743) and P_{GAL1}-*STE4* plasmids; (center, right) strain PPY1230 (*ste4*Δ *gpa1*Δ *ste5*Δ) carrying the same Gpa1 derivatives and the indicated Ste4 variants expressed from the native *STE4* promoter. PPY1230 also expressed either Ste5ΔN-CTM (pPP479) or Ste5ΔN-Sec22 (pPP1175) from the *GAL1* promoter. (Far right) Ste4 mutants also display qualitative differences in cells lacking Fus3. Patch mating assay conducted with PPY1937 (*fus3Δ ste4*Δ) harboring the indicated P_{GAL1}-*STE4* plasmids.

(B) Pheromone confusion assay showing that *fus3*Δ cells are chemotropically proficient. Strains, from top to bottom: PPY577, PPY824, PPY827, PPY836. Similar results were also seen in S288C and W303 strain backgrounds (P.M. Pryciak, personal communication).

(C) Quantitative mating assay of strains PPY663, PPY817, PPY498, PPY820 expressing galactose-inducible Ste12 (pPP271) performed ± exogenous α factor. Cells were mated for 18 hours. Bars, mean ± SD (n=3).

Fusion of Gβ to Gα suggests a role for the Nt interface in coupling between the receptor and Gαβγ

Finally, we addressed whether maintenance of the Nt interface was necessary for coupling of the heterotrimer (Gαβγ) to the receptor. A model for coupling between a GPCR and its associated heterotrimeric G protein indicates that the Nt interface lies tangential to the membrane (Hamm, 1998; Hamm, 2001), and the N-terminus of Gα has been implicated in receptor recognition (Taylor et al., 1994; Itoh et al., 2001; Cabrera-Vera et al., 2003). This suggested that the Nt interface mutations may not only disrupt interaction between Gβ and Gα, but they may also disrupt the way Gαβγ interacts with the receptor. However, the ability to test this notion was hindered by the fact that all of the Ste4 mutations caused constitutive signaling, which obscured whether the receptor might still exert some regulatory control over the G protein. To circumvent this difficulty, we took advantage of a previously described Ste4-Gpa1 fusion protein (Klein et al., 2000), with the rationale that forced association to Gpa1 may inhibit the constitutive signaling of the Ste4 mutants and thus allow us to assay receptor coupling.

Starting with the prior Ste4-Gpa1 fusion construct, we replaced the original *GAL1* promoter with the native *STE4* promoter, and then compared its function to wild type (non-fused) polypeptides. By multiple assays, we found the Gβ-Gα fusion (Ste4-Gpa1) to function in a manner that was virtually indistinguishable from when Gβ and Gα were expressed as separate polypeptides. This included growth arrest (Figure 2-6A, left), regulation by the RGS-family protein Sst2 (Figure 2-6A, right), and pheromone-induced transcription (Figure 2-6B). Furthermore, the Gβ-Gα fusion was able to mediate total

mating levels and chemotropic mating behavior that was similar to wild-type cells (Figures 2-6C and 2-6D). Thus, the fusion of Gβ to Gα does not interfere with Gαβγ function in either signaling or gradient detection.

Next, we incorporated the Nt interface and Sw interface mutations into the *STE4* portion of the *STE4-GPA1* fusion gene (in both the *GAL1* promoter and native *STE4* promoter contexts), and then performed *FUS1-lacZ* assays to determine if forced association with Gpa1 could suppress the constitutive signaling activity of the Ste4 mutants. Again, the Nt interface and Sw interface mutants showed distinct phenotypes, as fusion to Gpa1 could suppress the constitutive signaling of the Nt interface mutants but not that of the Sw interface mutants (Figure 2-6E, left and middle panels). There was a slight difference between the two Sw interface mutants in the native promoter fusion context, as fusion to Gpa1 partially reduced signaling by Ste4-LN/RK, but not Ste4-WL/RF (Figure 2-6E, top).

Further analysis of these mutant fusion proteins showed that although constitutive signaling by the Nt interface mutants could be suppressed by fusion to Gpa1, signaling could not be efficiently re-activated by the addition of pheromone, in contrast to the fusion containing wild-type Ste4 (Figure 2-6E, right panels). The absence of robust pheromone response suggests that mutations in the Nt interface disrupt coupling between Gαβγ and the receptor, which may explain their defective behavior in both chemotropism and *de novo* polarization assays. The Sw interface mutants, on the other hand, behave as if they remain unregulated by Gpa1 even in the fusion context (Figure 2-6E middle and right panels). This suggests that dissociation of the Sw interface is the primary regulator

of downstream signaling. Thus, while both Sw and Nt mutants show constitutive signaling when not fused to Gpa1, their different behaviors when fused to Gpa1 suggests the possibility that their different chemotropism/polarity phenotypes are a consequence of disrupted receptor-Gαβγ coupling in the Nt mutants, and by inference that this coupling can still occur in Sw mutants despite their constitutive signaling.

Figure 2-6

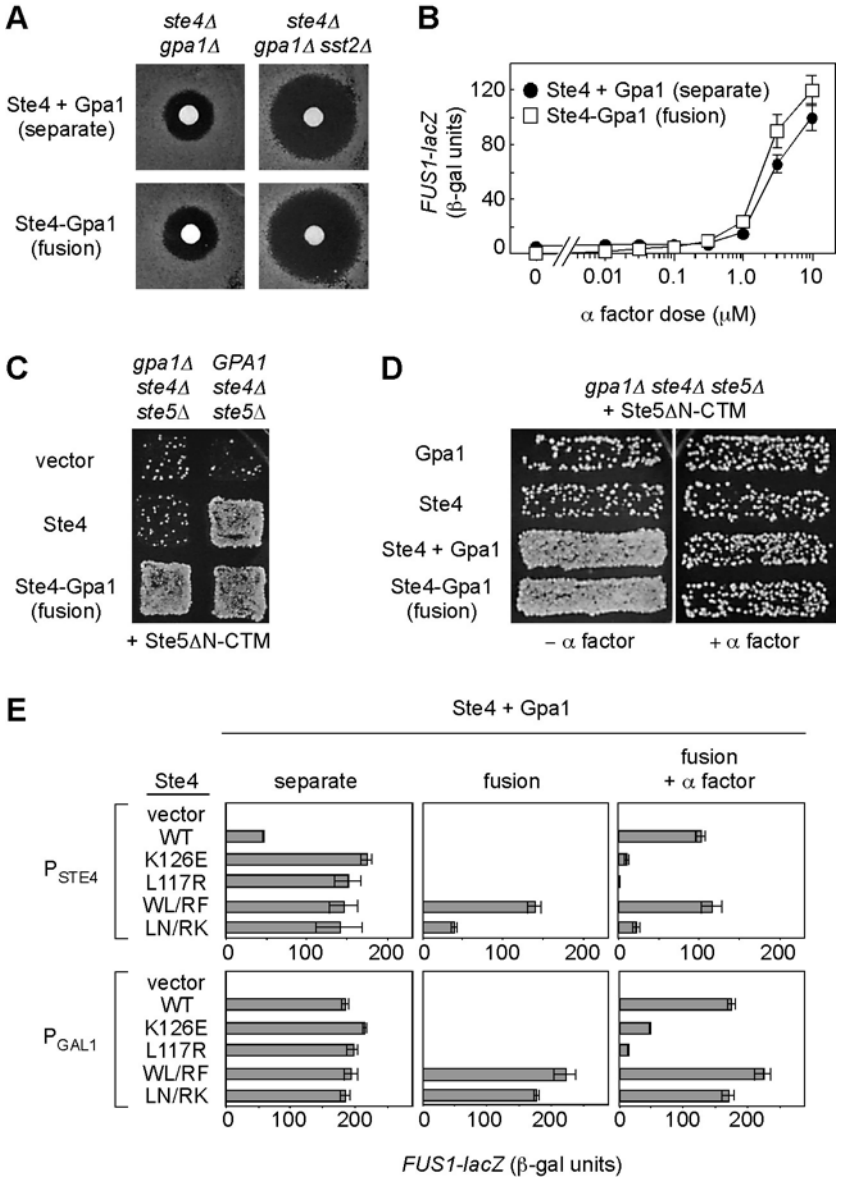
A
ste4Δ gpa1Δ
ste4Δ gpa1Δ sst2Δ
Ste4 + Gpa1 (separate)
Ste4-Gpa1 (fusion)
B
Ste4 + Gpa1 (separate)
Ste4-Gpa1 (fusion)
FUS1-lacZ (β-gal units)
120
80
40
0
0
0.01
0.1
1.0
10
α factor dose (μM)
C
gpa1Δ ste4Δ ste5Δ
GPA1 ste4Δ ste5Δ
vector
Ste4
Ste4-Gpa1 (fusion)
+ Ste5ΔN-CTM
D
gpa1Δ ste4Δ ste5Δ
+ Ste5ΔN-CTM
Gpa1
Ste4
Ste4 + Gpa1
Ste4-Gpa1 (fusion)
– α factor
+ α factor
E
Ste4 + Gpa1
Ste4
separate
fusion
fusion + α factor
vector
WT
K126E
L117R
WL/RF
LN/RK
P STE4
P GAL1
0
100
200
FUS1-lacZ (β-gal units)

Figure 2-6. Phenotypic consequences when Ste4 is forced to remain associated with Gpa1

(A) The Ste4-Gpa1 fusion expressed from the native *STE4* promoter functions indistinguishably from when Ste4 and Gpa1 are expressed as separate polypeptides. Growth arrest of *ste4*Δ *gpa1*Δ cells (PPY1228) or *ste4*Δ *gpa1*Δ *sst2*Δ cells (PPY1942) harboring Gpa1 and Ste4 as separate (YCplac22-GPA1-WT + pPP226) or fused (pPP1340 + pRS314 vector) polypeptides.

(B) *FUS1-lacZ* assays showing that the Ste4-Gpa1 fusion retains normal dose response to pheromone. PPY1663 (*ste4*Δ *gpa1*Δ) harbored plasmids as in panel A. Results are mean ± SD (n=4).

(C) Patch mating assay of strains PPY1230 (*ste5*Δ *ste4Δ gpa1Δ*) or PPY886 (*ste5*Δ *ste4Δ GPA1*) harboring P_{GAL1}-*STE5*Δ*N-CTM* (pPP473) plus pRS316, pPP226, or pPP1340.

(D) Patch mating assays showing that the Ste4-Gpa1 fusion protein remains proficient at chemotropism. Strain PPY1230 carried P_{GAL1}-*STE5*Δ*N-CTM* (pPP479) and plasmids: pRS316, pPP2711, pRS314, pPP226, pPP1340. (Vector plasmids were included when necessary to supplement an auxotropic deficiency to allow matings to be performed on the same plate.)

(E) In the Ste4-Gpa1 fusion context the Ste4 mutants show distinct signaling phenotypes. (Top) Strain PPY1662 (*ste4*Δ *ste7*Δ) harbored a P_{GAL1}-*STE7* construct (pPP2773) plus either vector (pRS316) or the indicated *STE4* or *STE4-GPA1* fusion alleles, expressed from the native *STE4* promoter. (Bottom) Strain PPY856 (*ste4*Δ) harbored either vector (pPP446) or the indicated P_{GAL1}-*STE4* or P_{GAL1}-*STE4-GPA1* fusion constructs. *FUS1-lacZ* activation was measured after induction with galactose ± 10μM α factor. The data in the top left graph is identical to that in Figure 2-3B (- α factor), and is shown here to facilitate comparison. Bars, mean ± SD (n=4).

GTP hydrolysis by Gα is required for de novo polarization and chemotropism

Our findings that pheromone and Gα, in addition to Gβγ, are required for *de novo* polarization (Figure 2-2B and 2-2C), and that the Nt mutants may disrupt receptor-Gαβγ coupling (Figure 2-6E), suggest that proper communication between Gαβγ and the receptor is necessary for directional responses even when the pheromone stimulus is provided uniformly. This receptor-Gαβγ communication might be required solely to promote GTP-GDP nucleotide exchange on Gα, perhaps allowing GTP-bound Gα to perform a polarization role that acts synergistically with Gβγ. Alternatively, receptor-Gαβγ communication might be required to generate asymmetry in the distribution of Gβγ activity (and/or Gα-GTP), which otherwise would remain symmetric (e.g., in *gpa1*Δ cells or with constitutively-active Ste4 mutants). To address these possibilities, we used a mutationally-activated form of the Gα subunit, Gpa1-Q323L (herein referred to as Gpa1-QL), which is defective at GTP hydrolysis (Dohlman et al., 1996; Apanovitch et al., 1998). We found that simultaneous activation of both Gα and Gβγ, by co-expressing Gpa1-QL with Ste4, was still not sufficient for *de novo* polarization in the absence of pheromone (Figure 2-7A and 2-7B). This was true regardless of whether Gpa1-QL was expressed with Ste4-WT or with the signaling-active Sw interface mutant, Ste4-WL/RF. In fact, we found that trapping Gpa1 in the GTP-bound state was detrimental, as cells expressing Gpa1-QL could not polarize even after exposure to pheromone (Figure 2-7A and 2-7B, + α factor). Therefore, polarization requires more than just the acquisition of both GTP-bound Gα and active Gβγ.

It seemed possible that activated Gα and Gβγ subunits might have to remain in close mutual proximity, and that this might be accomplished during receptor-mediated activation but not by co-expression of mutationally-activated subunits. Therefore, to force GTP-bound Gα to remain associated with Gβγ, we incorporated the Gpa1-QL mutation into the *STE4-GPA1* fusion constructs. In signaling assays, incorporation of either the Ste4-WL/RF or Gpa1-QL mutations (or both) into the Ste4-Gpa1 fusion caused constitutive activity (Figure 2-7C), yet none of these fusions could induce *de novo* polarization in the absence of pheromone (Figure 2-7A and 2-7B, - α factor). Notably, however, the fusions containing the Gpa1-QL mutation were able to promote a detectable increase in elongation (and more so than when the same subunits were expressed as separate polypeptides). Nevertheless, these elongated cells did not form the highly-polarized, pear-shaped shmoos seen during pheromone treatment. Thus some aspect of pheromone-induced polarization was still missing, such as the ability to maintain a persistent polarity axis and/or to focus morphogenesis to a restricted portion of the cell perimeter.

Furthermore, pheromone could still trigger *de novo* polarization when Ste4 was fused to Gpa1, but this was disrupted by the Gpa1-QL mutation (Figures 2-7A and 2-7B, + α factor). Consistent with these findings, the fusions containing the Gpa1-QL mutation were also defective in chemotropic mating assays (Figure 2-7D). In addition, the Gpa1-QL mutant (expressed as a separate polypeptide) eliminated the mating advantage of Sw interface mutants over Nt interface mutants (Figure 2-7E). Thus, interfering with GTP hydrolysis activates Gβγ signaling but disrupts cell polarization and chemotropism,

regardless of whether Gα is fused to Gβ or kept separate. Finally, it should be noted that when expressed at native levels, the Gpa1-QL mutant is recessive to wild-type Gpa1 and thus does not interfere with mating (Figure 2-8). Altogether, these observations suggest that the ability of pheromone-bound receptor molecules to guide cell polarization, either along a *de novo* polarization axis or along pheromone gradients, requires normal coupling to the Gα GTP-hydrolysis cycle.

Figure 2-7

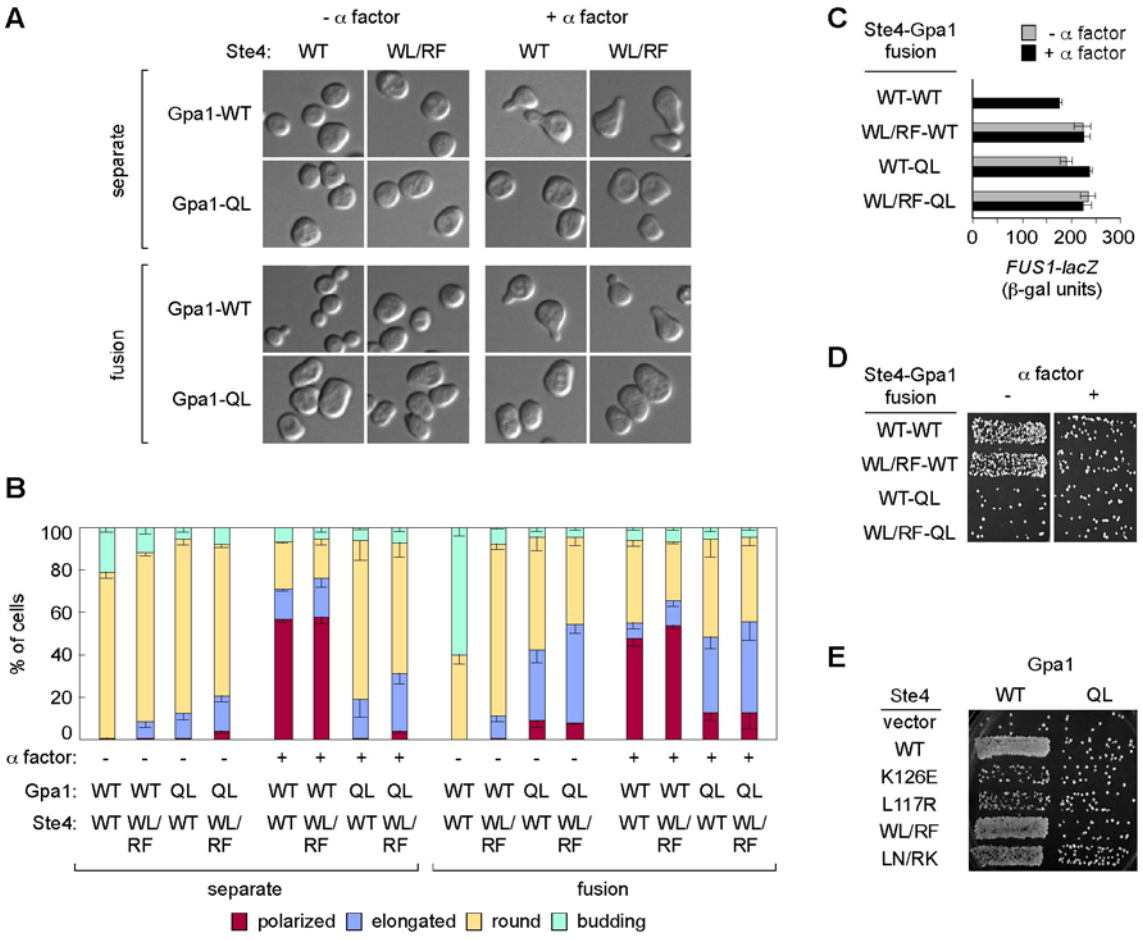
A
- α factor
+ α factor
Ste4: WT WL/RF WT WL/RF
separate
Gpa1-WT
Gpa1-QL
fusion
Gpa1-WT
Gpa1-QL
B
% of cells
100
80
60
40
20
0
α factor: - - - - + + + + - - - - + + + +
Gpa1: WT WT QL QL WT WT QL QL WT WT QL QL WT WT QL QL
Ste4: WT WL/RF WT WL/RF WT WL/RF WT WL/RF WT WL/RF WT WL/RF WT WL/RF WT WL/RF
separate
fusion
polarized
elongated
round
budding
C
Ste4-Gpa1 fusion
- α factor
+ α factor
WT-WT
WL/RF-WT
WT-QL
WL/RF-QL
0
100
200
300
FUS1-lacZ
(β-gal units)
D
Ste4-Gpa1 fusion
α factor
-
+
WT-WT
WL/RF-WT
WT-QL
WL/RF-QL
E
Gpa1
Ste4
WT
QL
vector
WT
K126E
L117R
WL/RF
LN/RK

Figure 2-7. Gpa1 GTP-hydrolysis mutant (Gpa1-QL) interferes with *de novo* polarization and mating

(A and B) *De novo* polarization was monitored using *ste4*Δ *gpa1*Δ *rsr1*Δ cells (PPY1380) expressing Ste4 and Gpa1 variants as either separate or fused polypeptides, after 4 hour induction with galactose ± 10μM α factor. Ste4 and Gpa1 subunits were expressed from pGT-STE4, pPP1228, pPP271, and pPP2802. Ste4-Gpa1 fusions were expressed from pSTE4-GPA1-b, pPP1230, pPP2806, and pPP2807. (A) Representative DIC images of predominant morphology for each condition. (B) Cell morphologies were quantified by counting 200 cells/condition. Cells were scored as polarized if they formed pear shaped shmoos or elongated to a point; whereas those scored as elongated did not form a point on one end but rather elongated so that one axis was longer than the other. Bars, mean - SD (n=3).

(C) Transcriptional induction. *ste4*Δ cells (PPY856) harboring the indicated fusion plasmids expressed from the *GAL1* promoter (from top to bottom: pSTE4-GPA1-b, pPP1230, pPP2806, pPP2807) were induced with galactose ± 10μM α factor and assayed for *FUS1-lacZ* activation. Results for the WT-WT and WL/RF-WT fusion proteins are identical to those for the P_{GAL1}-driven constructs in Figure 2-6E (bottom, middle and right) and are presented here for comparison.

(D) Fusion proteins harboring the Gpa1-QL mutation are defective at chemotropism. Patch mating assay of *ste4*Δ *gpa1*Δ *ste5*Δ cells (PPY1230) harboring galactose-inducible Ste5ΔN-CTM (pPP479) and the indicated fusion construct (plasmids as in C) in the absence (-) or presence (+) of 20 μM exogenous α factor.

(E) Gpa1-QL eliminates the chemotropic advantage of Sw interface mutants over Nt interface mutants. Patch mating assay performed with strain PPY1230 (*ste4*Δ *gpa1*Δ *ste5*Δ) expressing galactose-inducible Ste5ΔN-Sec22 (pPP1175) and the indicated combination of Gpa1 allele

(plasmids, from left to right: pPP2711, pPP2802) and Ste4 allele (plasmids, from top to bottom: pRS316, pPP226, pPP1377, pPP1378, pPP1379, pPP1380).

Figure 2-8

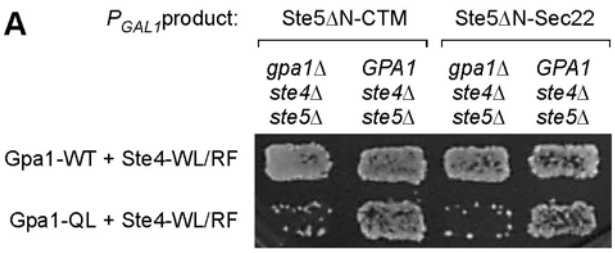
A
P_{GAL1}product:
Ste5ΔN-CTM
Ste5ΔN-Sec22
gpa1Δ ste4Δ ste5Δ
GPA1 ste4Δ ste5Δ
gpa1Δ ste4Δ ste5Δ
GPA1 ste4Δ ste5Δ
Gpa1-WT + Ste4-WL/RF
Gpa1-QL + Ste4-WL/RF

Figure 2-8. Gpa1-QL is recessive to wild type Gpa1

(A) Patch mating assay of *ste4*Δ *ste5*Δ *gpa1*Δ cells (PPY1230) and *ste4*Δ *ste5*Δ *GPA1* cells (PPY867) harboring the indicated Gpa1 derivatives (pPP2711 or pPP2802) and Ste4-WL/RF (pPP1379). These strains also expressed either Ste5ΔN-CTM (pPP479) or Ste5ΔN-Sec22 (pPP1175) from the *GAL1* promoter. The mating partner, PPY198 (MATα *ura3 trp1*) was used to select for retention of the plasmids (*TRP1* and *URA3*).

Discussion Chapter II

This work examines how a GPCR and its coupled Gαβγ heterotrimer coordinate an asymmetric response to external stimuli. Our findings indicate that although Gβγ is thought to be responsible for interacting with downstream polarity factors (e.g., Far1, Cdc24), chemotropism and *de novo* polarization both require an intact receptor-Gαβγ module (Figure 2-1). Furthermore, our results suggest qualitatively different roles for the two Gα-Gβ interaction interfaces. Sw interface mutants are proficient in chemotropism and *de novo* polarization assays, whereas the Nt interface mutants are defective (Figure 2-3D and 2-3E). Forced association of Gβ with Gα revealed that the Sw interface controls signaling, whereas the Nt interface governs coupling to the receptor (Figure 2-6E). As such, maintenance of the N-terminal interface is required for both chemotropism and *de novo* polarization. Finally, Gα GTP hydrolysis is required as a Gpa1-GTP hydrolysis mutant interfered with rather than promoted *de novo* polarization and chemotropism. Overall, these results suggest that proper communication between the receptor and Gαβγ is important for chemotropism and polarized growth, perhaps to regulate Gαβγ in a spatially asymmetric manner.

Distinctions between signaling and polarity roles of Gβγ

Bypassing the role of Gβγ in signaling revealed several interesting points regarding mating efficiency. First, the ability of exogenous pheromone to disrupt chemotropism does not require changes in MAP kinase cascade signaling, as signaling

levels were unaffected by exogenous pheromone and yet mating efficiency was decreased (Figures 2-1A and 2-1B). Thus, the roles of Gβγ and pheromone gradients in chemotropism are clearly separable from their control of MAP kinase cascade signaling and transcription. Second, the total level of mating efficiency is neither solely dictated by nor strongly dependent on transcription levels, as the two membrane-targeted Ste5 reagents activated transcription to either high (Ste5ΔN-CTM) or low (Ste5ΔN-Sec22) levels and yet yielded higher-efficiency mating than the Ste11 and Ste12 reagents (Figures 2-1A and 2-1B). Presumably, the Ste5 reagents promote the most efficient mating because they can activate the MAP kinase cascade (i.e., in contrast to Ste12 overexpression, which induces transcription only) but do not cross-activate other pathways that inhibit mating (i.e., in contrast to Ste11ΔN, which also activates the HOG pathway) (Harris et al., 2001). Third, the ability of pheromone gradients to increase mating success is independent of the baseline level of mating, as this behavior was observed whether the baseline level of mating is relatively high (Ste5ΔN-CTM and Ste5ΔN-Sec22) or relatively low (Ste11ΔN and Ste12) (Figures 2-1A and 2-1B).

Heterotrimeric G protein dissociation mechanisms

Several of our findings are relevant to the mechanism of Gαβγ dissociation. Although it is generally accepted that GTP-loading onto Gα causes Gα-GTP to dissociate from Gβγ (Gilman, 1987; Neer, 1995; Cabrera-Vera et al., 2003), some previous studies have raised the possibility that complete dissociation may not be necessary (Rebois et al., 1997; Klein et al., 2000; Levitzki and Klein, 2002; Bunemann et al., 2003; Gales et al.,

2006). Indeed, prior work showed that the yeast heterotrimer remained functional when Gα and Gβ were expressed as a Gβ-Gα fusion protein (Klein et al., 2000), which should restrict dissociation. We have extended these results further by showing that this Gβ-Gα fusion protein performs both signaling and polarity functions indistinguishably from the wild type, non-fused proteins, even when expressed at native levels (Figure 2-6 A-D). Furthermore, we find that the two Gα-Gβ interaction interfaces have qualitatively different roles. The chemotropic and *de novo* polarization proficiency of the Sw interface mutants indicates that despite being active for signaling, these mutants can still mediate a response to the pheromone ligand whereas the Nt interface mutants cannot mediate such a response (Figure 2-3D and 2-3E and Figure 2-6E), implying that the Sw mutants maintain a functional Nt interface. This raises the possibility that when the Sw interface is dissociated, the Gαβγ heterotrimer may remain tethered by the Nt interface, allowing continued communication with the receptor. By extension, it is conceivable that this "partial dissociation" state applies not only to the Sw interface mutants studied here, but also to receptor-activated Gαβγ. Namely, GTP-induced conformational changes in the switch region of Gα may trigger an initial state in which the Sw interface dissociates but the Nt interface does not.

Several structural considerations are pertinent to this partial dissociation model. First, the N-terminal helix of Gα has been previously implicated in receptor recognition and is thought to lie tangential to the membrane (Taylor et al., 1994; Bourne, 1997; Hamm, 1998; Hamm, 2001; Itoh et al., 2001; Cabrera-Vera et al., 2003), suggesting how an intact Nt interface may facilitate receptor coupling. Second, Gα and Gβγ are anchored

to the membrane by addition of lipophilic groups to the Gα N-terminus and the Gγ C-terminus (Wedegaertner et al., 1995), and these groups are predicted to lie adjacent to each other at one end of the Nt interface (Wall et al., 1995; Lambright et al., 1996). Membrane insertion of these groups increases the stability of the intact heterotrimer (Bigay et al., 1994; Chen and Manning, 2001), and thus may also help stabilize the weak interaction at the Nt interface and keep the partially dissociated structure intact. Solublizing the membrane with detergents would eliminate this contribution, explaining why GTP-activated heterotrimers (Gilman, 1987) and our Sw mutants appear fully dissociated in cell extracts. Third, the behavior of the Gβ-Gα fusion protein is compatible with the partial dissociation model, as the linkage formed between the Gβ C-terminus and the Gα N-terminus would constrain separation of the Nt interface but not the Sw interface. Fourth, crystal structures of Gαβγ show that the N-terminal helix of Gα makes no contacts with the remainder of Gα (Wall et al., 1995; Lambright et al., 1996), thus the linkage between them could freely rotate, potentially allowing the Gα and Gβ halves of the Sw interface to swivel away from each other. Fifth, the N-terminal helix of Gα is usually structurally disordered when Gα is free or bound to effectors (Sunahara et al., 1997; Tesmer et al., 1997a; Tesmer et al., 1997b; Medkova et al., 2002), potentially implying that it tends to remain in contact with Gβγ. Sixth, contacts between Gβγ and effector proteins in co-crystal structures generally involve Gβ residues in the Sw interface rather than the Nt interface (Gaudet et al., 1996; Lodowski et al., 2003), and thus are in principal compatible with partial dissociation.

Note that this partial dissociation model does not postulate that Gα and Gβγ are inseparable, but only that dissociation of the Sw interface (upon loading of Gα with GTP) does not automatically lead to dissociation of the Nt interface as a necessary and/or immediate consequence. Complete dissociation might follow at a subsequent point, perhaps if GTP hydrolysis is delayed or when Gα-GTP and Gβγ bind their targets. Indeed, structural analysis of a tripartite Gα-GRK2-Gβγ complex suggests that the separation between Gα and Gβγ is too great for them to retain contacts and thus they may be completely dissociated, although the status of the Gα N-terminus was ambiguous due to being disordered (Tesmer et al., 2005). Partial dissociation could be of some advantage in allowing an additional level of regulation of heterotrimer activity, or quickening heterotrimer reformation following GTP hydrolysis by Gα. In our physiological context, it could facilitate chemotropism and *de novo* polarization by allowing the activated Gβγ complex to remain in regulatory communication with the receptor.

Symmetry breaking

Symmetry breaking, in which cells or molecular modules self-organize without a localized cue, is thought to involve the amplification of an initial asymmetry that occurs through stochastic variation (Kirschner et al., 2000; Wedlich-Soldner and Li, 2003). In yeast, symmetry breaking can allow formation of polarized buds in the absence of directional cues (Chant and Herskowitz, 1991; Irazoqui et al., 2003). This has been proposed to result from stochastic variation in the local amount of activated (GTP-bound)

Cdc42, which is then amplified by positive feedback loops via two possible pathways (Irazoqui et al., 2003; Wedlich-Soldner et al., 2003). One pathway involves self-assembly of the adaptor protein Bem1, which links Cdc24 and Cdc42 (Butty et al., 2002; Irazoqui et al., 2003; Wedlich-Soldner et al., 2004). The other involves feedback between Cdc42-induced actin polymerization and polarized transport of secretory vesicles carrying Cdc42 as cargo (Gulli et al., 2000; Wedlich-Soldner et al., 2003; Wedlich-Soldner and Li, 2003).

Analogous mechanisms may apply during pheromone response to allow *de novo* polarization. Breaking the symmetry inherent in a uniform field of pheromone may begin with a small difference in receptor-Gαβγ activation, resulting either from a stochastic fluctuation in local ligand concentration or from discontinuities in the plasma membrane distribution of receptor and/or Gαβγ molecules. These differences could cause a slight asymmetry in the initial activation of Gβγ and the resultant recruitment of polarity proteins (Butty et al., 1998; Nern and Arkowitz, 1998; Nern and Arkowitz, 1999), generating a weak landmark for polarity establishment (Arkowitz, 1999) that could then be amplified to form a persistent polarity axis.

Our results implicate a role for continuous communication between pheromone-bound receptors and Gαβγ, since activated Gβγ and Gα alone cannot induce *de novo* polarization. Because pheromone receptors are rapidly internalized and new receptors are delivered by secretory transport along actin filaments (Jenness and Spatrick, 1986; Schandel and Jenness, 1994; Ayscough and Drubin, 1998), the slight initial asymmetry might become amplified by polarized delivery of new pheromone receptors to the initial

landmark, resulting in heightened pheromone response in that location which would reinforce the initial directional choice. The mutations that disrupt *de novo* polarization (i.e., *gpa1-Q323L*, or *ste4* Nt interface mutations) may disable this positive reinforcement by disrupting the ability to coordinate receptor localization with Gα activation and/or Gβγ activity/localization. On the other hand, the chemotropism and *de novo* polarization proficiency of the Sw interface mutants suggests that, despite constitutively-active Gβγ signaling, these mutant heterotrimers remain in regulatory communication with the receptor. Unfortunately, it remains unclear what this communication achieves in molecular terms, though it does require the Gα subunit and GDP-GTP cycling. Speculatively, we envision three scenarios that might explain the ability of pheromone to regulate polarization of cells that express a partially-dissociated, constitutively-active Sw mutant Gαβγ heterotrimer: (1) interaction with asymmetrically-localized receptors might influence localization of the heterotrimer, thereby causing asymmetrically-localized Gβγ activity; (2) the Sw mutants might still allow nucleotide exchange on the Gα subunit at sites of pheromone-bound receptors, potentially promoting localized Gα-GTP, which could control polarization in synergy with Gβγ; or (3) pheromone-bound receptors might interact directly with downstream polarity factors, but normal affinity of receptors for ligand might require coupling to a Gαβγ heterotrimer with an intact Nt interface and normal GDP-GTP exchange properties. Distinguishing among these scenarios will require further study.

Conclusions

The findings reported here reveal several unexpected lessons that may be applicable to other examples of cell polarity control and/or of heterotrimeric G protein function. First, the activated Gαβγ heterotrimer (and the resulting downstream signaling) is not inherently able to organize a directionally-persistent polarization axis. Second, the requirements of the receptor-Gαβγ module are similar for gradient-controlled polarization and *de novo* polarization. Third, the two structurally-distinct Gα-Gβ interfaces have functionally-distinct roles. Fourth, the yeast heterotrimer may be able to function in a partially-dissociated state that allows continued regulatory communication with the receptor. In future studies, it will be interesting to compare these behaviors shown by the yeast system to those of other systems.

CHAPTER III

A MECHANISM FOR CELL-CYCLE REGULATION OF MAP KINASE SIGNALING IN A YEAST DIFFERENTIATION PATHWAY

Figure 3-4 D and Figure 3-8 D and H were contributed by Matt Winters.

Figure 3-7 A was contributed by Dr. Giora Ben-Ari and Dr. Mike Tyers.

Figure 3-6 A, Figure 3-8 C, Figure 3-9, and Figure 3-10 were contributed by Dr. Peter Pryciak.

Rachel Lamson provided technical assistance.

These results were published in:

Strickfaden, S.C., Winters, M.J., Ben-Ari, G., Lamson, R.E., Tyers, M., Pryciak, P.M. (2007). A Mechanism for Cell-Cycle Regulation of MAP Kinase Signaling in a Yeast Differentiation Pathway. Cell 128, 519-531.

Summary

Yeast cells arrest in the G1 phase of the cell cycle upon exposure to mating pheromones. As cells commit to a new cycle, G1 CDK activity (Cln/CDK) inhibits signaling through the mating MAPK cascade. Here, we show that the target of this inhibition is Ste5, the MAPK cascade scaffold protein. Cln/CDK phosphorylates a cluster of sites flanking a small, basic membrane-binding motif in Ste5, thereby disrupting Ste5 membrane localization. Effective inhibition of Ste5 signaling requires multiple phosphorylation sites and a substantial accumulation of negative charge, suggesting that Ste5 acts as a sensor for high G1 CDK activity. Thus, Ste5 is an integration point for both external and internal signals. When Ste5 cannot be phosphorylated, pheromone triggers an aberrant arrest of cells outside G1, either in the presence or absence of the CDK inhibitor protein Far1. These findings define a mechanism and physiological benefit of restricting antiproliferative signaling to G1.

Introduction Chapter III

Cellular decisions are commonly regulated by external signals via MAP kinase cascades (Qi and Elion, 2005). MAP kinase pathways are widely appreciated to stimulate cell proliferation, but they can also regulate cell differentiation. Relatively little is known about how differentiation and antiproliferative signals may be integrated with, or counteracted by, the cell division status of individual cells. In yeast, mating pheromones activate a MAP kinase cascade to trigger fusion between two haploid gamete cells (Dohlman and Thorner, 2001). This mating reaction exhibits fundamental hallmarks of differentiation, in that cells exit the cell cycle, induce a unique program of gene expression, and undergo morphogenetic changes that allow them to adopt a new fate. Mating pheromones cause cells to arrest specifically in the G1 stage of the cell cycle, prior to the G1 to S transition step known as Start. However, once cells pass Start they become committed to finishing that round of division. As such, when post-Start cells are exposed to pheromone they will complete the current division cycle and arrest in the next G1 phase (Hartwell et al., 1974).

Mutual antagonism between the Cln/CDK complexes and Far1, the CDK inhibitor, contributes to the G1 specificity of pheromone induced cell cycle arrest (McKinney et al., 1993; Peter and Herskowitz, 1994; Henchoz et al., 1997; Gartner et al., 1998; Jeoung et al., 1998). In addition, Cln/CDK activity also plays a role in restricting arrest to G1 by inhibiting signaling though the mating MAPK cascade (Oehlen and Cross,

1994; Wassmann and Ammerer, 1997). This ability of the G1 CDKs has been recognized for many years, but the target and mechanism were unknown.

Here, we report that G1 CDK activity inhibits pheromone signaling by inhibiting membrane recruitment of the MAPK cascade scaffold protein, Ste5. The Ste5 PM domain is flanked by multiple CDK sites that are phosphorylated by G1 CDKs *in vivo* and *in vitro*, and the addition of multiple negatively-charged phosphates impedes binding to acidic phospholipid membranes. Furthermore, we show that when CDK regulation of Ste5 is disrupted, pheromone signaling blocks cell cycle progression even after cells pass Start, and even in the absence of Far1, providing a physiological rationale for antagonizing pheromone signaling as cells begin a new division cycle.

Results Chapter III

G1 CDKs inhibit the function of the Ste5 PM domain

To identify the target of Cln/CDK inhibition we used several new tools to dissect early steps in the mating pathway. First, we expressed activated forms of various pathway components (Figure 3-1B) from a strong, galactose-inducible promoter (P_{GAL1}), to bypass upstream signaling steps. We then compared signaling with and without overexpression of Cln2, the G1 cyclin that is most potent at inhibiting pheromone response (Oehlen and Cross, 1994). While each activation method caused strong signaling, only those that require the Ste5 PM domain could be inhibited by Cln2 (Figure 3-1C). Especially revealing is the comparison between Ste5-Q59L and Ste5-CTM. Both activate signaling by targeting Ste5 to the plasma membrane, and both bypass Gβγ but still require Ste20 (Pryciak and Huntress, 1998; Winters et al., 2005). Yet they behaved oppositely with regard to Cln2 sensitivity: Ste5-Q59L (which is targeted to the membrane by an enhanced PM domain; (Winters et al., 2005)) was sensitive to Cln2 inhibition, whereas Ste5-CTM (which is targeted to the membrane by a foreign transmembrane domain; (Pryciak and Huntress, 1998)) was resistant. Furthermore, when comparing two Ste11 derivatives, we found that Ste11-Cpr (which requires the Ste5 PM domain; (Winters et al., 2005)) remained sensitive to Cln2 inhibition, whereas Ste11ΔN (which bypasses Ste5 altogether; (Pryciak and Huntress, 1998)) was resistant. These results argue that G1 CDK inhibition does not act on Gβγ, Ste20, Ste11, or even the ability of Ste5 to facilitate

signaling through the MAP kinase cascade. Instead, signaling is inhibited only when membrane localization by the Ste5 PM domain is required.

In addition to promoting the initial Ste20 to Ste11 step, membrane localization of Ste5 serves a second, Ste20-independent role in boosting signal transmission from active Ste11 through the MAP kinase cascade (Lamson et al., 2006). Because of this "amplification" effect, pheromone can stimulate signaling in *ste20*Δ cells that harbor a pre-activated Ste11 mutant, Ste11-Asp3 (Lamson et al., 2006). Cln2 still inhibited this Ste20-independent response (Figure 3-1D), indicating that there must be a target other than Ste20. Notably, however, partial Cln2 resistance was observed. Yet because this was true for both the Ste20-independent signaling by Ste11-Asp3 (Figure 3-1D) and the Ste20-dependent signaling by Ste11-Cpr (Figure 3-1C), it did not reflect the participation of Ste20 *per se*. Rather, we suggest that Cln2 inhibition is strongest when it can antagonize two successive signaling steps that each rely on Ste5 membrane localization, and becomes incomplete when the first step is bypassed by pre-localization or pre-activation of Ste11.

Further experiments showed that Cln2/CDK inhibition of pheromone response could be reversed by strengthening the Ste5-membrane interaction. First, mutations in the PM domain (Winters et al., 2005) that enhance membrane binding (T52L, Q59L, or a T52L Q59L double mutant) reduced Cln2 inhibition (Figure 3-1F, left), from 89% (WT) to 34% (T52L Q59L). Second, by replacing the native Ste5 PM domain with foreign membrane-binding motifs (Winters et al., 2005), we found that signaling remained Cln2-sensitive when using a relatively weak motif, the PH domain from PLCδ, but became

Cln2-resistant when using two tandem copies of this same motif (Figure 3-1F, right). The PM domain can also target Ste5 into the nucleus (Winters et al., 2005), but Cln2 sensitivity was not changed by a PM domain mutation (NLSm; Figure 3-1E) that specifically disrupts nuclear localization (Winters et al., 2005). Collectively, our results suggest that Cln/CDK antagonizes the ability of the Ste5 PM domain to mediate membrane-localized signaling.

Figure 3-1

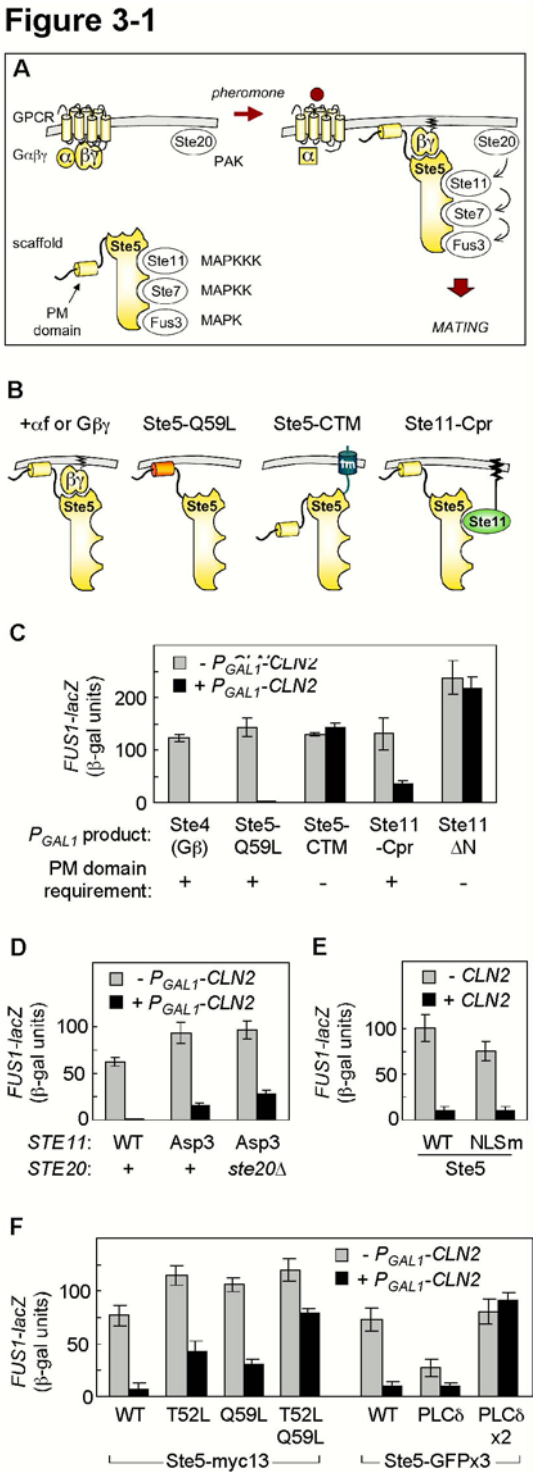
A
pheromone
GPCR
Gαβγ
Ste20
PAK
Ste5
Ste11
Ste7
Fus3
scaffold
MAPKKK
MAPKK
MAPK
PM domain
MATING
B
+αf or Gβγ
Ste5-Q59L
Ste5-CTM
Ste11-Cpr
tm
C
FUS1-lacZ (β-gal units)
- PGAL1-CLN2
+ PGAL1-CLN2
PGAL1 product:
Ste4 (Gβ)
Ste5-Q59L
Ste5-CTM
Ste11-Cpr
Ste11 ΔN
PM domain requirement:
D
STE11:
STE20:
WT
Asp3
ste20Δ
E
- CLN2
+ CLN2
WT
NLSm
Ste5
F
T52L
Q59L
T52L Q59L
PLCδ
PLCδ x2
Ste5-myc13
Ste5-GFPx3

Figure 3-1. Cln2/CDK antagonizes membrane-localized signaling mediated by the Ste5 PM domain

(A) Pheromone response pathway, showing membrane recruitment of Ste5.

(B) Methods for activating membrane-localized signaling. From left to right: α factor (αf) treatment or Gβ overexpression (Whiteway et al., 1990); hyperactive membrane localization of Ste5 via an enhanced PM domain (Winters et al., 2005); membrane targeting of Ste5 via a foreign transmembrane domain (Pryciak and Huntress, 1998); membrane targeting of Ste11 via a prenylation/palmitoylation motif (Winters et al., 2005).

(C) Cln2/CDK inhibition correlates with dependence on the Ste5 PM domain. Pathway-activating components were expressed from the *GAL1* promoter and compared for their ability to induce *FUS1-lacZ* transcription in *ste4*Δ strains ± P_{GAL1}-*CLN2* (n = 4).

(D) Ste20-independent signaling is sensitive to Cln2 inhibition. Wild-type Ste11 (WT) or a Ste20-independent mutant (Ste11-Asp3) was expressed in *ste11*Δ or *ste11*Δ *ste20*Δ strains ± P_{GAL1}-*CLN2*. *FUS1-lacZ* induction was measured after α factor treatment (n = 6).

(E) PM domain mutations that disrupt nuclear targeting (NLSm) do not affect Cln2 inhibition. *FUS1-lacZ* was induced by α factor treatment in *ste5*Δ ± P_{GAL1}-*CLN2* strains expressing Ste5-WT or Ste5-NLSm (n = 9).

(F) Increased Ste5 membrane affinity causes increased resistance to Cln2. *Left*, Ste5 variants contained PM domain mutations that increase membrane affinity. *Right*, the native PM domain was replaced with 1 or 2 copies of the PLCδ PH domain. All forms were expressed from the native *STE5* promoter in *ste5*Δ strains ± P_{GAL1}-*CLN2*, and response to α factor was measured (n = 4-9).

Data in all bar graphs show the mean ± SD.

Multiple CDK sites flanking the Ste5 PM domain regulate signaling

Of fifteen possible CDK sites (i.e., SP or TP) within Ste5, eight are concentrated around the PM domain (Figure 3-2A). This conspicuous clustering, coupled with results described above, suggested that phosphorylation at one or more of these sites might regulate Ste5 signaling. Indeed, small deletions on either side of the Ste5 PM domain conferred partial Cln2 resistance (Figure 3-3B). Therefore, we replaced the Ser or Thr residues at all eight SP/TP sites with non-phosphorylatable Ala residues. This "Ste5-8A" mutant remained fully capable of pheromone response but was now completely resistant to Cln2 inhibition (Figures 3-2B and 3-3C). This phenotype was specific to the Ste5-8A mutant, as a previously-described Ste20 mutant lacking 13 CDK sites, Ste20-13A (Oda et al., 1999), conferred no Cln2 resistance in parallel tests (Figure 3-2B). Furthermore, the Cln2 resistance displayed by Ste5-8A was separable from any possible effects on Ste5-Gβγ binding, because Gβγ-independent signaling by P_{GAL1}-*STE5-Q59L* became resistant to Cln2 when Ste5 harbored the 8A mutations (Figure 3-2C).

We also examined Ste5-8A signaling in synchronous cultures (Figure 3-2D). As cells progressed through the cell cycle, pheromone response was monitored by transcriptional induction of a *FUS1-lacZ* reporter and by phosphorylation of the MAPK Fus3. By either assay, Ste5-8A largely disrupted the normal cell cycle periodicity of pheromone response. Some fluctuation remained, especially at times immediately after release from *cdc15* arrest, which could represent a minor effect of cell cycle position on other targets or a nonspecific effect of the temperature shift protocol. Overall, however, it is clear that

the Ste5-8A mutant confers a very strong, if not complete, resistance to G1 CDK regulation of pheromone response.

To ask which of these eight Ste5 sites governs CDK regulation, we replaced individual Ser or Thr sites with Ala residues. Remarkably, none of the eight single ("1A") mutants displayed the complete Cln2 resistance shown by Ste5-8A, and instead most conferred weak partial resistance (Figure 3-2E), with some variation in strength. By making combined mutants, we observed gradually increasing resistance to Cln2 as more sites were removed (Figure 3-2E), yet complete resistance was seen only when all eight sites were eliminated. Conversely, however, while Cln2 could inhibit signaling to a measurable degree when Ste5 retained 4 or 5 CDK sites, inhibition was much stronger when Ste5 retained 6, 7, or 8 CDK sites. Clearly then, no single site controls sensitivity to Cln2. Rather, multiple CDK sites are required to fully inhibit Ste5 signaling.

Figure 3-2

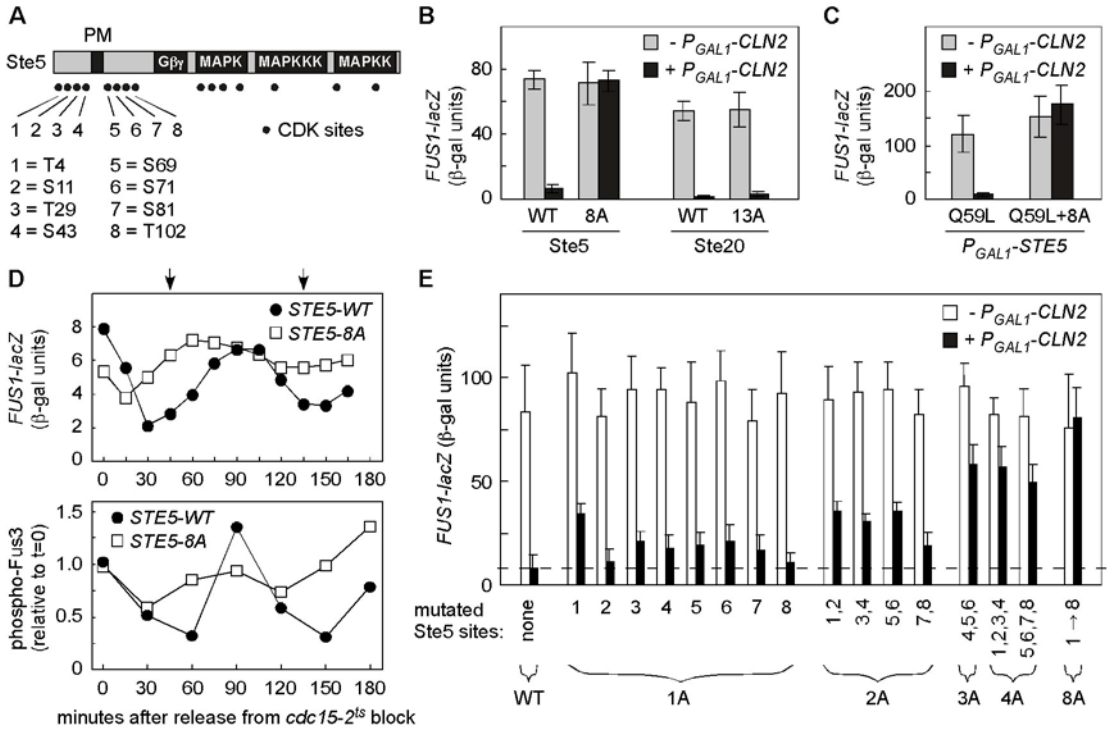
A
PM
Ste5
Gβγ
MAPK
MAPKKK
MAPKK
1 2 3 4 5 6 7 8
• CDK sites
1 = T4
2 = S11
3 = T29
4 = S43
5 = S69
6 = S71
7 = S81
8 = T102
B
- P_GAL1-CLN2
+ P_GAL1-CLN2
FUS1-lacZ (β-gal units)
WT 8A WT 13A
Ste5
Ste20
C
- P_GAL1-CLN2
+ P_GAL1-CLN2
FUS1-lacZ (β-gal units)
Q59L Q59L+8A
P_GAL1-STE5
D
STE5-WT
STE5-8A
FUS1-lacZ (β-gal units)
phospho-Fus3 (relative to t=0)
minutes after release from cdc15-2ts block
E
- P_GAL1-CLN2
+ P_GAL1-CLN2
FUS1-lacZ (β-gal units)
mutated Ste5 sites:
none 1 2 3 4 5 6 7 8 1,2 3,4 5,6 7,8 4,5,6 1,2,3,4 5,6,7,8 1→8
WT 1A 2A 3A 4A 8A

Figure 3-2. Multiple CDK sites flanking the Ste5 PM domain control Cln2/CDK inhibition

(A) Locations of potential CDK phosphorylation sites (SP or TP) in Ste5.

(B) Elimination of 8 N-terminal CDK sites in Ste5 (Ste5-8A) causes resistance to Cln2. Response to α factor was measured in *ste5*Δ ± P_{GAL1}-*CLN2* cells expressing Ste5 variants (WT or 8A) from the native *STE5* promoter, or in *ste20*Δ ± P_{GAL1}-*CLN2* cells expressing Ste20 variants (WT or 13A) from the native *STE20* promoter. Bars, mean ± SD (n = 8).

(C) CDK resistance caused by 8A mutations restores membrane signaling independent of Ste5-Gβγ interaction. Gβγ-independent signaling was activated by P_{GAL1}-*STE5-Q59L* ± *8A* in *ste4*Δ *ste5*Δ cells ± P_{GAL1}-*CLN2*. Bars, mean ± SD (n=7).

(D) The Ste5-8A mutant disrupts cell cycle periodicity of pheromone response. Cells (*cdc15-2* or *cdc15-2 STE5-8A*) were synchronized in late M phase by arrest at 36˚C, and then transferred to 25˚C. At various times, response to brief treatment with α factor was monitored (see Appendix A Materials and Methods Chapter II). Top, *FUS1-lacZ* induction (mean of 4 trials). Bottom, Fus3 activation (phospho-Fus3) was measured using phospho-specific antibodies (mean of 6 trials). Arrows mark the times of bud emergence (see Figures 3-3D and 3-7G).

(E) Ste5 phosphorylation sites were replaced with Ala residues either singly (1A) or in various combinations (2A, 3A, 4A, 8A). Response to α factor was tested in *ste5*Δ strains ± P_{GAL1}-*CLN2* (mean + SD, n = 8-16).

Figure 3-3

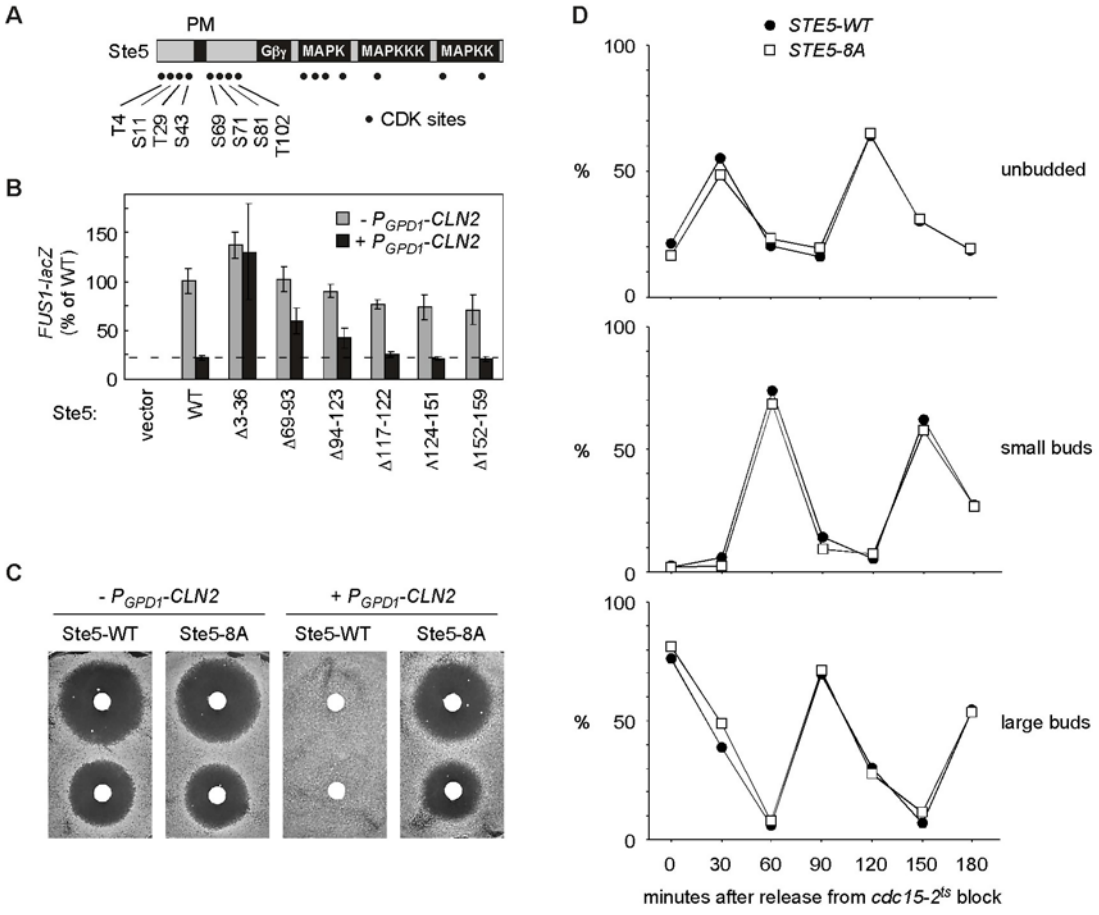
A
PM
Ste5
Gβγ
MAPK
MAPKKK
MAPKK
T4
S11
T29
S43
S69
S71
S81
T102
• CDK sites
B
FUS1-lacZ (% of WT)
- PGPD1-CLN2
+ PGPD1-CLN2
Ste5:
vector
WT
Δ3-36
Δ69-93
Δ94-123
Δ117-122
Δ124-151
Δ152-159
C
- PGPD1-CLN2
+ PGPD1-CLN2
Ste5-WT
Ste5-8A
Ste5-WT
Ste5-8A
D
STE5-WT
STE5-8A
%
unbudded
small buds
large buds
minutes after release from cdc15-2ts block

Figure 3-3. Mutations flanking the Ste5 PM domain affect sensitivity to Cln2 inhibition

(A) Schematic depiction of CDK sites in Ste5. The residue numbers are shown for the eight sites surrounding the PM domain for comparison to the deletion mutations in panel B.

(B) Ste5 derivatives with small deletions flanking the Ste5 PM domain (Winters et al., 2005) were compared for their sensitivity to Cln2 inhibition. Induction of *FUS1-lacZ* by α factor (mean ± SD, n=4) was assayed in *ste5*Δ ± P_{GPD1}-*CLN2* strains expressing the Ste5 derivatives from the native *STE5* promoter. Partial resistance to Cln2 inhibition was observed for deletions that removed some CDK sites (Δ3-36, Δ69-93, Δ94-123), but not for others (Δ117-122, Δ124-151, Δ152-159).

(C) Halo assays showing that Ste5-8A resists the ability of Cln2 overexpression to inhibit pheromone-induced growth arrest. Strains expressed Ste5-WT or Ste5-8A from the endogenous (genomic) *STE5* locus, either with or without an integrated P_{GPD1}-*CLN2* construct. Cells were plated on YPD and overlaid with filter disks containing α factor (20 μl of 100 or 20 μM). Plates were photographed after 2 days.

(D) Synchrony of *cdc15* block and release cultures. Budding morphology was used to monitor cell cycle progression during synchronous culture experiments reported in Figure 3-2D. At 30 min. intervals, aliquots of the cultures (*cdc15-2* or *cdc15-2 STE5-8A*) were fixed in 3.7% formalydehyde, and scored for the percentage of unbudded, small budded, and large budded cells (n = 300). The examples shown here represent the mean of two parallel trials of each strain. The timing of morphological transitions was similar in other experiments (see Figure 3-7G for additional examples). Note that entry into the cell cycle (as judged by the appearance of small buds) correlates with decreased pheromone response in wild-type (but not *STE5-8A*) cells (Figure 3-2D).

Inhibition is proportional to added negative charge

We hypothesized that the addition of anionic phosphates next to the basic-rich PM domain interferes with its electrostatic attraction to acidic phospholipid membranes. Although our findings hinted that full interference might require phosphorylation at multiple Ste5 sites, it was equally possible that multiple sites merely serve to increase the likelihood of phosphorylation at one or a few sites. To address these issues, we replaced the same Ser/Thr residues with negatively-charged Glu residues (Figure 3-4A). Placement of Glu residues at all 8 sites (Ste5-8E) did reduce pheromone response, but not as strongly as when Ste5-WT was inhibited by Cln2 (Figure 3-4B). To explain this partial effect, we reasoned that if electrostatic interference was the operative mechanism, then the net charge might dictate the level of inhibition. Because Ser/Thr phosphorylation introduces a charge of –2, phosphorylation at 8 sites would add a net charge of –16, whereas 8 Glu residues would add a net charge of only –8 and thus would be less inhibitory. To test this notion, we sought to better mimic the –2 charge of each phosphate by using two Glu residues, and so we replaced the SP or TP dipeptides at each of the 8 Ste5 sites with EE dipeptides (Figure 3-4A). Indeed, pheromone response by this "Ste5-16E" mutant was reduced to a level similar to when Ste5-WT was inhibited by Cln2 (Figure 3-4B). This strong effect required EE dipeptides at all 8 sites, because EE dipeptides at only 4 sites either before or after the PM domain (Ste5-up8E or Ste5-dn8E) caused only a partial reduction similar to when the eight Glu residues were distributed among all 8 sites (Ste5-8E), except that signaling could be further inhibited by Cln2 via the remaining 4 CDK sites.

Several observations suggest that the strong signaling deficit of the Ste5-16E mutant reflects a specific effect on the Ste5 PM domain and not a complete inactivation of Ste5. First, the Ste5-16E mutant showed normal protein levels (Figure 3-4C), and it still bound Ste4 (Gβ) (Figure 3-4D). Second, the Ste5-16E mutant could still mediate basal signaling from an activated Ste11 derivative, Ste11-4 (Figure 3-4E), which does not require the Ste5 PM domain (Mahanty et al., 1999; Winters et al., 2005). Third, as with inhibition by Cln2 (see Figure 3-1C), the 16E mutation inhibited Ste5-Q59L but not Ste5-CTM (Figure 3-4F) and therefore only blocks membrane signaling that requires the Ste5 PM domain. A control mutant with AA dipeptides at all 8 sites was not informative because it was poorly expressed (Figure 3-4C), which we traced to the fact that an AA dipeptide was not tolerated at site #3 or #4. By allowing sites #3 and #4 to harbor only single replacements (either A or E) and replacing the six other sites with AA or EE dipeptides, generating "Ste5-14A" and "Ste5-14E", we found that Ste5-14A remained functional (and fully resistant to Cln2), whereas Ste5-14E was strongly inhibited (Figure 3-4B). Therefore, the EE phenotypes reflect the addition of charge rather than the multiplicity of mutations.

As with inhibition by Cln2, the Glu replacements affected membrane-based signaling in general, rather than Gβγ-triggered signaling in particular, because they also disrupted Gβγ-independent signaling by Ste11-Cpr (Figure 3-4G). Again, the degree of inhibition was proportional to the added negative charge. Notably, Ste5-14E retained more function than Ste5-16E, suggesting that 16 negative charges are more inhibitory than 14, which agrees with our finding that removing single CDK sites confers partial

Cln2 resistance. Because the Ste5 PM domain normally acts cooperatively with Ste5-Gβγ binding (Winters et al., 2005), we predicted that the inhibitory effect of a small number of negative charges would be enhanced when Ste5-Gβγ affinity is reduced. Indeed, when using Ste4 (Gβ) mutants with reduced binding to Ste5, we could now detect inhibition by 1 to 4 added Glu residues (Figure 3-4H). Thus, a small number of charges has measurable inhibitory potential, but multiple charges are necessary when the interactions governing Ste5 membrane recruitment occur with normal affinity. Collectively, the Glu replacement phenotypes show that added negative charges disrupt membrane signaling mediated by the Ste5 PM domain, and that the requirement for multiple CDK sites truly reflects a need for adding multiple phosphates.

Figure 3-4

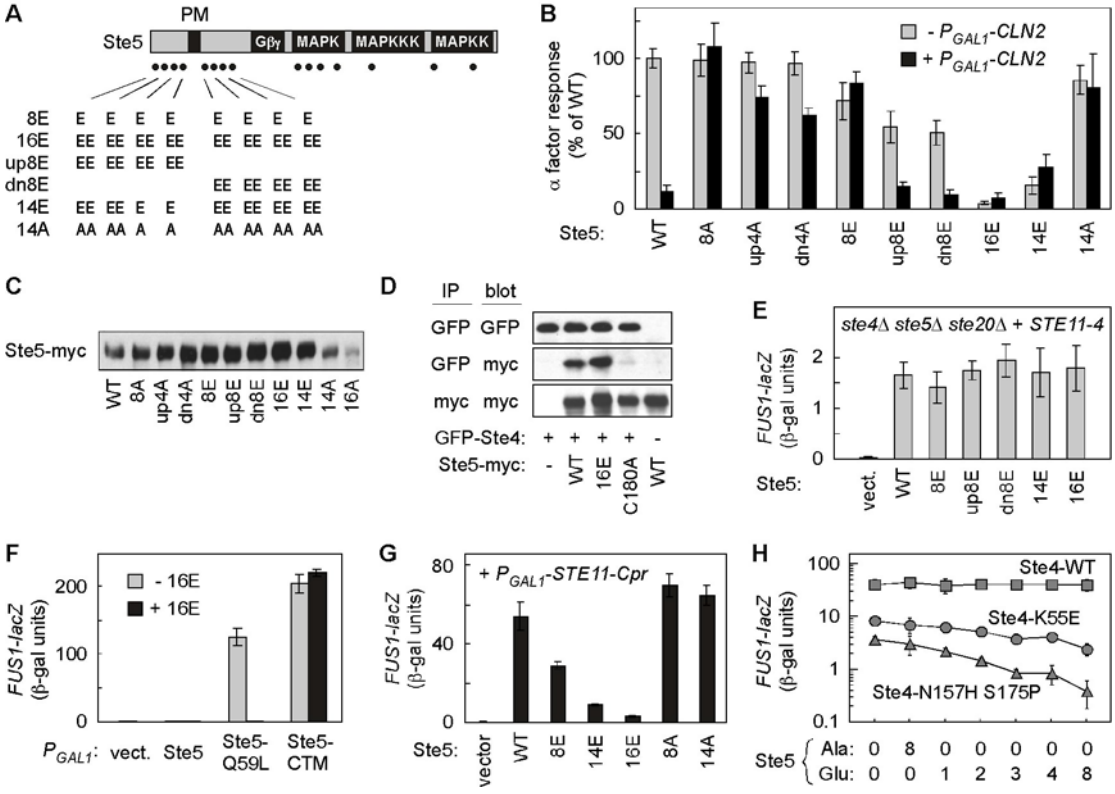
A
PM
Ste5
Gβγ
MAPK
MAPKKK
MAPKK
8E E E E E E E E E
16E EE EE EE EE EE EE EE EE
up8E EE EE EE EE
dn8E EE EE EE EE
14E EE EE E E EE EE EE EE
14A AA AA A A AA AA AA AA
B
α factor response (% of WT)
- P_GAL1-CLN2
+ P_GAL1-CLN2
Ste5: WT 8A up4A dn4A 8E up8E dn8E 16E 14E 14A
C
Ste5-myc
WT 8A up4A dn4A 8E up8E dn8E 16E 14E 14A 16A
D
IP blot
GFP GFP
GFP myc
myc myc
GFP-Ste4: + + + + -
Ste5-myc: - WT 16E C180A WT
E
ste4Δ ste5Δ ste20Δ + STE11-4
FUS1-lacZ (β-gal units)
Ste5: vect. WT 8E up8E dn8E 14E 16E
F
FUS1-lacZ (β-gal units)
- 16E
+ 16E
P_GAL1: vect. Ste5 Ste5-Q59L Ste5-CTM
G
+ P_GAL1-STE11-Cpr
FUS1-lacZ (β-gal units)
Ste5: vector WT 8E 14E 16E 8A 14A
H
FUS1-lacZ (β-gal units)
Ste4-WT
Ste4-K55E
Ste4-N157H S175P
Ste5 Ala: 0 8 0 0 0 0 0
Glu: 0 0 1 2 3 4 8

Figure 3-4. Strong inhibition of Ste5 signaling requires a large number of negative charges

(A) Glu replacement mutations at CDK sites. S/T residues were replaced with E or A, and SP/TP dipeptides were replaced with EE or AA, as indicated.

(B) Inhibition of Ste5 signaling is proportional to added negative charge. Ste5 mutants were tested for α factor response in *ste5*Δ cells ± P_{GAL1}-*CLN2*. Ste5 "up4A" and "dn4A" refer to Ala mutations at sites #1-4 and #5-8, respectively. Bars, *FUS1-lacZ* levels, relative to Ste5-WT (mean ± SD, n = 6).

(C) Anti-myc blot showing levels of Ste5-myc_{13} mutants expressed in *ste5*Δ cells.

(D) The Ste5-16E mutant can still bind Ste4. Extracts of *ste4*Δ *ste5*Δ cells coexpressing Ste5-myc and GFP-Ste4 (after 3 hr induction of P_{GAL1}-*GFP-STE4*) were analyzed by immunoprecipitation (IP) and immunoblotting (blot) as indicated. Ste5-C180A served as a control that is defective at binding Ste4 (Feng et al., 1998).

(E) Ste5 Glu mutants are competent to mediate basal signaling (i.e., no α factor) activated by Ste11-4 in *ste4*Δ *ste5*Δ *ste20*Δ cells. Bars, mean ± SD (n = 4).

(F) The 16E mutations only inhibit signaling that requires the Ste5 PM domain. *FUS1-lacZ* (mean ± SD, n = 3-6) was induced in *ste4*Δ *ste5*Δ cells (without α factor) by P_{GAL1}-driven expression of Ste5, Ste5-Q59L, or Ste5-CTM, each of which either contained the 16E mutations (+16E) or did not (-16E). Anti-GFP blots confirmed that protein levels were unaffected by the 16E mutations (data not shown).

(G) Glu mutants disrupt Gβγ-independent, membrane-localized signaling. Signaling (mean ± SD, n = 6) was activated in *ste4*Δ *ste5*Δ cells (without α factor) by coexpression of P_{GAL1}-*STE11-Cpr* with the indicated Ste5 derivatives.

(H) Ste5 derivatives containing various Ala or Glu mutations were coexpressed in *ste4*Δ *ste5*Δ cells with either Ste4-WT or Ste4 mutants (K55E or N157H S175P) that weaken Ste5 binding

(Leeuw et al., 1998; Winters et al., 2005). Response to α factor was measured (mean ± SD, n=6).

G1 CDK activity disrupts Ste5 membrane localization

Using a Ste5-GFP_{x3} fusion expressed at native levels (Winters et al., 2005), we found that P_{GAL1}-*CLN2* inhibited pheromone-induced membrane recruitment of Ste5-WT, but not Ste5-8A (Figure 3-6A). We also examined membrane localization mediated specifically by the Ste5 PM domain, in isolation from upstream factors (e.g., pheromone, Gβγ) or downstream signaling consequences (e.g., transcriptional induction, cell cycle arrest), by using the hyperactive Ste5 variant Ste5-Q59L (Winters et al., 2005). Expression of Cln2 displaced Ste5-Q59L from the plasma membrane (Figure 3-5A), and this effect was blocked by the 8A mutations (Ste5-Q59L+8A). Results were similar in strains lacking Ste20 or the MAPKs Fus3 and Kss1 (Figure 3-6B), ruling out any contribution from Cln2/CDK phosphorylation of Ste20 (Oehlen and Cross, 1998; Wu et al., 1998) or MAPK phosphorylation of Ste5 (Kranz et al., 1994; Flotho et al., 2004; Bhattacharyya et al., 2006). Because these experiments were performed in non-signaling strains, the effect of Cln2 was not due to a shift from G1-arrested cells to cycling cells. Thus, Cln2/CDK actively inhibits Ste5 membrane localization mediated by the PM domain.

To address whether these localization effects were due to added negative charge, we examined the Glu replacement mutations. In agreement with their signaling phenotypes (see Figure 3-4F), the 16E mutation disrupted membrane localization of Ste5-Q59L, which depends on the PM domain, but not Ste5-CTM, which is independent of the PM domain (Figure 3-5B). Furthermore, displacement of Ste5 can be ascribed to a local effect on the PM domain (rather than more global changes in Ste5), because Glu

mutations blocked membrane localization of N-terminal Ste5 fragments (Figure 3-5C). When membrane binding by an N-terminal fragment was enhanced using the Q59L mutation (Figure 3-5C, bottom), displacing it required greater negative charge (i.e., 16E, rather than 8E), suggesting that competition between attractive and repulsive interactions determines the net membrane affinity. Collectively, these results indicate that phosphorylation near the Ste5 PM domain disrupts plasma membrane binding.

Figure 3-5

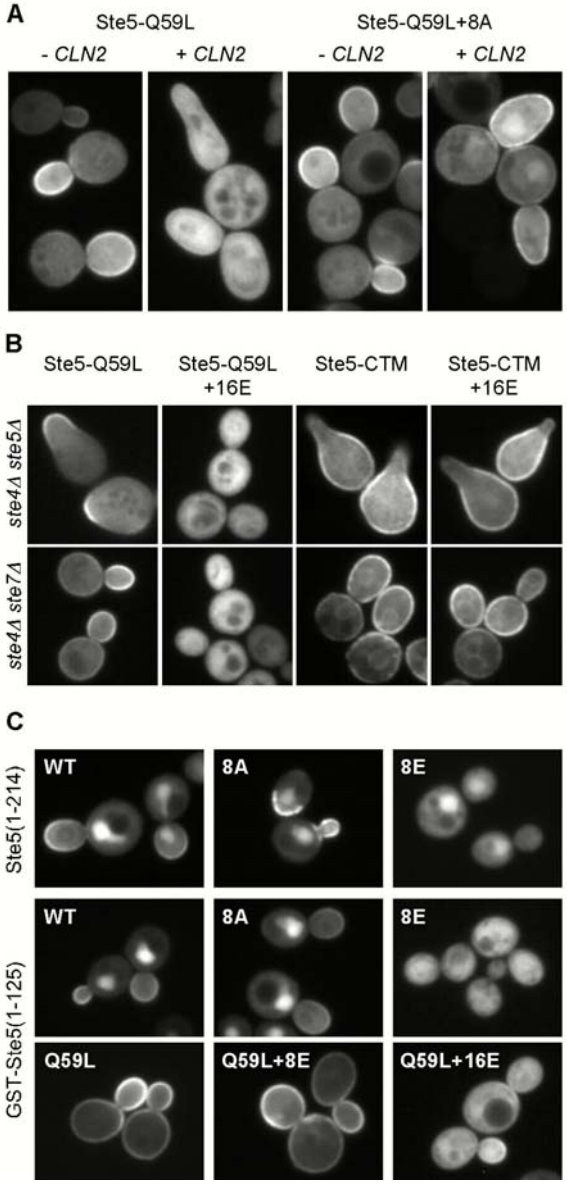
A
Ste5-Q59L
Ste5-Q59L+8A
- CLN2
+ CLN2
- CLN2
+ CLN2
B
Ste5-Q59L
Ste5-Q59L +16E
Ste5-CTM
Ste5-CTM +16E
ste4Δ ste5Δ
ste4Δ ste7Δ
C
Ste5(1-214)
GST-Ste5(1-125)
WT
8A
8E
WT
8A
8E
Q59L
Q59L+8E
Q59L+16E

Figure 3-5. Disruption of Ste5 membrane localization by G1 CDK activity or negative charge

(A) Localization of GFP-Ste5-Q59L ± 8A, expressed from the *GAL1* promoter in *ste4*Δ *ste7*Δ cells ± P_{GAL1}-*CLN2*. Note that hyperpolarized bud growth is due to Cln2 overexpression, not mating signaling. Also see Figure 3-6B.

(B) The 16E mutations disrupt Ste5 membrane localization mediated by the PM domain (Q59L), but not that mediated by a foreign transmembrane domain (CTM). Top, membrane localization induces mating pathway signaling, causing pear-shaped "shmoo" morphology. Bottom, localization results were similar in a non-signaling strain (*ste4*Δ *ste7*Δ).

(C) Negative charge disrupts membrane localization of Ste5 N-terminal fragments. Localization was compared (in *ste4*Δ *ste7*Δ cells) for WT and mutant derivatives of GFP-Ste5(1-214) and GST-GFP-Ste5(1-125), which can localize to the membrane in the absence of pheromone, Gβγ, and other Ste5 sequences (Winters et al., 2005).

Figure 3-6

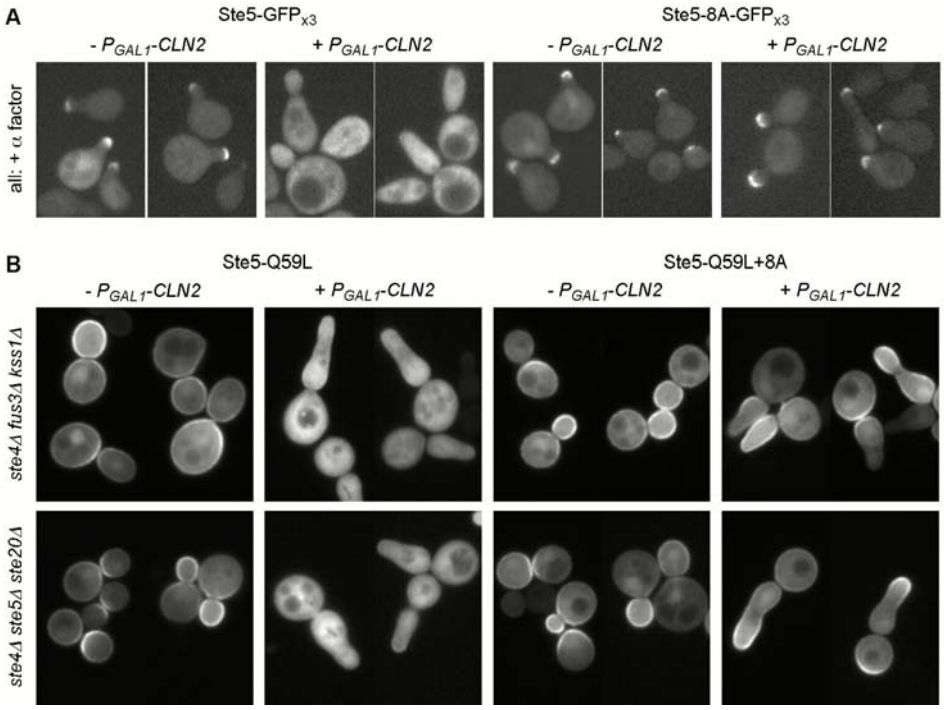
A
Ste5-GFP$_{x3}$
Ste5-8A-GFP$_{x3}$
- P_{GAL1}-CLN2
+ P_{GAL1}-CLN2
- P_{GAL1}-CLN2
+ P_{GAL1}-CLN2
all: + α factor
B
Ste5-Q59L
Ste5-Q59L+8A
- P_{GAL1}-CLN2
+ P_{GAL1}-CLN2
- P_{GAL1}-CLN2
+ P_{GAL1}-CLN2
ste4Δ fus3Δ kss1Δ
ste4Δ ste5Δ ste20Δ

Figure 3-6. Cln2 expression disrupts Ste5 membrane localization

(A) Cln2 inhibits pheromone-stimulated membrane recruitment of Ste5. A Ste5-GFP_{x3} fusion (Winters et al., 2005) and a derivative harboring the 8A mutations (Ste5-8A-GFP_{x3}) were each expressed from the native *STE5* promoter in *ste5*Δ cells ± P_{GAL1}-*CLN2*. Cells growing in 2% raffinose medium were induced with 2% galactose for 1 hr prior to pheromone treatment, then α factor (5 μM) was added for 1 hr (in the continued presence of galactose). After this time, an additional pulse of pheromone was applied by pelleting and resuspending cells in fresh medium (-Ura /raffinose/galactose) containing 20 μM α factor. Cells were then spotted onto microscope slides and visualized immediately.

(B) Localization of GFP-Ste5-Q59L and GFP-Ste5-Q59L+8A (each expressed from the *GAL1* promoter) was examined in the indicated strains ± P_{GAL1}-*CLN2*. As in Figure 3-5A, expression of Cln2 disrupts membrane localization of Ste5-Q59L and this effect is blocked by incorporation of the 8A mutations. The experiments here were performed in *ste4*Δ *ste5*Δ *ste20*Δ or *ste4*Δ *fus3*Δ *kss1*Δ cells, ruling out the possibility of indirect effects due to Cln2/CDK phosphorylation of Ste20 (Oehlen and Cross, 1998; Wu et al., 1998) or Fus3/Kss1 MAPK phosphorylation of Ste5 (Kranz et al., 1994; Flotho et al., 2004; Bhattacharyya et al., 2006).

Cln2-dependent phosphorylation of Ste5

To test if Cln2/CDK directly phosphorylates Ste5, we performed *in vitro* kinase assays. As a substrate we used a purified Ste5 fragment (residues 1-125) encompassing the PM domain and all eight N-terminal CDK sites. Purified Cln2/Cdc28 phosphorylated the wild type Ste5 fragment, and this was severely reduced by the 8A or 8E mutations (Figure 3-7A). Thus, the N-terminus of Ste5 can serve as a direct Cln2/CDK substrate, and the CDK sites are required for phosphorylation.

In vivo, Cln2 overexpression promoted phosphorylation of Ste5, as evidenced by reduced electrophoretic mobility (Figure 3-7B) that was reversed by subsequent phosphatase treatment (Figure 3-7C). This agrees with a previous report that the phosphorylation status of Ste5 *in vivo* depends on Cdc28 (Flotho et al., 2004). The Ste5 mobility shift was consistent with multiply phosphorylated forms, as it was comparable to the Ste5-16E mutant, which mimics phosphorylation at all 8 N-terminal sites (Figure 3-7B). Furthermore, the effect of Cln2 on Ste5 mobility required the N-terminal CDK sites, because Ste5-8A and Ste5-16E were unaltered by Cln2 (Figure 3-7B). Results were similar in strains lacking Fus3 and Kss1 (Figure 5B, bottom), ruling out any contribution from Ste5-affiliated MAPKs (which can also phosphorylate SP/TP motifs). Unlike Cln2, overexpression of other cyclins (i.e., Cln3, Clb5, or Clb2) did not alter Ste5 mobility (Figure 3-7D), which agrees with their inability to inhibit pheromone signaling (Oehlen and Cross, 1994; Oehlen et al., 1998). Thus, Ste5 is a specific substrate of Cln2/CDK activity *in vivo*, and the relevant phosphorylation sites correspond to those that allow Cln2 to regulate Ste5 signaling.

Next, we wished to follow cell cycle-dependent changes in Ste5 phosphorylation, but our efforts were hindered by the low fraction of Ste5 showing a clear mobility shift. While a technical issue could be partly to blame (e.g., phosphatase activity in cell lysates), we wondered if Ste5 molecules in different subcellular locales might be modified to different extents. Indeed, when Ste5 was restricted to the cytoplasm by using the "ΔNLS" allele (Winters et al., 2005), Cln2 expression could modify nearly all Ste5 molecules (Figures 3-7D and 3-7E). In other respects phosphorylation of $Ste5^{\Delta NLS}$ resembled that of wild-type Ste5, including a specific requirement for Cln2 and for the 8 N-terminal CDK sites (Figures 3-7D and 3-7E). Exploiting these favorable detection properties, we saw that $Ste5^{\Delta NLS}$ phosphorylation was elevated in cells arrested immediately after Start (*cdc4*, *cdc53*, or *cdc34*), but not when Cln1/2 were absent (*cdc34 cln1 cln2*) or in cells arrested in G1 (*cdc28-4*, *cdc28-13*) (Figure 3-7F). Furthermore, in synchronous cultures, phosphorylation of $Ste5^{\Delta NLS}$ fluctuated during the cell cycle, peaking at the onset of budding (Figure 3-7G). Thus, modification of the N-terminal CDK sites in Ste5 occurs as cells pass Start.

Figure 3-7

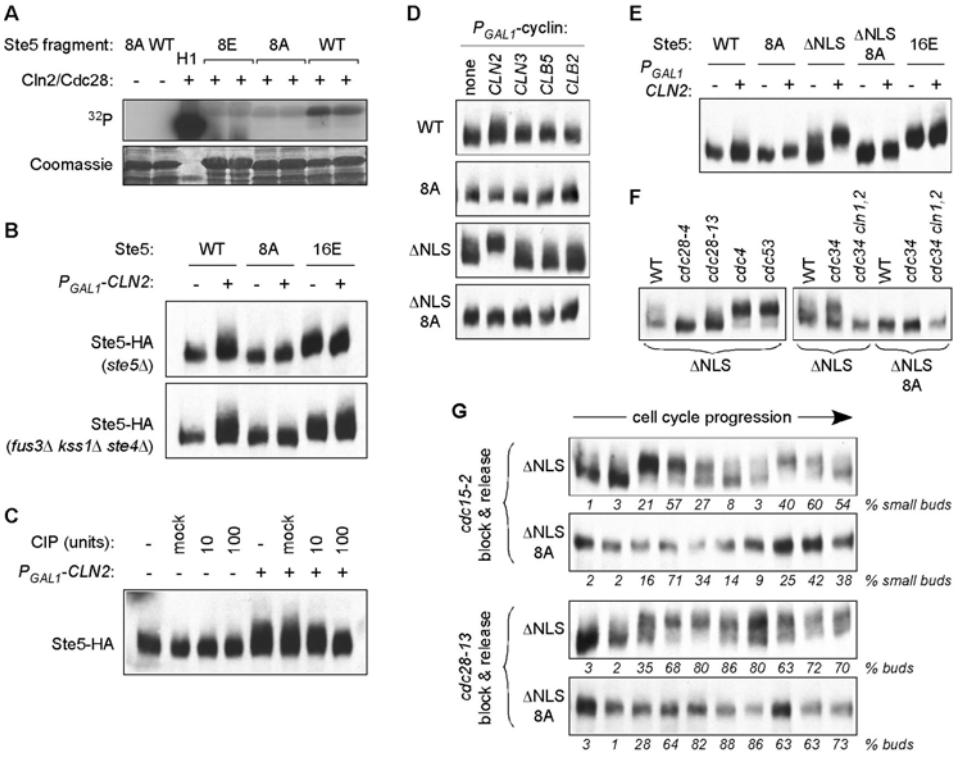
A
Ste5 fragment: 8A WT H1 8E 8A WT
Cln2/Cdc28: - - + + + + + + +
32P
Coomassie
B
Ste5: WT 8A 16E
PGAL1-CLN2: - + - + - +
Ste5-HA (ste5Δ)
Ste5-HA (fus3Δ kss1Δ ste4Δ)
C
CIP (units): - mock 10 100 - mock 10 100
PGAL1-CLN2: - - - - + + + +
Ste5-HA
D
PGAL1-cyclin:
none CLN2 CLN3 CLB5 CLB2
WT
8A
ΔNLS
ΔNLS 8A
E
Ste5: WT 8A ΔNLS ΔNLS 8A 16E
PGAL1 CLN2: - + - + - + - + - +
F
WT cdc28-4 cdc28-13 cdc4 cdc53 WT cdc34 cdc34 cln1,2 WT cdc34 cdc34 cln1,2
ΔNLS
ΔNLS
ΔNLS 8A
G
cell cycle progression
cdc15-2 block & release
ΔNLS
1 3 21 57 27 8 3 40 60 54 % small buds
ΔNLS 8A
2 2 16 71 34 14 9 25 42 38 % small buds
cdc28-13 block & release
ΔNLS
3 2 35 68 80 86 80 63 72 70 % buds
ΔNLS 8A
3 1 28 64 82 88 86 63 63 73 % buds

Figure 3-7. Phosphorylation of Ste5 by Cln2/CDK

(A) Phosphorylation of the Ste5 N-terminus by Cln2/Cdc28 *in vitro*. Bacterially-expressed GST-Ste5$^{1-125}$ fusions (WT, 8A, and 8E) were phosphorylated by recombinant Cln2-Cdc28. Histone H1 served as a control substrate.

(B) Cln2 expression *in vivo* alters Ste5 electrophoretic mobility. HA-tagged Ste5 (WT, 8A, and 16E) was immunoprecipitated from the indicated strains after 3 hr galactose induction (to express Cln2), resolved by SDS-PAGE, and analyzed by anti-HA immunoblot.

(C) The Ste5 mobility shift is due to phosphorylation. Ste5-HA_3 was immunoprecipitated from *ste5*Δ ± P_{GAL1}-*CLN2* strains, and treated with calf intestinal phosphatase (CIP).

(D) Effects on Ste5 mobility are specific to Cln2. Ste5-HA_3 derivatives (WT, 8A, ΔNLS, ΔNLS+8A) were analyzed as in panel B, using various P_{GAL1}-cyclin strains.

(E) Ste5$^{\Delta NLS}$ is more fully modified by Cln2. Ste5-HA_3 derivatives were analyzed as in B.

(F) Ste5$^{\Delta NLS}$ modification is elevated after Start and requires Cln1/2. WT and mutant strains ("*cln1,2*" = *cln1 cln2*) expressing Ste5-HA_3 (ΔNLS or ΔNLS+8A) were incubated for 3 hr at 37˚C.

(G) Modification of the Ste5 N-terminus is cell cycle dependent. Cells (*cdc15-2* or *cdc28-13*) harboring Ste5-HA_3 (ΔNLS or ΔNLS+8A) were arrested at 37˚C for 3 hr, then transferred to 25˚C to resume cycling. Samples were collected at 20 min intervals (0-180 min). As *cdc15* cells arrest with large buds, emergence of small buds was used to follow cell cycle progression (c.f., Figure 3-3D).

In panels B-G, Ste5-HA_3 derivatives were expressed from the native *STE5* promoter.

CDK-resistant signaling causes aberrant cell cycle arrest

To ask why it is beneficial to inhibit pheromone signaling as cells pass Start, we explored the physiological consequences of CDK-resistant Ste5 mutants. First, we examined the G1 specificity of pheromone arrest. Unlike wild-type cells, which arrested uniformly in G1, a significant fraction of *STE5-8A* cells (~15%) arrested at a post-Start stage with 2N DNA content (Figure 3-8A). The Ste5-8A phenotype was dominant to wild type, and an increasing fraction of 2N arrest was observed as more CDK sites were removed from Ste5 (Figure 3-8B), suggesting that it reflects ectopic (non-G1) signaling by CDK-resistant Ste5 (rather than a leaky G1 arrest). Indeed, the post-Start arrest phenotype required the *STE5-8A* cells to be cycling at the time of pheromone addition, and was not observed when pheromone was added to a uniform population of G1 cells (Figures 3-8C and 3-9). Also, pheromone treatment of cycling *STE5-8A* cells induced a unique morphology in which mating projections appeared to emanate from cell buds (Figures 3-8C and 3-10), suggesting that signaling responses occurred during the budding phase of the cell cycle. Remarkably, elimination of only one or two CDK sites in Ste5 caused a measurable increase in 2N arrest (Figure 3-8B), showing that full inhibition of Ste5 via multiple CDK sites serves a physiologically important function. Accordingly, expression of Ste5-8E, which mimics the addition of 4 phosphates but cannot be inhibited further by Cln2/CDK, also allowed a substantial level of 2N arrest. We conclude that a failure of G1 CDKs to downregulate the mating MAP kinase pathway is detrimental, as it allows pheromone to arrest cells at an inappropriate cell cycle stage.

Because *STE5-8A* cells can arrest at either G1 or post-Start stages, the percentage

that arrest at the latter stage (usually ~15% 2N) likely reflects the fraction of cells in the asynchronous culture that were between the two arrest points. Indeed, when pheromone was added to *STE5-8A* cultures at different times after leaving G1, the level of 2N arrest roughly correlated with the fraction of the initial cell population that were in S phase (Figure 3-9). Hence, cells outside this susceptible window likely arrest in G1. Consistent with this view, the majority of *STE5-8A* cells could be trapped at the 2N stage when G1 arrest mechanisms were bypassed. Specifically, overexpression of the B-type cyclin Clb5 can push cells through Start even in the presence of pheromone, thereby making wild-type cells pheromone-resistant ((Oehlen et al., 1998) and references therein). In *STE5-8A* cells, however, Clb5 overexpression could still push cells through Start but the cells arrested in response to pheromone, and did so almost entirely at the 2N stage (Figure 3-8D). Therefore, signaling by CDK-resistant Ste5 has a dangerous potential to disrupt events during a post-Start window of the cell cycle.

CDK-resistant Ste5 permits Far1-independent arrest

To further explore the consequences of CDK-resistant signaling, we tested the role of Far1, which is ordinarily required for pheromone-induced arrest (Chang and Herskowitz, 1990). Strikingly, the CDK-resistant Ste5-8A mutant restored pheromone arrest to *far1*Δ cells (Figure 3-8E). Removal of as few as one or two CDK sites in Ste5 allowed significant suppression of the *far1*Δ arrest defect, with stronger suppression as more sites were removed (Figures 3-8F and 3-11A). Thus, Far1 becomes dispensable when Ste5 signaling cannot be inhibited. Indeed, *far1*Δ cells could be arrested (Figure 3-

8G) by activating the mating pathway with CDK-resistant constructs (P_{GAL1}-*STE5-Q59L+8A*, P_{GAL1}-*STE5-CTM*), but not with CDK-sensitive constructs (P_{GAL1}-*STE4*, P_{GAL1}-*STE5-Q59L*). Far1-independent arrest has been observed in previous studies but remains poorly understood (Chang and Herskowitz, 1990; Valdivieso et al., 1993; Tyers, 1996; Oehlen et al., 1998; Cherkasova et al., 1999). Our results indicate that pheromone signaling is capable of robust growth arrest without Far1, but this is masked in *far1*Δ cells because the absence of Far1 allows Cln/CDK to downregulate Ste5.

Pheromone signaling in *far1*Δ *STE5-8A* cells caused arrest at more than one stage, because treated cultures showed a heterogeneous mix of 1N and 2N cells (Figure 3-8H and 3-11B), as well as unbudded and budded cells (data not shown), despite an immediate cessation of proliferation (Figure 3-11C). The G1 arrest appeared somewhat leaky and could be counteracted by G1 CDK activity (Figure 3-11B). Most notably, Far1 proved entirely dispensable for the post-Start arrest, because the near-uniform 2N arrest seen in *STE5-8A* cells overexpressing Clb5 (Figure 3-8D) was independent of Far1 (Figure 3-8H). Altogether, our results indicate that CDK-resistant signaling by Ste5-8A can impede cell cycle progression of both G1 and post-Start cells in a Far1-independent manner. Therefore, cell cycle control of Far1 (McKinney et al., 1993; Henchoz et al., 1997) is not sufficient for cells to escape the arrest effects of pheromone, and instead downregulation of Ste5 is also critical.

Figure 3-8

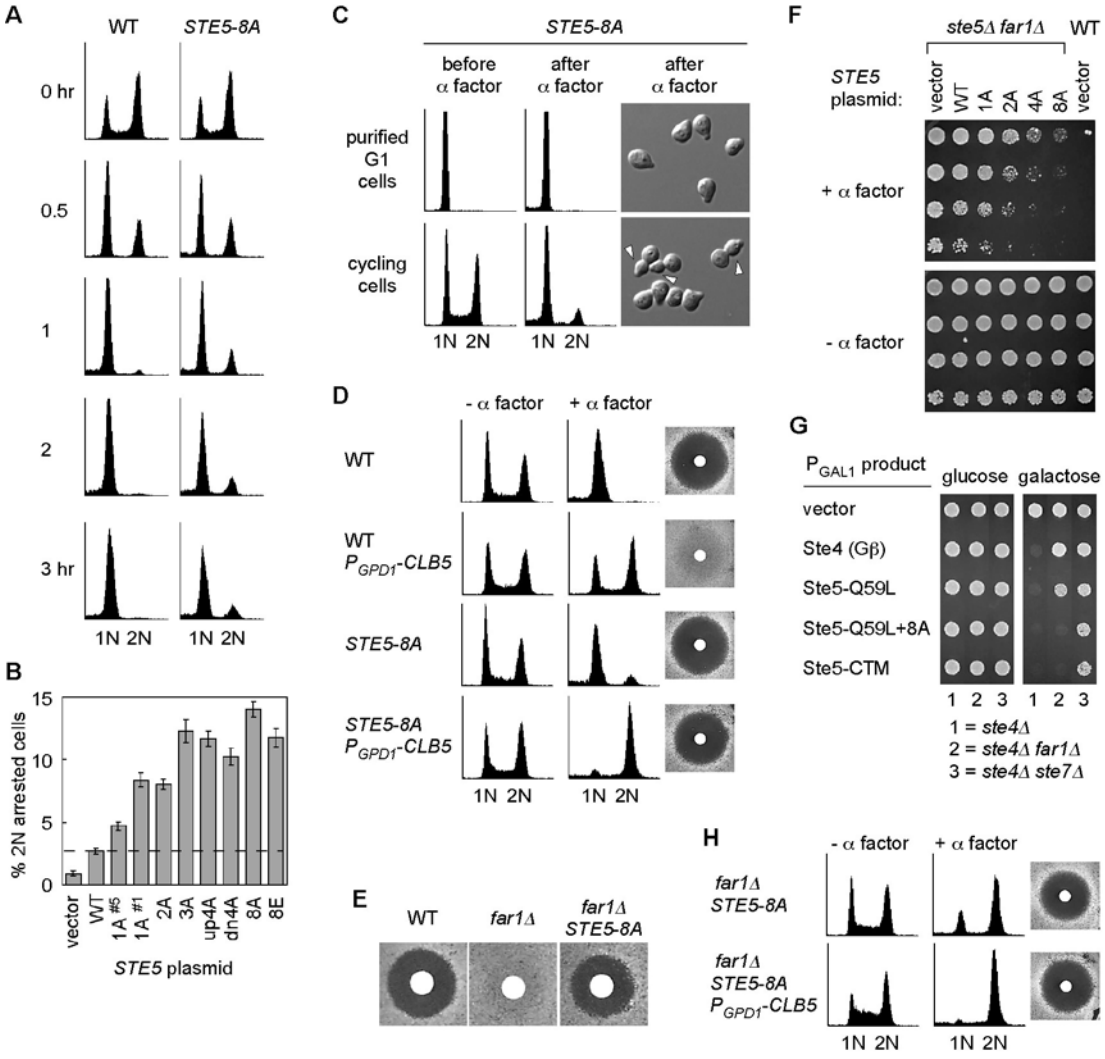
A
WT
STE5-8A
0 hr
0.5
1
2
3 hr
1N 2N
1N 2N
B
% 2N arrested cells
15
10
5
0
vector
WT
1A #5
1A #1
2A
3A
up4A
dn4A
8A
8E
STE5 plasmid
C
STE5-8A
before α factor
after α factor
after α factor
purified G1 cells
cycling cells
1N 2N
1N 2N
D
- α factor
+ α factor
WT
WT PGPD1-CLB5
STE5-8A
STE5-8A PGPD1-CLB5
1N 2N
1N 2N
E
WT
far1Δ
far1Δ STE5-8A
F
ste5Δ far1Δ
WT
STE5 plasmid:
vector
WT
1A
2A
4A
8A
vector
+ α factor
- α factor
G
PGAL1 product
glucose
galactose
vector
Ste4 (Gβ)
Ste5-Q59L
Ste5-Q59L+8A
Ste5-CTM
1 2 3 1 2 3
1 = ste4Δ
2 = ste4Δ far1Δ
3 = ste4Δ ste7Δ
H
- α factor
+ α factor
far1Δ STE5-8A
far1Δ STE5-8A PGPD1-CLB5
1N 2N
1N 2N

Figure 3-8. CDK-resistant Ste5 allows aberrant arrest

(A) Pheromone arrests some *STE5-8A* cells at a post-Start (2N) stage. Cells were treated with α factor for the indicated times. FACS profiles show DNA content.

(B) The post-Start arrest phenotype is dominant and reflects the level of CDK-resistance of Ste5. Wild type cells harboring *STE5* plasmids ($1A^{\#5}$ = site #5; $1A^{\#1}$ = site #1; 2A = sites #5-6) were treated with α factor for 3.25 hrs. The percent of cells with 2N DNA content was quantified by FACS (mean ± SD; n = 4). The dashed line marks the %2N value observed when the *STE5-WT* plasmid is present in wild-type cells.

(C) G1 phase *STE5-8A* cells were purified by centrifugal elutriation, and treated with α factor either immediately or after cells resumed cycling. Arrest phenotypes were then compared. See Figures 3-9 and 3-10 for the complete data set. *Arrowheads*, cell buds with α factor-induced projections.

(D) *STE5-8A* allows near-uniform 2N arrest when G1 arrest is bypassed using P_{GPD1}-*CLB5*. *Left*, DNA content of cells after 3 hr ± α factor. *Right*, halo assays showing growth arrest by α factor.

(E) Halo assays showing that *STE5-8A* restores pheromone arrest to *far1*Δ cells.

(F) Suppression of the *far1*Δ arrest defect increases as more CDK sites are eliminated from Ste5. Fivefold serial dilutions of strains harboring *STE5* plasmids (1A = site #5; 2A = sites #5-6; 4A = sites #1-4) were incubated on –Ura plates ± 1 μM α factor.

(G) Pathway activation by CDK-resistant constructs causes Far1-independent arrest. Deletion strains harboring P_{GAL1}-regulated activators of the mating pathway were grown on –Ura glucose or galactose plates.

(H) The post-Start arrest triggered by Ste5-8A signaling is independent of Far1. The indicated strains were analyzed in parallel with those in panel D.

Figure 3-9

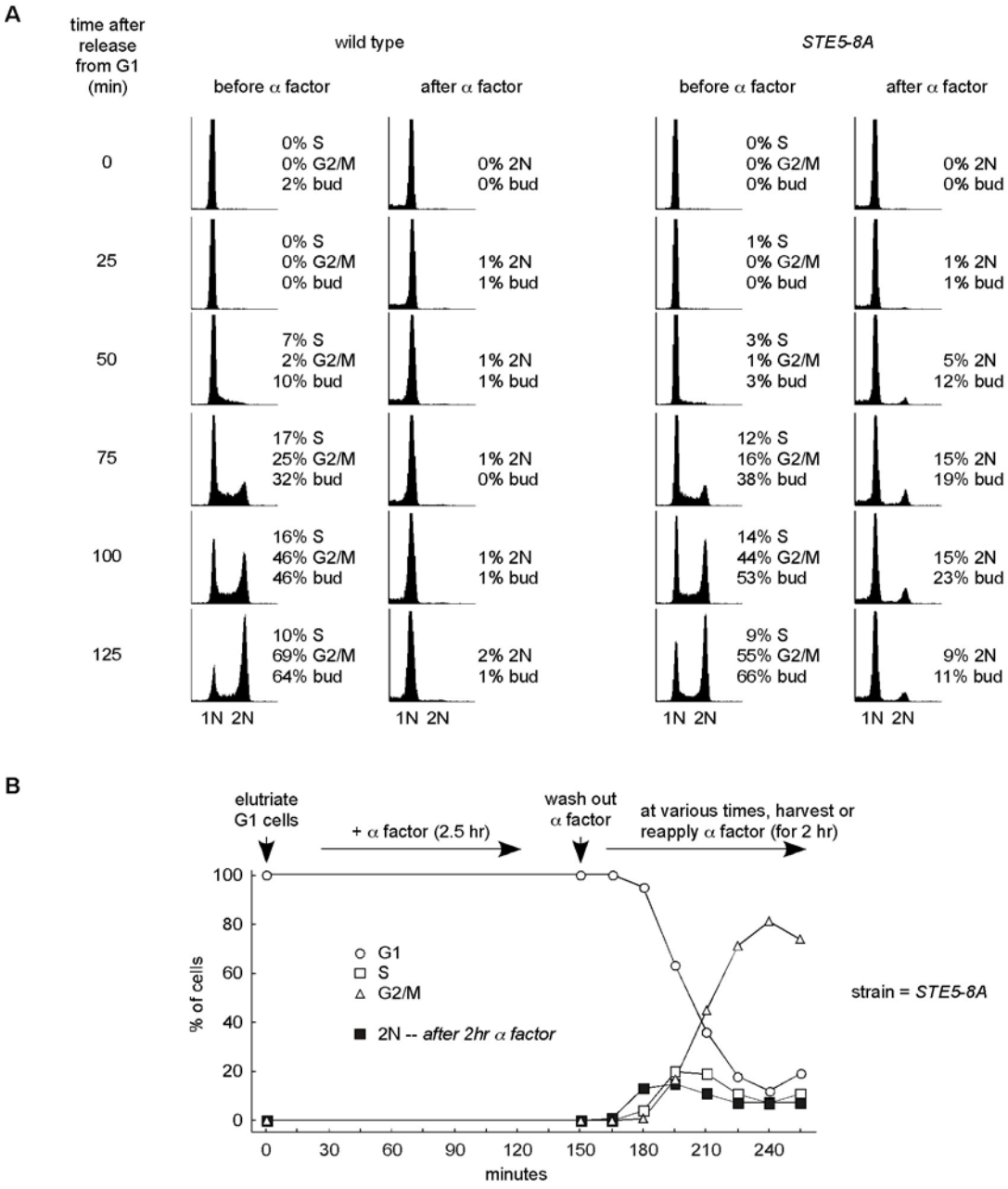
A
time after release from G1 (min)
wild type
STE5-8A
before α factor
after α factor
before α factor
after α factor
0
0% S
0% G2/M
2% bud
0% 2N
0% bud
0% S
0% G2/M
0% bud
0% 2N
0% bud
25
0% S
0% G2/M
0% bud
1% 2N
1% bud
1% S
0% G2/M
0% bud
1% 2N
1% bud
50
7% S
2% G2/M
10% bud
1% 2N
1% bud
3% S
1% G2/M
3% bud
5% 2N
12% bud
75
17% S
25% G2/M
32% bud
1% 2N
0% bud
12% S
16% G2/M
38% bud
15% 2N
19% bud
100
16% S
46% G2/M
46% bud
1% 2N
1% bud
14% S
44% G2/M
53% bud
15% 2N
23% bud
125
10% S
69% G2/M
64% bud
2% 2N
1% bud
9% S
55% G2/M
66% bud
9% 2N
11% bud
1N 2N
1N 2N
1N 2N
1N 2N
B
elutriate G1 cells
+ α factor (2.5 hr)
wash out α factor
at various times, harvest or reapply α factor (for 2 hr)
100
80
60
40
20
0
% of cells
G1
S
G2/M
2N -- after 2hr α factor
strain = STE5-8A
0
30
60
90
120
150
180
210
240
minutes

Figure 3-9. Only cycling *STE5-8A* cells are susceptible to the post-Start arrest

(A) G1 phase wild type and *STE5-8A* cells were purified by centrifugal elutriation, and then inoculated into YPD growth medium and incubated at 30˚C. At various times afterward, aliquots were removed and split in two. One half was fixed immediately (before α factor), and the other half was treated with α factor (1 μM) for 2 hours prior to fixation (after α factor). FACS profiles from cycling cells were used to determine boundaries for the assignment of cells into G1 (1N), G2/M (2N), and S phase (between 1N and 2N). The same boundaries were then applied to all profiles in the data set, to quantify the percentage of cells in S or G2/M before α factor treatment and the percentage of cells arrested at the post-Start (2N) stage after α factor treatment. The percentage of budded cells (% bud) was scored visually (n = 400). Note that the budded cells in α factor-treated *STE5-8A* cultures display an unique morphology (see Figure 3-10).
(B) *STE5-8A* cells in G1 phase were purified by elutriation, inoculated into YPD growth medium, and immediately treated with 0.1 μM α factor for 2.5 hrs at 30˚C. The α factor was washed out to allow cells to resume cycling, and then at 15 min intervals aliquots of cells were collected, half of which was fixed immediately and the other half re-treated with α factor for 2 hr. FACS was used to quantify the percentage of cells in the G1, S and G2/M phases of the cell cycle before reapplication of α factor (*open symbols*) as well as the percent of cells arrested at the 2N stage 2 hr after reapplication of α factor (*closed symbols*).

Both panels A and B show the following: (i) the post-Start (2N) arrest was observed only when pheromone was added to *STE5-8A* cells that had begun to leave G1; and (ii) the amount of 2N arrest roughly correlated with the percentage of cells in S phase, rather than G1 or G2/M, suggesting that the cell cycle window in which cells are susceptible to the post-Start arrest roughly overlaps S phase. Results in panel B make the following additional points: (i) the uniform G1 arrest seen when elutriated *STE5-8A* cells are treated with α factor is stable for up to 4.5 hours

(i.e. the filled square at 150 min. represents elutriated G1 cells treated for 2.5 hours, then immediately re-treated for an additional 2 hours); and (ii) the similar results seen when using freshly elutriated G1 cells (panel A) or cells held in G1 for a prolonged period by α factor arrest (panel B) argues that *STE5-8A* cells become susceptible to post-Start arrest only as a result of leaving G1, and not as a result of fulfilling a minimum incubation time after elutriation.

Figure 3-10

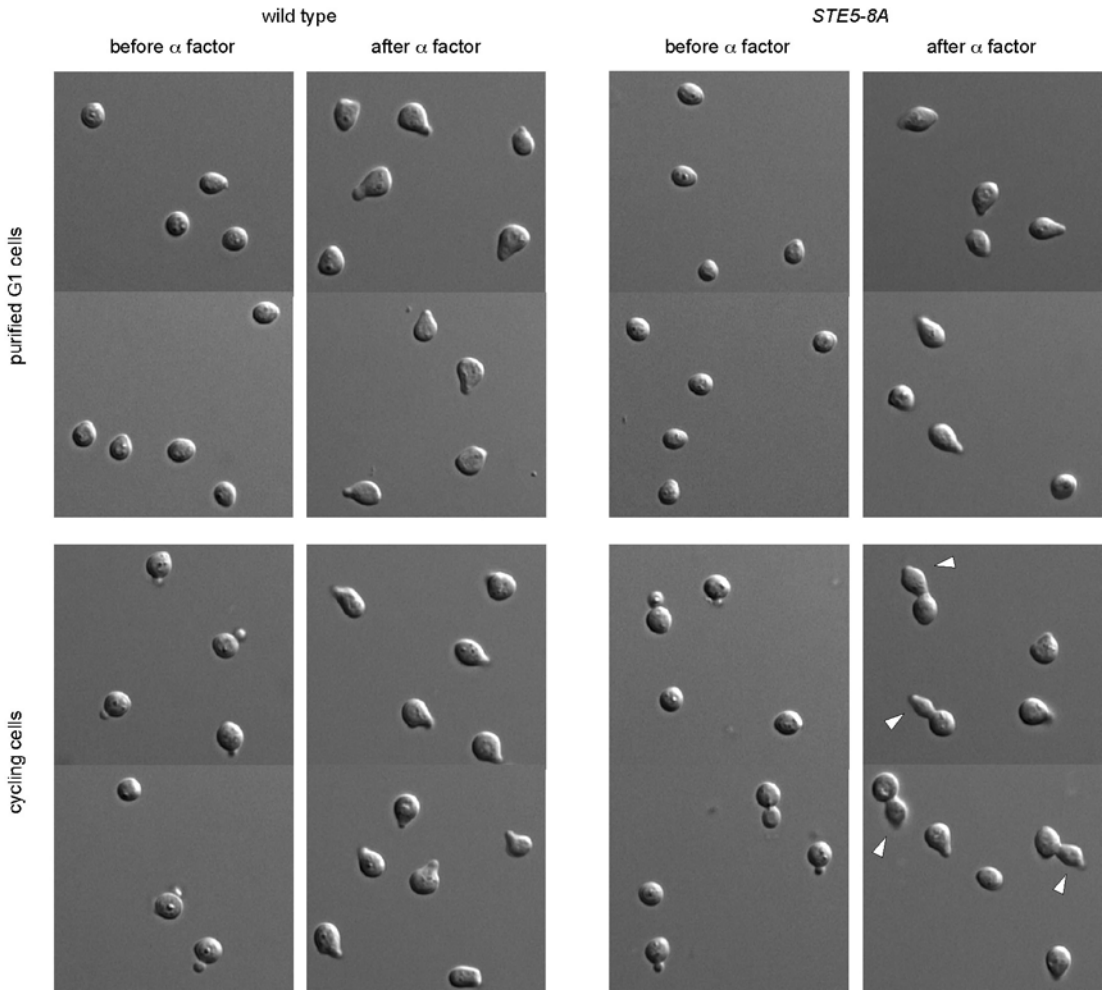
wild type
STE5-8A
before α factor
after α factor
before α factor
after α factor
purified G1 cells
cycling cells

Figure 3-10. Pheromone treatment of cycling *STE5-8A* cells induces a unique morphology

These images show examples of cell morphology from the experiments in Figure 3-9A. Specifically, cells are shown before and after α factor treatment of cultures that had been released from G1 for 0 min (purified G1 cells) or 100 min (cycling cells). Note that α factor treatment of cycling *STE5-8A* cultures caused some cells to adopt an unusual morphology in which buds contained pointed projections (arrowheads), suggesting that they responded to pheromone while budding. Presumably, these are the cells that arrested with 2N DNA content (see Figure 3-9A), whereas the unbudded shmoo cells represent those that arrested in G1. Also note that the unusual morphology was not observed in wild-type cells or when *STE5-8A* cells in G1 were treated with α factor.

Figure 3-11

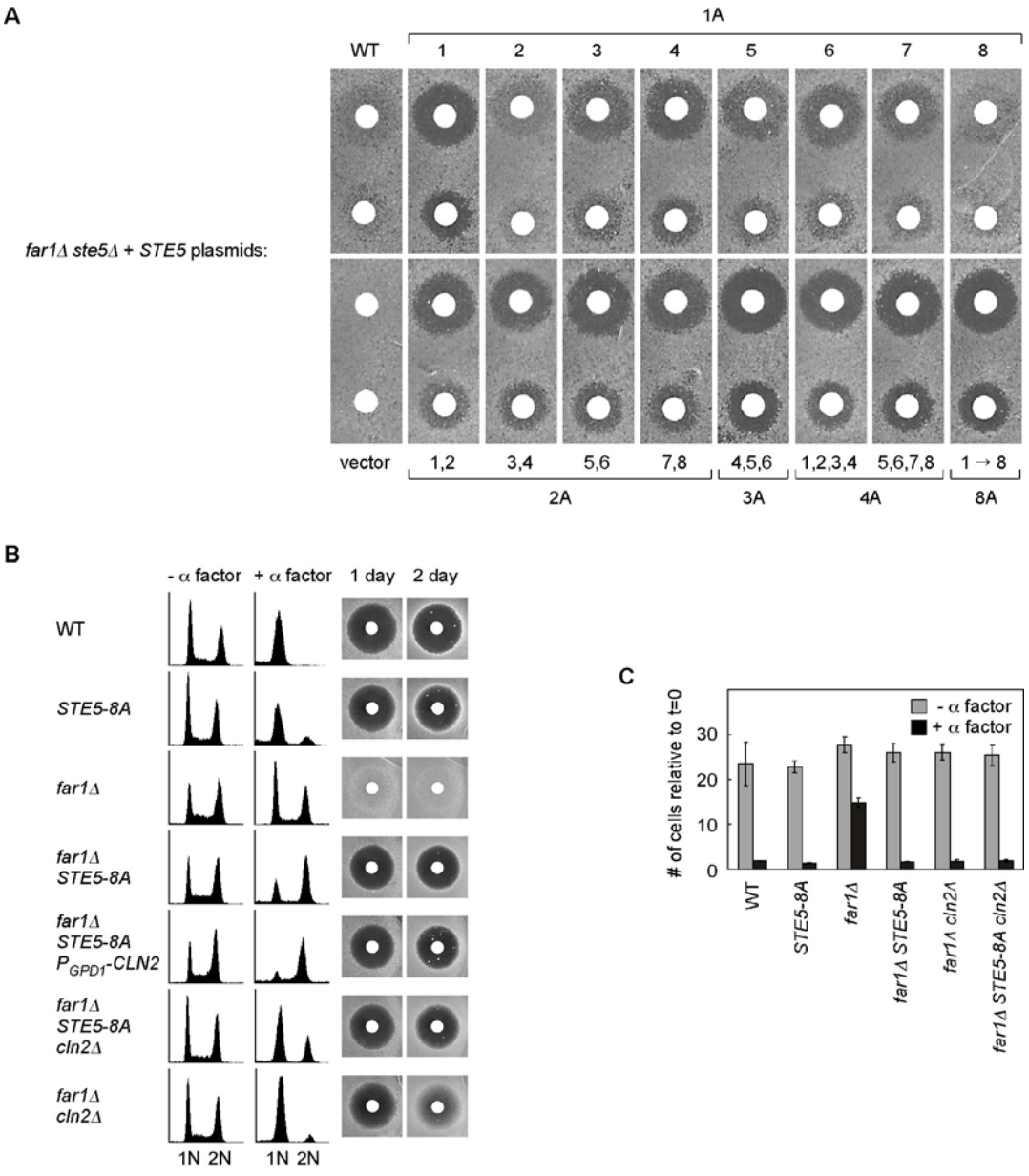
A
1A
WT
1
2
3
4
5
6
7
8
far1Δ ste5Δ + STE5 plasmids:
vector
1,2
3,4
5,6
7,8
4,5,6
1,2,3,4
5,6,7,8
1 → 8
2A
3A
4A
8A
B
- α factor
+ α factor
1 day
2 day
WT
STE5-8A
far1Δ
far1Δ STE5-8A
far1Δ STE5-8A P_GPD1-CLN2
far1Δ STE5-8A cln2Δ
far1Δ cln2Δ
1N 2N
1N 2N
C
# of cells relative to t=0
- α factor
+ α factor
0
10
20
30
WT
STE5-8A
far1Δ
far1Δ STE5-8A
far1Δ cln2Δ
far1Δ STE5-8A cln2Δ

Figure 3-11. CDK-resistant Ste5 allows Far1-independent arrest

(A) Suppression of the *far1*Δ arrest defect increases as more CDK sites are removed from Ste5. Lawns of *ste5*Δ *far1*Δ cells harboring vector, Ste5-WT, or the indicated Ste5-Ala mutants were plated on –Ura plates and overlaid with filter disks containing 20 μl of 1 mM (top) or 200 μM (bottom) α factor. Note that the suppression of the *far1*Δ defect parallels their resistance to Cln2/CDK inhibition (see Figure 3-2E). Specifically, there is increasingly stronger *far1*Δ suppression as more CDK sites are eliminated, and the effects of single Ala mutations in both assays are strongest at site #1 and weakest at sites #2 and #8. These results suggest that *far1*Δ suppression results directly from the CDK resistance of Ste5 signaling.

(B) Disrupting Cln2/CDK regulation of Ste5 allows pheromone to arrest both G1 and post-Start (2N) cells in the absence of Far1. *Left*, FACS profiles show DNA content of cells after 3 hours ± 1 μM α factor. *Right*, growth arrest of the same strains exposed to α factor for 1 or 2 days at 30°C. Note that in pheromone-treated *far1*Δ *STE5-8A* cultures, the relative proportion of 1N versus 2N arrested cells could be altered by varying the gene dosage of *CLN2*. Given the role of Cln2 in promoting exit from G1, the observed pattern suggests that the Far1-independent G1 arrest is somewhat leaky and can be counteracted by elevated Cln/CDK activity or stabilized by reducing Cln/CDK activity, whereas the post-Start arrest remains intact. As noted previously (Chang and Herskowitz, 1990), *far1*Δ *cln2*Δ cells could arrest in response to pheromone and did so predominantly in G1, though the long-term maintenance of growth arrest was more stable and the proportion of 2N cells was higher in *far1*Δ *STE5-8A cln2*Δ cells, suggesting that in the *far1*Δ *cln2*Δ cells Ste5 can be inhibited by other G1 cyclins (e.g., Cln1; (Oehlen and Cross, 1994)).

(C) Pheromone triggers an immediate cessation of proliferation in strains that show Far1-independent arrest. Cultures were split in two and incubated for 6 hours either with or without 1μM α factor. Cell numbers were counted using a hemacytometer, and compared to the number

of cells in the original culture immediately prior to the split (t = 0). The ratio is shown on the y-axis (mean ± SD, n = 3). Note that, in strains where the *far1*Δ arrest defect is suppressed (see panel B), the immediacy of α factor-induced growth arrest is comparable to wild-type cells.

Discussion Chapter III

Mechanism for cell cycle regulation of MAP kinase cascade signaling

In this study we define a mechanism by which G1 CDKs inhibit signaling through the yeast mating MAP kinase cascade. We show that the MAP kinase cascade scaffold protein Ste5 is the target of this inhibition, and that G1 CDK activity inhibits signaling by phosphorylating sites flanking a membrane-binding domain in Ste5. Our findings support a model in which these negatively-charged phosphates disrupt Ste5 membrane association by electrostatic interference (Figure 3-12A). Hence, through the use of two weak interactions that cooperatively control its membrane recruitment, Ste5 serves as an integration point for both external and internal regulatory cues (Figure 3-12B), such that signaling is activated only when two conditions are satisfied—i.e., when pheromone is present and the cell cycle stage is appropriate. The physiological benefit of this arrangement is that it restricts pheromone arrest to G1, thus preventing inappropriate disruption of cell cycle progression in cells that have passed Start.

The regulatory CDK sites in Ste5 lie in sequences flanking the PM domain that are dispensable for its normal signaling role ((Winters et al., 2005); see also Figure 3-3B), and are predicted to be mostly random coil (Figure 3-13). Hence, rather than affecting a specific tertiary structure, the phosphorylated N-terminus of Ste5 may behave as an unstructured electronegative mass, making juxtaposition to its target energetically unfavorable. This mode of regulation may be generally applicable where phosphorylation serves to disrupt interactions. Phosphorylation of Ste5 provides a variation of

"electrostatic switch" mechanisms seen in other signaling proteins such as Src or MARCKS, where membrane interactions are disrupted by phosphorylation within a membrane-binding domain (McLaughlin and Aderem, 1995). In Ste5, the use of sites distal to the membrane-binding domain may impose a requirement for multiple phosphorylations, which is likely to be advantageous to the regulatory circuit (see below).

Figure 3-12

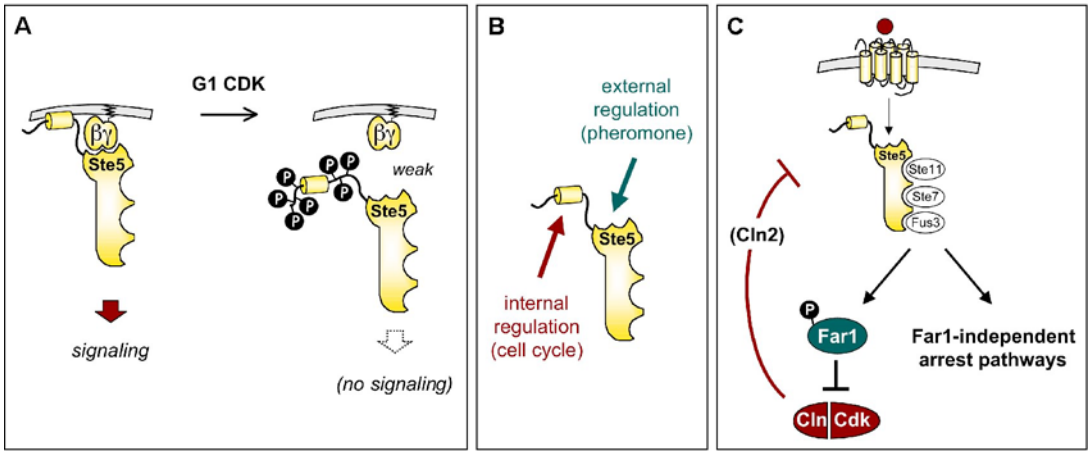
A
G1 CDK
βγ
Ste5
signaling
weak
(no signaling)
B
external
regulation
(pheromone)
internal
regulation
(cell cycle)
C
Ste11
Ste7
Fus3
(Cln2)
Far1
Far1-independent
arrest pathways
Cln
Cdk

Figure 3-12. Model for G1 CDK inhibition of Ste5 signaling

(A) As cells pass Start, G1 CDK activity inhibits pheromone signaling by phosphorylating CDK sites flanking the PM domain in Ste5. The negatively-charged phosphates interfere with binding between the basic PM domain and the anionic phospholipid membrane.

(B) Ste5 serves as an integration point for both external and internal regulatory cues, which act through the Gβγ-binding domain and the membrane-binding domain.

(C) Far1 promotes pheromone arrest by inhibiting Cln/CDK activity, but Far1-independent arrest pathways also exist and are revealed when Ste5 signaling cannot be downregulated by Cln/CDK activity.

Figure 3-13

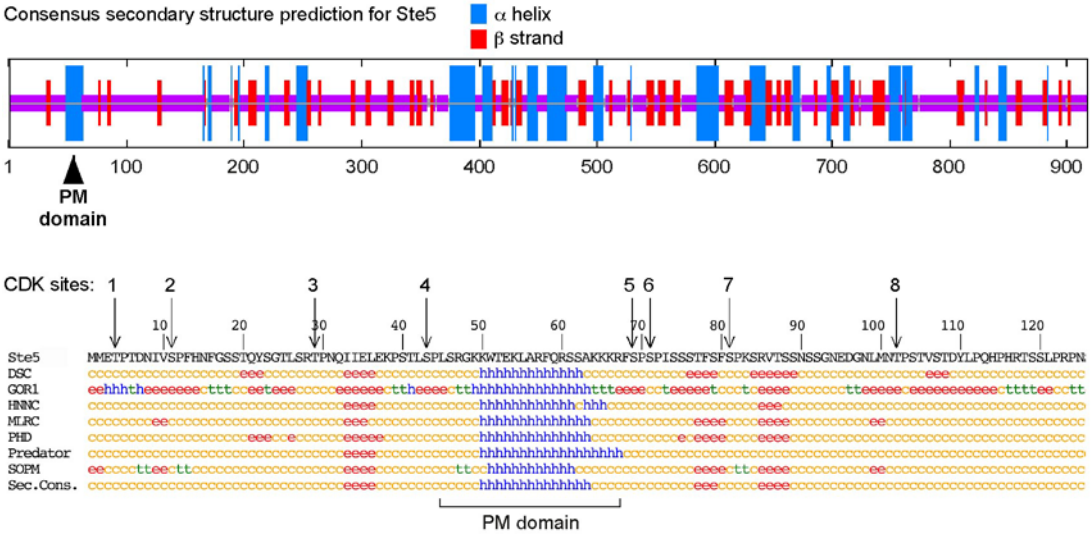
Consensus secondary structure prediction for Ste5
α helix
β strand
1
100
200
300
400
500
600
700
800
900
PM
domain
CDK sites: 1 2 3 4 5 6 7 8
10
20
30
40
50
60
70
80
90
100
110
120
Ste5
DSC
GOR1
HNNC
MLRC
PHD
Predator
SOPM
Sec.Cons.
PM domain

Figure 3-13. Regulatory CDK sites reside in sequences that are predicted to be largely unstructured

Top, consensus secondary structure prediction for full-length Ste5 (residues 1-917). Bottom, alignment of multiple secondary structure prediction algorithms for Ste5 residues 1-125, which contains the PM domain and all 8 N-terminal CDK sites. The last line shows the consensus prediction (Sec. Cons.). c = random coil; h = α helix; e = extended β strand; t = β turn. Sequence analysis was performed using "NPS@: Network Protein Sequence Analysis" (http://npsa-pbil.ibcp.fr/). Note the prevalence of random coil in sequences surrounding the helical PM domain, and the consensus prediction that all 8 CDK sites lie in random coil.

Multisite phosphorylation as a sensor for high CDK activity

Inhibition of Ste5 signaling requires phosphorylation at multiple CDK sites, and maximal inhibition of Ste5 is required to avoid aberrant arrest. This behavior suggests that multisite phosphorylation of Ste5 serves as a sensor for high G1 CDK activity, so that signaling is not fully inhibited until CDK activity is high enough to promote cell cycle entry. Conceptually, this tactic is similar to that used by the B-type cyclin/CDK inhibitor protein Sic1, which must be phosphorylated on at least six CDK sites to trigger its degradation and the resultant progression into S and M phases (Nash et al., 2001). In each example, multisite phosphorylation likely enables a sharp phenotypic switch between distinct cell cycle stages. Unlike Sic1, we saw no indication that CDK phosphorylation (or added Glu residues) affects Ste5 protein stability. Moreover, CDK effects on Ste5 may be rapidly reversible, because chemical inactivation of Cdc28 can immediately restore pheromone response to post-Start cells (Colman-Lerner et al., 2005). Thus, robust dephosphorylation by cellular phosphatases may also help enforce a demand for high G1 CDK levels to inactivate Ste5 signaling.

Cell cycle arrest by pheromone

Cell cycle control of Ste5 signaling is necessary to avoid an aberrant pheromone arrest. The best-known mediator of pheromone arrest is the CDK inhibitor Far1, yet for years it has been evident that Far1-independent arrest pathways must exist, because Far1 is dispensable in cells lacking Cln2 (Chang and Herskowitz, 1990) or all 3 G1 cyclins (Tyers, 1996; Oehlen et al., 1998). Our results show that MAPK signaling can arrest

growth without Far1, but this is ordinarily masked in *far1*Δ cells because Ste5 gets inactivated by G1 CDKs (Figure 3-12C). Hence, when Ste5 cannot be inhibited, the Far1-independent arrest is revealed. This can explain the preferential ability of *cln2*Δ to suppress *far1*Δ (Chang and Herskowitz, 1990), because Cln2 is the strongest of the 3 G1 cyclins at inhibiting pheromone response (Oehlen and Cross, 1994). Therefore, although cells eliminate Far1 as they pass Start (McKinney et al., 1993; Henchoz et al., 1997), this regulation is essentially futile without also downregulating Ste5 signaling.

The mechanisms by which CDK-resistant Ste5 signaling can impede cell cycle progression are largely unknown. The ability of Ste5-8A to trigger a G1 arrest (or delay) without Far1 is consistent with reports that pheromone can repress G1/S transcription (Valdivieso et al., 1993; Cherkasova et al., 1999). This repression may normally act in conjunction with Far1 to promote a robust, stable G1 arrest, yet may still allow a weak G1 arrest in *far1*Δ cells. The post-Start arrest is more enigmatic. A similar phenotype was seen in cells lacking G1 cyclins (Oehlen et al., 1998) or expressing a stable form of Far1 (McKinney and Cross, 1995). In light of our findings, these prior cases may result from disrupted Cln/CDK regulation of Ste5. The window of susceptibility to post-Start arrest roughly overlaps S phase, consistent with the period in which pheromone signaling is normally downregulated (Oehlen and Cross, 1994), and preliminary work suggests that the 2N cells cannot enter mitosis (S.C.S. and P.M.P., personal observations. These are preliminary results that will be pursued by other lab members), but the molecular cause remains unknown. Possibly, signaling events that ordinarily help promote G1 arrest (e.g., CDK inhibition, transcriptional repression) can also block later cell cycle steps if

signaling is unabated. Or MAPK signaling during S phase might induce DNA damage or replication errors, triggering a checkpoint arrest. Alternatively, physiological changes induced by the mating pathway (e.g., cytoskeletal rearrangements) may clash with cell division due to biochemical incompatibility or competition. In any scenario, downregulation of Ste5 would allow cells to properly commit to a new division cycle, by eliminating impediments to cell cycle progression.

Coordinating signaling with cell cycle stage

The discovery that cells sharply alter their sensitivity to extrinsic stimuli upon commitment to division played an important role in the formulation of early models for the cell cycle (Hartwell et al., 1974). Sharp transitions between distinct cell cycle stages can be ensured by feedback loops (Brandman et al., 2005). In the pheromone response pathway, mutual reinforcement between Ste5 and Far1 (in which Ste5-dependent signaling activates Far1, and Far1 blocks inactivation of Ste5) establishes a positive feedback loop. Conversely, Cln/CDK inhibition of both proteins can facilitate a decisive switch between conflicting states (i.e., arrest vs. proliferation).

During animal development, control of cell fate by external signals often occurs in the context of carefully orchestrated patterns of cell division (Vidwans and Su, 2001). Thus, it may be generally important to coordinate the response to differentiation signals with cell division status. While it is common for MAP kinase cascades to regulate the cell cycle, the reciprocal regulation is less well appreciated, yet its utility is clearly demonstrated by the behavior of the pheromone response pathway. Such mutual

antagonism can also occur in pathways not involving MAP kinases, as in the TGFβ pathway where antiproliferative signaling by Smad3 is inhibited by G1 CDKs (Matsuura et al., 2004). Thus, while the mechanisms may vary, we expect that the beneficial role of coordinating signaling with cell cycle stage will be shared by other antiproliferative pathways.

CHAPTER IV

GENERAL DISCUSSION AND UNPUBLISHED RESULTS

This work used the yeast pheromone response pathway to examine how cellular responses to external stimuli are regulated. In yeast, exposure to mating pheromone promotes entry into a differentiation pathway that leads to formation of a diploid zygote. Cellular responses involved in this process include cell cycle arrest, expression of mating specific genes, and morphology changes. These responses are triggered by the heterotrimeric G protein βγ (Gβγ) dimer, which mediates recruitment of the proteins necessary for cell polarization and activation of signaling through the MAP kinase cascade.

Chapter II of this thesis examines one of the cellular responses to pheromone. Here, we studied how Gβγ activity is regulated to promote the formation of an elongated mating projection when a localized polarity cue is present (i.e., chemotropism in response to a gradient of pheromone) or absent (i.e., *de novo* polarization in a uniform concentration of pheromone). We found that in both settings, despite Gβγ's role in recruiting the polarity proteins, Gβγ alone was not sufficient. Rather an intact receptor-Gαβγ module was required for chemotropism and *de novo* polarization. Further investigation revealed qualitatively different roles for the two Gα-Gβ interaction interfaces and suggests that the Sw interface controls signaling, whereas the Nt interface governs coupling to the receptor. As such, an intact Nt interface is required for both

chemotropism and *de novo* polarization. In addition, we found that GTP hydrolysis by Gα is required for polarization and mating. Altogether these results indicate that communication between the receptor and Gαβγ is important for chemotropism and *de novo* polarization, possibly to regulate Gαβγ in a spatially asymmetric manner.

In Chapter III another cellular response triggered by Gβγ was examined. Here we investigated how signaling through the MAP kinase cascade is regulated by G1 CDKs to coordinate mating response with cell cycle stage. We show that Cln2/CDK activity inhibits signaling by phosphorylating sites surrounding the PM domain in the MAPK cascade scaffold protein Ste5, to disrupt its membrane localization. This inhibition requires many phosphorylation sites and substantial accumulation of negative charge. Furthermore, we found that disrupting this inhibition allows cells to undergo aberrant post-Start arrest regardless of whether the arrest factor Far1 is present or not. Our findings define a mechanism and physiological benefit of restricting mating pathway signaling to G1.

These studies provide insight into how cellular responses to external stimuli are regulated. However, there are still remaining questions. Some of the remaining questions and related unpublished data are discussed below.

Role for asymmetric localization of Gβγ activity in polarity establishment

Polarity establishment involves interaction between Gβγ and the polarity proteins Far1 and Cdc24 (Butty et al., 1998; Nern and Arkowitz, 1998; Nern and Arkowitz, 1999). However, our results in Chapter II show that free Gβγ is not sufficient for polarity

establishment and further indicate that communication between the receptor and Gαβγ is important. The inability of free Gβγ to promote polarization may result from a uniform distribution of Gβγ and suggests that Gβγ activity may need to be spatially localized or clustered as mediated by receptor induced Gαβγ activation. Clustering could allow for asymmetric recruitment of the polarity proteins, Cdc24 and Far1, and thus provide a means for localized activation of Cdc42. It has been found that, in wild type cells, uniform recruitment of Far1 to the plasma membrane, by fusion to a foreign myristoylation sequence, is toxic. In this setting, cells arrest as large unbudded cells (Wiget et al., 2004). Therefore, rather than promoting polarization, uniform recruitment has detrimental effects, which are thought to be due to uniform recruitment of Cdc24 and thus activation of Cdc42 (Wiget et al., 2004). This suggests that normally, in response to pheromone Gβγ recruits Far1 to the plasma membrane in a spatially asymmetric manner to promote polarization. The findings of Wiget et. al. and those in Chapter II indicate that asymmetric localization of Gβγ activity may be important for polarity establishment.

Possible role for Gα-GTP interaction with downstream polarity factors

Our results in Chapter II indicate that communication between the receptor and Gαβγ is important for polarity establishment. This communication may allow receptor induced GTP loading onto Gα (Gpa1) to occur in a localized manner. It is possible that activated Gpa1 interacts with a downstream polarity factor and asymmetric activation of Gpa1 is important for this. Although we found that interaction between Gpa1 and Fus3 is

not required for chemotropism, this does not rule out a role for Gpa1 interaction with some other target.

We have unpublished observations that support such a possible role. We examined whether overexpression of Gpa1 could suppress the mating deficiency of cells lacking Ste4. Here the ability to bypass Gβγ's role in activating signaling proved beneficial as it provided us with a setting in which we could detect a potential role for Gα in promoting chemotropism independent of Gβγ. Signaling was activated using the bypass methods (Ste5ΔN-CTM or Ste5ΔN-Sec22) discussed in Chapter II and the mating ability of *ste4*Δ *ste5*Δ cells harboring Gpa1 expressed from a low copy CEN plasmid, high copy 2μM plasmid or from *GAL1* promoter was examined. We found that overexpression of Gpa1 (either from a high copy 2μM plasmid or from the *GAL1* promoter) increased the mating success of cells lacking Ste4 (Figure 4-1A-D), In addition, we found that unlike wild type Gpa1, overexpression of Gpa1-QL cannot suppress the mating deficiency of cells lacking Ste4, suggesting that GTP hydrolysis by Gpa1 is required for this suppression (Figure 4-1C and D). Overall, we found that overexpression of wild type Gpa1 can suppress the chemotropism defect of cells lacking Ste4.

We do not know how overexpressed wild type Gpa1 is able to suppress this defect. The suppression might be due to interaction between Gpa1 and an unknown downstream factor important for chemotropic proficiency. Alternatively, in this setting, interaction between Gpa1 and Fus3 might be required. Previously, it has been found that Fus3 interacts with the formin Bni1 (Matheos et al., 2004). Thus it is possible that

interaction between Gpa1, Fus3 and Bni1 could promote actin assembly and polarized growth.

To promote polarized growth the interaction between Gpa1 and its target (either the unknown protein or Fus3) would need to occur in a localized fashion, but how this occurs is also unknown. This may be mediated by interaction with the receptor, as efficient mating requires cells to sense and respond in the direction of the partner. Normally, the intact heterotrimer is required for efficient interaction with the receptor, but maybe in this setting Gpa1 has some ability to interact with the receptor and this could allow localization of Gpa1. However, it is also possible that localized polarized growth is not required and overexpressed Gpa1 suppresses the mating deficiency of *ste4*Δ cells in some other way. Further characterization of this suppression will require examination of a *ste4*Δ *ste5*Δ strain lacking Fus3 and a *ste4*Δ *ste5*Δ strain lacking Ste2. Although the mechanism is unknown, the ability of overexpressed Gpa1 to suppress the mating defect of cells lacking Ste4 suggests that under normal mating conditions Gα-GTP may act synergistically with Gβγ to promote polarity establishment.

Figure 4-1

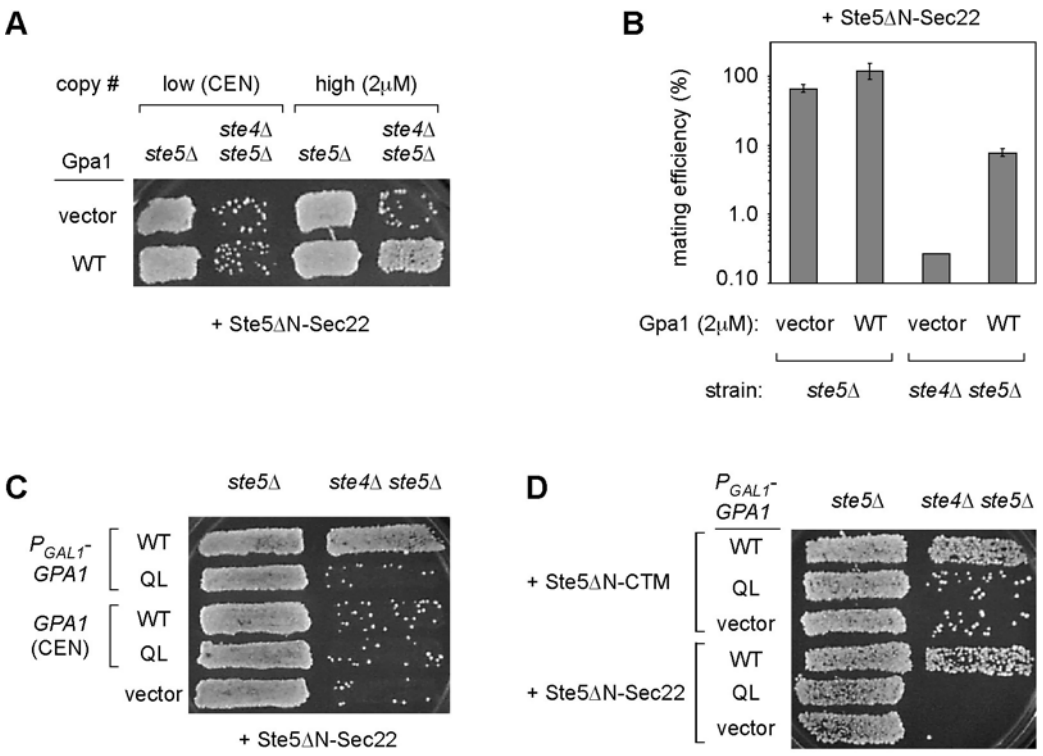
A
copy #
low (CEN)
high (2μM)
Gpa1
ste5Δ
ste4Δ ste5Δ
ste5Δ
ste4Δ ste5Δ
vector
WT
+ Ste5ΔN-Sec22
B
+ Ste5ΔN-Sec22
mating efficiency (%)
100
10
1.0
0.10
Gpa1 (2μM): vector WT vector WT
strain: ste5Δ ste4Δ ste5Δ
C
ste5Δ
ste4Δ ste5Δ
PGAL1-GPA1
WT
QL
GPA1 (CEN)
WT
QL
vector
+ Ste5ΔN-Sec22
D
PGAL1-GPA1
ste5Δ
ste4Δ ste5Δ
+ Ste5ΔN-CTM
WT
QL
vector
+ Ste5ΔN-Sec22
WT
QL
vector

Figure 4-1. Overexpression of Gpa1 can increase the mating efficiency of cells lacking Ste4 when signaling is activated independent of Gβγ

(A) Patch mating assays were performed using strains PPY861 (W303 *MAT***a** *ste5*Δ) and PPY867 (W303 *MAT***a** *ste5*Δ *ste4*Δ) harboring vector (pRS314), wild type Gpa1 expressed from a low copy CEN plasmid (pPP2711) or wild type Gpa1 expressed from a high copy 2μM plasmid (pPP2712). These strains also carried P_{GAL1}-*STE5*Δ*N-SEC22* (pPP1169).

(B) Quantitative mating assay of the same strains as panel A. Matings were performed as described in the methods for Chapter II (see Appendix A). Cells were mated for 5.5 hr and mating efficiency was determined as the percentage of input **a** cells that formed diploids. Bars, mean ± SD (n=2).

(C) Wild type Gpa1 expressed from the *GAL1* promoter suppresses the mating deficiency of cells lacking Ste4. Also, these results show that unlike wild type Gpa1, overexpression of Gpa1-QL cannot increase the mating success of cells lacking Ste4. Gpa1 derivatives were expressed from the *GAL1* promoter (pPP1836 or pPP1837), or a low copy CEN plasmid (pPP2711 or pPP2802). Vector, (pRS316). These strains (PPY861 and PPY867) also harbored P_{GAL1}-*STE5*Δ*N-SEC22* (pPP1175).

(D) Overexpression of Gpa1 increases the mating success of cells lacking Ste4 when either P_{GAL1}-*STE5*Δ*N-SEC22* or P_{GAL1}-*STE5*Δ*N-CTM* is used to activate signaling and thus does not depend on a specific signaling activation method (i.e., Ste5ΔN-Sec22). Strains (PPY861, PPY867) harbored P_{GAL1}-*GPA1* derivatives (pPP1836 or pPP1837) or vector (pRS316), plus P_{GAL1}-*STE5*Δ*N-CTM* (pPP473) or P_{GAL1}-*STE5*Δ*N-SEC22* (pPP1175).

All patch mating assays shown here were performed as described in the methods for Chapter II (see Appendix A) and used the mating partner PT2α.

Does the receptor interact with the N terminus of Gα?

In Chapter II we found that the two interaction interfaces between Gα and Gβ have qualitatively different roles. Our results suggest that an intact Nt interface is required to maintain communication with the receptor. In support of this a model for coupling between a mammalian receptor and Gαβγ indicates that the N terminal interface lies tangential to the membrane (Hamm, 1998; Hamm, 2001). Also, the Gα N terminus has been implicated in receptor recognition. In particular, it has been implicated in recognizing the third intracellular (ic3) loop of the receptor (Taylor et al., 1994; Itoh et al., 2001).

To further investigate a role for the N terminus of Gpa1 in coupling to the receptor, we sought to disrupt this interaction. To do so we mutated ten residues in the N-terminus of Gpa1. In yeast, the N-terminus of Gα contacts Gβγ at residues N24, I27, E28, L31, E34 (Lambright et al., 1996). Therefore, to try and maintain interaction with Gβγ while specifically disrupting interaction with the receptor we mutated residues that are next to those that contact Gβγ. These include Q19, N20, D25, V26, Q29, S30, L33, Q36, R37 and D38 (the mutations are as follows, Q19 to A, N20 to A, D25 to A, V26 to A, Q29 to A, S30 to A, L33 to A, Q36 to A, R37 to G and D38 to A. The resulting Gpa1 mutant is herein referred to as Gpa1-10A). We found that the Gpa1-10A mutant functioned similarly to wild type in mating, growth arrest, and signaling assays (Figure 4-2 A and B).

This lack of phenotype might suggest that the N-terminus of Gpa1 does not extensively interact with the receptor. Alternatively, it might indicate that mutating these

residues to Ala was not a severe enough change. It has been found that an overall net positive charge of the ic3 loop of the yeast receptor, Ste2, is important for its function. Mutations that remove positively charged residues decrease pheromone response (Celic et al., 2003). The authors suggest that the positively charged residues could be important for function as they might mediate interaction with negatively charged residues on Gα (Celic et al., 2003). The N-terminus of Gpa1 has eight negatively charged residues, which include D12, D15, D25, E28, E34, D38, E41 and E51. Our Gpa1-10A mutant changed two of these residues. Thus, the lack of phenotype associated with our Gpa1-10A mutant may be due to insufficient disruption of the interaction. Mutating more of these negatively charged sites to alanine or changing the ten sites we mutated to positively charged residues may have a greater disruptive effect on interaction between the receptor and Gαβγ.

Figure 4-2

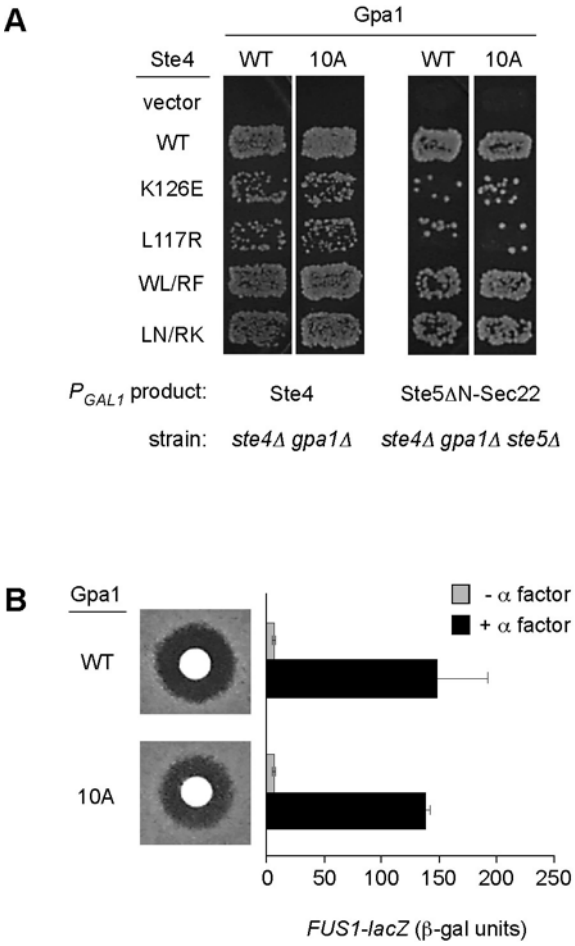
A
Gpa1
Ste4
WT
10A
WT
10A
vector
WT
K126E
L117R
WL/RF
LN/RK
P_{GAL1} product:
Ste4
Ste5ΔN-Sec22
strain:
ste4Δ gpa1Δ
ste4Δ gpa1Δ ste5Δ
B
Gpa1
WT
10A
- α factor
+ α factor
0
50
100
150
200
250
FUS1-lacZ (β-gal units)

Figure 4-2. Mutating ten residues in the N-terminus of Gpa1 does not disrupt function

(A) The Gpa1-10A mutant functions similarly to wild type Gpa1 in chemotropism assays and does not alter the chemotropic advantage of the Sw interface mutants over the Nt interface mutants. Patch mating assays were performed as described in the methods for Chapter II (see Appendix A) using PT2α as a mating partner. (Left) strain PPY1228 (*ste4*Δ *gpa1*Δ) harbored wild type Gpa1 (pPP2711) or Gpa1-10A (pPP2766) and P_{GAL1}-*STE4* plasmids (see Table A-2); (right) strain PPY1230 (*ste4*Δ *gpa1*Δ *ste5*Δ) carried the same Gpa1 derivatives, the indicated Ste4 variants expressed from the *STE4* promoter (see Table A-2), and Ste5ΔN-Sec22 (pPP1175) expressed from the *GAL1* promoter.

(B) Gpa1-10A functions similarly to wild type Gpa1 in growth arrest and signaling assays. (Left) lawns of *ste4*Δ *gpa1*Δ cells (PPY1228) harboring wild type Ste4 (pPP226) and wild type Gpa1 (pPP2711) or Gpa1-10A (pPP2766) were plated on –Ura –Trp plates and overlaid with filter disks containing 20 μl of 1 mM α factor. Plates were incubated for 3 days at 30°C. (Right) Transcriptional induction. *ste4*Δ *gpa1*Δ cells (PPY1228) harboring the same plasmids as (left) and a *FUS1-LacZ* plasmid (pPP1044) were treated with or without 10μM α factor for 2 hrs and then assayed for *FUS1-LacZ* activation. Bars, mean ± SD (n=4).

Role for GTP hydrolysis

Our results in Chapter II show that expression of a Gα GTP hydrolysis mutant, Gpa1-Q323L, interfered with mating and *de novo* polarization (Figure 2-7), revealing that Gpa1 may require the ability to hydrolyze GTP in order to promote receptor-guided polarization. Several studies have found that GTP hydrolysis is important for the functions of another GTP binding protein, the Rho-family GTPase, Cdc42. With mammalian Cdc42, disrupting the hydrolysis cycle affects cell proliferation (Vanni et al., 2005). For yeast Cdc42, it was found that GTP hydrolysis is important for cell fusion (Barale et al., 2006) and cell polarization in the absence of localized polarity cues (symmetry breaking) (Irazoqui et al., 2003). These studies indicated that the ability to cycle between GDP and GTP bound states was important for targeting and/or localizing Cdc42 activity.

Normally, localized activation of Cdc42 is governed by localized polarity cues. During budding, the localized activation of another GTPase, Rsr1, a general bud site selection protein, is thought to promote local activation of Cdc42 by recruiting its activator Cdc24 to the proper bud site (Park et al., 1997; Park et al., 2002). The GTPase cycle of Rsr1 is important for this targeting as expression of an Rsr1 mutant that cannot hydrolyze GTP disrupts localization of Cdc24 (Park et al., 2002). Thus the GTPase cycle of Rsr1 is important for proper bud site selection.

Similarly, localized receptor-induced GTP loading onto Gα could promote formation of a mating projection. Here localized GTP-loading onto Gα and subsequent activation of Gβγ activity may allow interaction between Gβγ and the polarity proteins,

Far1 and Cdc24, to occur in a spatially restricted manner. This could promote local activation of Cdc42. These interactions could promote localized polarization of the cytoskeleton and stabilize the axis of polarization (Nern and Arkowitz, 2000a). Thus the Gα GTP hydrolysis cycle may provide the necessary asymmetric spatial cue to establish and maintain a polarized mating projection.

How does signaling by CDK-resistant Ste5 promote cell cycle arrest?

In Chapter III we found that CDK-resistant Ste5-8A allowed cell cycle arrest at both G1 and post-Start cell cycle stages. Furthermore, this arrest was independent of the arrest factor Far1 (Strickfaden et al., 2007). This raises the important question of how signaling mediated by CDK-resistant Ste5 promotes arrest. In particular, what are the mechanisms for the G1 and post-Start arrest?

Potential mechanism for the Far1-indpendent G1 arrest

The G1 arrest mediated by Ste5-8A may be due to repression of genes necessary for the G1 to S transition. Previous studies have reported that pheromone can repress G1/S transcription (Valdivieso et al., 1993; Cherkasova et al., 1999) but the mechanism remains unknown. Two heterodimeric transcription factors, SBF (composed of Swi4 and Swi6) and MBF (composed of Mbp1 and Swi6), regulate the transcription of genes required for Start including *CLN1* and *CLN2* (SBF regulated) and *CLB5* and *CLB6* (MBF regulated) (Wittenberg, 2005). Activation of the SBF complex is inhibited by the transcriptional repressor Whi5. Whi5 is phosphorylated by Cln3/CDK to promote its

dissociation from SBF and thereby allow transcriptional activation of *CLN1* and *CLN2* (Costanzo et al., 2004; de Bruin et al., 2004).

It is possible that pheromone-induced signaling could disrupt the activation/activity of SBF and MBF thereby promoting the Far1-indpendent G1 arrest. In addition to Whi5, Swi6 and Swi4 are also phosphoproteins, which can be phosphorylated by CDKs (Ubersax et al., 2003). Since MAPKs can also phosphorylate CDK SP/TP sites, it is possible that the mating pathway MAPKs could phosphorylate these components at a subset of these CDK sites to mediate transcriptional repression. Pathway signaling could directly inhibit activation of SBF or MBF through phosphorylation of Swi6 or Swi4. It is also possible that MAPK mediated phosphorylation of Whi5 at a subset of its twelve CDK sites could prevent its dissociation from SBF and thereby prevent transcriptional activation.

To begin to investigate a role for Whi5 or Swi6 in mediating the G1 arrest we asked if deletion of *WHI5* or *SWI6* in *STE5-8A far1*Δ cells would eliminate the G1 arrest. If Whi5 or Swi6 was required to mediate the G1 arrest, then the loss of these proteins in *STE5-8A far1*Δ cells would cause the cells to accumulate entirely at the 2N arrest stage in response to pheromone. We deleted *WHI5* or *SWI6* in a *STE5-8A far1*Δ strain and analyzed these cells by FACS after exposure to α factor. We found that these cells still arrested with both 1N and 2N DNA content, showing that loss of these proteins was not sufficient to eliminate the G1 arrest (S.C.S and P.M.P, personal observations. These are preliminary results that will be pursued by other lab members). This indicates that some other factor is responsible for the G1 arrest. It is possible that Swi4 may be responsible

for mediating the G1 arrest as it may be subject to inhibitory phosphorylation from MAP kinases. It is also possible that signaling activates some other repressor that blocks transcription of genes necessary for the G1 to S transition. Further investigation is needed to determine the mechanism of the Far1 independent G1 arrest.

Potential mechanism for the post-Start arrest

How the post-Start arrest is mediated remains an interesting and important unanswered question. Preliminary investigations suggest that cells arrested at the post-Start position cannot enter mitosis (S.C.S and P.M.P., personal observations. This work will be pursued by other lab members). DAPI staining of *STE5-8A far1*Δ cells after exposure to α factor for 3 hours revealed that these cells were mononucleate even though 60%-70% of the cells arrested with 2N DNA content, indicating that these cells arrest before nuclear division. Interestingly, use of tubulin-GFP (Tub1-GFP) revealed that the *STE5-8A far1*Δ cells did not form bipolar spindles even though a high percentage of the cells arrested at the 2N position. Rather, these cells had a monopolar spindle (i.e., a single dot of tubulin fluorescence with microtubules emanating from it) (P.M.Pryciak, personal communication). This monopolar spindle may represent SPBs that have duplicated but not separated or it may be a single unduplicated SPB. A more detailed analysis of the monopolar spindle is needed to determine if it is due to a duplication or separation defect.

Spindle pole body duplication occurs during the G1 stage of the cell cycle and Cln/CDK activity plays a role. Cln/CDKs have been shown to phosphorylate a key

component of the SPB, Spc42, and a regulator of the SPB, Mps1, and this is thought to be important for SPB duplication (Jaspersen et al., 2004). CDK activity is also involved in SPB separation. Here it is mediated by the Clb cyclins (Bloom and Cross, 2007). Many SPB components have been identified as CDK substrates, but the role of phosphorylation by CDKs is not understood (Jaspersen and Winey, 2004). Thus altered CDK activity, due to potential CDK inhibition or transcriptional repression caused by signaling mediated by Ste5-8A, may disrupt the normal regulation of SPB components and this could affect duplication and/or separation. Also, it is possible that activation of the mating pathway MAPKs outside of G1 could allow inappropriate phosphorylation of SPB components and disrupt duplication and/or separation.

In addition to possible role in regulating components of the SPB, uninhibited MAPK signaling may alter the activity of motors involved in SPB separation. Separation involves the movement of one SPB to the other side of the nucleus and this requires microtubules and microtubule motors (Jaspersen and Winey, 2004). It is possible that altered CDK or MAPK activity could disrupt the function of the motors involved in separation thereby promoting a separation defect. Also it is possible that during the post-Start arrest, the cells are simultaneously trying to organize the cytoskeleton for karyogamy, the nuclear fusion that follows mating, and mitosis. This could cause severe defects as there could be competition for components involved in each process and thus neither process can be completed. What the mechanism is for the post-Start arrest remains an interesting question.

Why do cells need Far1?

We have found that although yeast have elaborate mechanisms for cell-cycle regulation of the arrest factor Far1, this is essentially futile if they cannot also regulate Ste5. CDK-resistant signaling mediated by Ste5-8A allows for Far1 independent cell cycle arrest (Strickfaden et al., 2007). This raises the question of why Far1 is necessary? Our results suggest Far1 is necessary to promote a robust and stable G1 arrest. In *STE5-8A* cells loss of *FAR1* causes a higher percentage of cells to arrest at the post-Start (2N) stage, which can be seen by comparing *STE5-8A* and *STE5-8A far1*Δ cells (Figure 3-8 and 3-11). We have preliminary evidence suggesting that the post-Start arrest may be irreversible. We compared the viability of wild type, *STE5-8A*, *far1*Δ and STE5-*8A far1*Δ cells after treatment with α factor. Cells were exposed to α factor for 3 or 6 hours and then plated to allow colony formation. After incubation at 30°C for 2 days colonies were counted and cell viability was determined by comparing the number of colonies formed to those of untreated cells. We found that overall the cells remained viable after short (3 hr) treatment with α factor, but there was a slight decrease in viability for the *STE5-8A far1*Δ cells. However, unlike wild type, cells that display post-Start arrest have decreased viability after longer (6 hr) exposure to α factor. Furthermore, the loss of viability seemed to correlate with the percentage of 2N arrest as *STE5-8A far1*Δ cells experienced a greater loss in viability than *STE5-8A* cells (Figure 4-3). This correlation between decreased viability and percentage of 2N arrest suggests that the post-Start arrest is detrimental. Thus expression of Far1 is needed to provide a robust and stable G1 arrest.

Figure 4-3

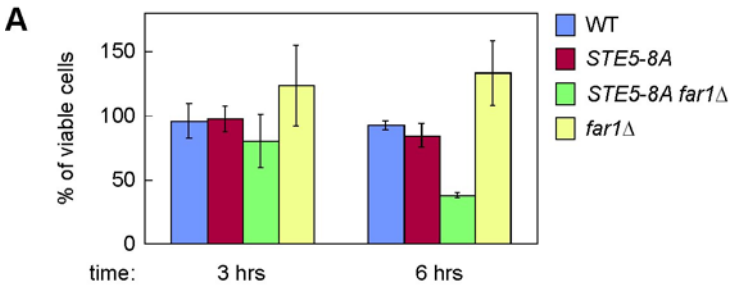
A
% of viable cells
150
100
50
0
time:
3 hrs
6 hrs
WT
STE5-8A
STE5-8A far1Δ
far1Δ

Figure 4-3. Pheromone treatment causes decreased viability in strains that show post-Start arrest

(A) Cultures of wild type (DK186), *STE5-8A* (PPY1748), *far1*Δ (PPY1777) and *STE5-8A far1*Δ (PPY1778) cells were grown at 30°C and sonicated. A aliquot was immediately harvested (untreated cells), and the remaining culture was exposed to 0.1μM α factor. Aliquots of the treated cultures were then harvested at 3 hrs and 6 hrs. The aliquots were diluted and plated. After incubation for 2 days at 30°C the plates were scored for colony formation. The percent of cells that remained viable after α factor treatment was determined by comparing the number of colonies formed after α factor treatment to those of the untreated cells. The % of viable cells is shown on the y-axis (mean ± SD, n=2).

Concluding Remarks

Over the years, study of the yeast pheromone response pathway has advanced our understanding of how cellular responses to external stimuli are regulated. Here, we learned lessons regarding how an asymmetric polarization response is generated. These studies revealed several interesting findings regarding heterotrimeric G protein function including i) the requirement for an intact receptor/Gαβγ module for response to both a localized and uniform polarity cue, ii) that the two interaction interfaces between Gα and Gβ have qualitatively different roles and iii) that the heterotrimer may function in a partially dissociated state. In addition, we gained insight into how CDK activity restricts MAPK signaling to a specific cell cycle stage. We also learned the importance of coordinating response to differentiation signals with cell-division status. As the signaling modules that comprise the yeast pheromone response pathway are conserved in higher eukaryotes, the lessons we learned here may be relevant for regulation of cell polarization and differentiation in other systems. In the future it will be interesting to see if these cellular responses are subject to similar types of regulation in higher eukaryotes.

APPENDIX A

MATERIALS AND METHODS

Materials and Methods Chapter II

Yeast strains

Yeast strains used in this study are listed in Table A-1. P_{GAL1}-*STE5*Δ*N*-*CTM* was integrated at the *HIS3* locus by transformation with *Nhe*I-digested pPP1268 to create strains PPY1303, PPY1304, PPY1306 and PPY1307. P_{GAL1}-*STE11*Δ*N*-*STE7* was integrated at the *HIS3* locus by transformation with *Nhe*I-digested pPP1270 to create strains PPY1309, PPY1310, PPY1311, PPY1312, PPY1313, PPY1314, PPY1951 and PPY1952.

Plasmids

Plasmids used in this study are listed in Table A-2. The *STE4* mutants defective for interaction with Gpa1 were isolated through a variety of screens and site directed mutagenesis. The *STE4* mutations that caused the most severe disruption of Gpa1-Ste4 binding were transferred to a variety of contexts for further study. The *STE4* mutants K126E, L117R, W136R/L138F and L154R/N156K were transferred as *Msc*I-*Xho*I fragments from the two-hybrid constructs (pPP2865, pPP2866, pPP266 and pPP966) into the P_{GAL1}-*STE4* construct pGT-STE4 (Klein et al., 2000), creating pPP1233, pPP1229, pPP1228 and pPP1209. Then, the mutants were placed under control of the native *STE4*

promoter by transferring *Msc*I-*BspE*I fragments from these P_{GAL1}-*STE4* constructs into pPP1340, creating pPP1377, pPP1378, pPP1379 and pPP1380. In addition, the mutations were transferred as *Msc*I-*Xho*I fragments into a P_{GAL1}-*STE4-GPA1* fusion construct pSTE4-GPA1-b (Klein et al., 2000) to produce pPP1231, pPP1232, pPP1230 and pPP1210. These *STE4-GPA1* fusions were then placed under control of the native *STE4* promoter by transferring *Msc*I-*BspE*I fragments from the P_{GAL1}-*STE4-GPA1* fusion constructs into pPP226, generating pPP1340, pPP1341, pPP1342, pPP1343 and pPP1344. (pPP226 contains *STE4* on a ~4-kb *EcoR*I fragment, from -2045 to +2003, cloned into the *EcoR*I site of pRS316 (Sikorski and Hieter, 1989)).

STE4-GPA1 fusions harboring the *GPA1-Q323L* mutation were constructed as follows. First, the Q323L mutation was transferred on a *Sph*I-*Sph*I fragment from pRS316-GPA1-Q323L (Apanovitch et al., 1998) into the *STE4-GPA1* fusion construct pPP1340, creating pPP1859. Then, the *Bgl*II-*Bsp*EI fragment from pPP1859 was transferred into pPP1343 to create pPP2801. To place these mutant *STE4-GPA1* fusions under control of the *GAL1* promoter, the *Msc*I-*Bsp*EI fragments from pPP1859 and pPP2801 were transferred into pSTE4-GPA1-b (Klein et al., 2000), creating pPP2806 and pPP2807.

Plasmid pPP2711 (CEN *TRP1 GPA1*) was created by PCR amplification of *GPA1* (-201 to +1707) from YCp50-C3 (Dietzel and Kurjan, 1987), and ligation as a *Sac*I-*Kpn*I fragment into pRS314 (Sikorski and Hieter, 1989). The *GPA1* mutations Q323L and K21E R22E were transferred into pPP2711 as *Bsr*GI-*Bst*BI fragments from pRS316-GPA1-Q323L (Apanovitch et al., 1998) and YCplac22-GPA1-K21ER22E (Metodiev et

al., 2002), to create pPP2802 and pPP2743, respectively. The *GPA1* mutations E28K and E28A were generated by site-directed mutagenesis of YCpGPA1 (Stone and Reed, 1990) and pPP247 (Pryciak and Hartwell, 1996), creating plasmids pPP1501, pPP1502, pPP1503 and pPP1505. The P_{GAL1}-*STE7* construct pPP2773 was made by transferring *STE7* as a *Bam*HI-*Pst*I fragment from pG7 (Harris et al., 2001) into the CEN *TRP* P_{GAL1} vector pPP449 (Pryciak and Huntress, 1998)).

Microscopy

For *de novo* and default polarization assays, transformants were grown in selective raffinose media. 2% galactose was added to induce expression of P_{GAL1}-driven constructs and, where indicated, 10μM α factor was also added. After 2-8 hour induction cells were visualized without fixation. For the *de novo* polarization assays in Figure 7A and 7B, images were captured for each condition, coded and then randomized to allow blind counts to be performed.

Mating assays

For patch mating assays, **a** cells were patched directly onto a lawn of partner PT2α cells, incubated overnight at 30° and then diploids were selected by replication to minimal media. After an immediate (1°) replica was made, more dilute replications were made by repeating the replication of the master plate two more times, using a fresh velvet each time, to create 2° and 3° replicas (Harris et al., 2001; Lamson et al., 2002). The replicas were then incubated for 2 days at 30°. For pheromone confusion assays, patch matings

were performed as described above, except α factor was spread on one plate (+ α factor) to give a final concentration of 30 μM, unless otherwise indicated, and allowed to dry before the PT2α lawn was spread.

Quantitative mating assays were performed as described in (Pryciak and Huntress, 1998; Lamson et al., 2002). In brief, cells were grown overnight in selective raffinose medium and then 0.5 x 10^6 – 5 x 10^6 **a** cells were mixed with 0.5 x 10^6 – 1 x10^7 partner cells and collected onto filters. (The mating partner is PT2α unless otherwise indicated.) The filters were placed on SC/raffinose/galactose plates and cells were allowed to mate for 6 - 7 hours (unless otherwise indicated) at 30°. After mating, filters were suspended in PBS and serial dilutions were plated on minimal media to select for diploids. Mating efficiency was determined as the percentage of total plasmid-containing (**a** + **a**/α) cells that were diploid. The quantitative mating in Figure 2-4D was performed similarly except the mating efficiency was determined as the percentage of input **a** cells that formed diploids (from two 6 hour and one 28 hour mating experiments) and is expressed relative to that of the wild type Ste4 and Gpa1 combination. For quantitative matings done in the presence of exogenous α factor, α factor was spread on the mating (SC/Raffinose/Galactose) plate to give a final concentration of 30 μM before the filters were added.

For zygote formation 5 x 10^6 **a** cells were mixed with 5 x 10^6 PT2α cells, collected onto filters and placed on SC/raffinose/galactose plates. After incubation at 30° for 5.5 hours, filters were harvested into PBS, sonicated, fixed in 5% formaldehyde and then visualized. DIC and fluorescence (GFP) images were captured.

Pheromone response and β-galactosidase assays

Halo assays of growth arrest were performed by plating cells on -Trp -Ura plates and overlaying with filters containing 20μl of 1mM α-factor (Lamson et al., 2002). Plates were photographed after incubation for 2 days at 30°.

FUS1-lacZ transcriptional induction assays were performed as described previously (Pryciak and Huntress, 1998; Lamson et al., 2002). *FUS1-lacZ* induction by pathway-activating constructs under control of the *GAL1* promoter was measured 4 hrs after addition of 2% galactose ± 10μM α factor to cultures grown in raffinose medium. To measure the effects of the Ste4 mutations on *FUS1-lacZ* activation in response to pheromone, cells were grown in raffinose media, induced with 2% galacatose for 1 hr, and then incubated ± 10μM α factor for an additional 2 hours. For dose response assays comparing pheromone response of separate versus fused Ste4 and Gpa1 polypeptides, cells were grown in glucose and treated with the indicated concentration of α factor for 2 hours. Two-hybrid liquid β-galactosidase assays were performed as previously described (Lamson et al., 2002).

Table A-1. Yeast strains used in Chapter II

strain bkgnd*	strain name	genotype	source §
(a)	PPY258	*MAT*α	this study
(a)	PPY498	*MAT***a** *fus3*Δ *kss1*Δ	this study
(a)	PPY577	*MAT***a** *FUS1::FUS1-lacZ::LYS2*	this study
(a)	PPY663	*MAT***a** *FUS1::FUS1-lacZ::LYS2*	1
(a)	PPY817	*MAT***a** *FUS1::FUS1-lacZ::LYS2 far1::ADE2*	1
(a)	PPY820	*MAT***a** *FUS1::FUS1-lacZ::LYS2 fus3::LEU2 kss1::ura3^{FOA} far1::ADE2*	this study
(a)	PPY824	*MAT***a** *FUS1::FUS1-lacZ::LYS2 fus3::LEU2*	this study
(a)	PPY827	*MAT***a** *FUS1::FUS1-lacZ::LYS2 fus3::LEU2 far1::ADE2*	this study
(a)	PPY836	*MAT***a** *far1::ADE2*	this study
(b)	PPY398	*MAT***a**	2
(b)	PPY794	*MAT***a** *ste4::ura3^{FOA}*	3
(b)	PPY842	*MAT***a** *ste4::ura3^{FOA} ste5::ADE2 ste20-1::TRP1*	4
(b)	PPY856	*MAT***a** *FUS1::FUS1-lacZ::LEU2 ste4::ura3^{FOA}*	4
(b)	PPY858	*MAT***a** *FUS1::FUS1-lacZ::LEU2 ste5::ADE2*	3
(b)	PPY861	*MAT***a** *ste5::ADE2*	this study
(b)	PPY863	*MAT***a** *ste5::ADE2 ste20::TRP1*	this study
(b)	PPY867	*MAT***a** *ste4::ura3^{FOA} ste5::ADE2*	this study
(b)	PPY886	*MAT***a** *FUS1::FUS1-lacZ::LEU2 ste4::ura3^{FOA} ste5::ADE2*	3
(b)	PPY978	*MAT***a** *FUS1::FUS1-lacZ::LEU2 ste5::ADE2 gpa1::URA3*	this study
(b)	PPY979	*MAT***a** *FUS1::FUS1-lacZ::LEU2 ste5::ADE2 ste2::URA3*	this study
(b)	PPY989	*MAT***a** *FUS1::FUS1-lacZ::LEU2 ste18::URA3 ste5::ADE2*	this study
(b)	PPY1228	*MAT***a** *ste4::ura3^{FOA} gpa1::ura3^{FOA}*	this study
(b)	PPY1230	*MAT***a** *ste4::ura3^{FOA} gpa1::ura3^{FOA} ste5::ADE2*	this study
(b)	PPY1248	*MAT***a** *ste4::ura3^{FOA} rsr1::ura3::HIS3*	this study
(b)	PPY1259	*MAT***a** *rsr1::ura3::HIS3*	this study
(b)	PPY1303	*MAT***a** *HIS3::P$_{GAL1}$-STE5*Δ*N-CTM*	this study
(b)	PPY1304	*MAT***a** *HIS3::P$_{GAL1}$-STE5*Δ*N-CTM ste5::ADE2*	this study
(b)	PPY1306	*MAT***a** *HIS3::P$_{GAL1}$ -STE5*Δ*N-CTM rsr1::URA3*	this study
(b)	PPY1307	*MAT***a** *HIS3::P$_{GAL1}$ -STE5*Δ*N-CTM rsr1::URA3 ste5::ADE2*	this study
(b)	PPY1309	*MAT***a** *HIS3::P$_{GAL1}$ -STE11*Δ*N-STE7*	this study
(b)	PPY1310	*MAT***a** *HIS3::P$_{GAL1}$ -STE11*Δ*N-STE7 ste5::ADE2*	this study
(b)	PPY1311	*MAT***a** *HIS3::P$_{GAL1}$ -STE11*Δ*N-STE7 ste5::ADE2 ste4::ura3^{FOA}*	this study
(b)	PPY1312	*MAT***a** *HIS3::P$_{GAL1}$-STE11*Δ*N-STE7 rsr1::URA3*	this study
(b)	PPY1313	*MAT***a** *HIS3::P$_{GAL1}$ -STE11*Δ*N-STE7 rsr1::URA3 ste5::ADE2*	this study
(b)	PPY1314	*MAT***a** *HIS3::P$_{GAL1}$ -STE11*Δ*N-STE7 rsr1::URA3 ste5::ADE2 ste4::ura3^{FOA}*	this study
(b)	PPY1380	*MAT***a** *gpa1::ura3^{FOA} ste4::ura3^{FOA} rsr1::ura3^{FOA}*	this study
(b)	PPY1662	*MAT***a** *FUS1::FUS1-lacZ::LEU2 ste4::ura3^{FOA} ste7::ADE2*	this study
(b)	PPY1663	*MAT***a** *FUS1::FUS1-lacZ::LEU2 ste4::ura3^{FOA} gpa1::ura3^{FOA}*	this study
(b)	PPY1937	*MAT***a** *fus3::LEU2 ste4::ura3^{FOA}*	this study
(b)	PPY1942	*MAT***a** *ste4::ura3^{FOA} gpa1::ura3^{FOA} sst2::LEU2*	this study
(b)	PPY1951	*MAT***a** *HIS3::P$_{GAL1}$-STE11*Δ*N-STE7 ste5::ADE2 gpa1::ura3^{FOA}*	this study
(b)	PPY1952	*MAT***a** *HIS3::P$_{GAL1}$-STE11*Δ*N-STE7 ste5::ADE2 gpa1::ura3^{FOA} rsr1::URA3*	this study
(c)	PPY762	*MAT***a** *LYS2::(lexAop)$_4$-HIS3 URA3::(lexAop)$_8$-lacZ ste11::ADE2*	5
(d)	PT2α	*MAT*α *hom3 ilvi can1*	3
(e)	PPY198	*MAT*α *his7 lys9 trp1 ura3 can1 cyh2*	3

* Strain background: (a) 381G (*cry1 ade2-1^{oc} ade3 his4-580^{am} leu2-3,112 lys2^{oc} trp1^{am} ura3-52 SUP4-3^{ts}*); (b) W303 (*ade2-1 his3-11,15 leu2-3,112 trp1-1 ura3-1 can1*); (c) S288c (a*de2 his3-Δ200 leu2-3,112 trp1-901*); (d) other; (e) A364A.

§ Source: (1) (Strickfaden et al., 2007); (2) (Harris et al., 2001); (3) (Pryciak and Huntress, 1998); (4) (Winters et al., 2005); (5) (Butty et al., 1998).

Table A-2. Plasmids used in Chapter II

Name	Alias	Description	Source §
pPP120	pRD-STE11-H3	CEN URA3 P_{GAL1}-GST-STE11ΔN	1
pPP126	YCpGPA1	CEN LEU2 GPA1	2
pPP134	pNC252	2μm URA3 P_{GAL1}-STE12	3
pPP226	p316-ST4-a	CEN URA3 P_{STE4}-STE4	this study
pPP244	pGAD424	2μm LEU2 GAL4-AD vector	4
pPP247	pBTM-GPA1	2μm TRP1 lexA-DBD-GPA1	3
pPP249	pGAD-STE4	2μm LEU2 GAL4-AD-STE4	3
pPP266	pGAD-21.1	2μm LEU2 GAL4-AD-STE4(W136R,L138F)	this study
pPP268	pGAD-YS4	2μm LEU2 GAL4-AD-STE4	this study
pPP271	pGS12-T	2μm TRP1 P_{GAL1}-STE12	this study
pPP446	pRD53-2μm	2μm URA3 P_{GAL1} vector	this study
pPP452	pGS5	CEN TRP1 P_{GAL1}-STE5	5
pPP473	pGS5ΔN-CTM	CEN TRP1 P_{GAL1}-ste5ΔN-CTM (= Snc2 TM domain)	5
pPP479	pH-GS5ΔN-CTM	CEN HIS3 P_{GAL1}-ste5ΔN-CTM (= Snc2 TM domain)	5
pPP513	pGFP-GS5ΔN-CTM	CEN TRP1 P_{GAL1}-GFP-ste5ΔN-CTM (= Snc2 TM domain)	5
pPP524	pGFP-GS5ΔN-SEC22	CEN TRP1 P_{GAL1}-GFP-ste5ΔN-Sec22 TM domain	5
pPP575	pGS11ΔN-T	CEN TRP1 P_{GAL1}-GST-STE11ΔN	6
pPP636	pGADXP	2μm LEU2 strong P_{ADH1}-GAL4-AD vector	7
pPP643	pGADXP-STE4	2μm LEU2 strong P_{ADH1}-GAL4-AD-STE4	7
pPP679	pRS314	CEN TRP1 vector	8
pPP681	pRS316	CEN URA3 vector	8
pPP741	pNC252-HIS3	2μm HIS3 P_{GAL1}-STE12	this study
pPP966	pGAD-YS4-L154R,N156K	2μm LEU2 GAL4-AD-STE4(L154R,N156K)	this study
pPP968	pGAD-21.1-L154R,N156K	2μm LEU2 GAL4-AD-STE4(W136R,L138F,L154R,N156K)	this study
pPP969	pGAD-YS4-N92G,K94E,S96A	2μm LEU2 GAL4-AD-STE4(N92G,K94E,S96A)	this study
pPP971	pGAD-YS4-W411R	2μm LEU2 GAL4-AD-STE4(W411R)	this study
pPP1121	pXP4-3-C7	2μm LEU2 strong P_{ADH1}-GAL4-AD-STE4(K126E)	this study
pPP1150	pSTE4-GPA1-b	CEN URA3 P_{GAL1}-STE4-GPA1 fusion (1 a.a. linker)	9
pPP1151	pGT-STE4	CEN URA3 P_{GAL1}-STE4	9
pPP1175	pH-GFP-GS5ΔN-SEC22	CEN HIS3 P_{GAL1}-GFP-ste5ΔN-Sec22 TM domain	this study
pPP1209	pGT4-LN/RK	CEN URA3 P_{GAL1}-STE4(L154R,N156K)	this study
pPP1210	pGT4GA-LN/RK	CEN URA3 P_{GAL1}-STE4(L154R,N156K)-GPA1 fusion	this study
pPP1228	pGT4-WL/RF	CEN URA3 P_{GAL1}-STE4(W136R,L138F)	this study
pPP1229	pGT4-L117R	CEN URA3 P_{GAL1}-STE4(L117R)	this study
pPP1230	pGT4GA-WL/RF	CEN URA3 P_{GAL1}-STE4(W136R,L138F)-GPA1 fusion	this study
pPP1231	pGT4GA-K126E	CEN URA3 P_{GAL1}-STE4(K126E)-GPA1 fusion	this study
pPP1232	pGT4GA-L117R	CEN URA3 P_{GAL1}-STE4(L117R)-GPA1 fusion	this study
pPP1233	pGT4-K126E	CEN URA3 P_{GAL1}-STE4(K126E)	this study
pPP1268	pIH-GS5ΔN-CTM	integrating HIS3 P_{GAL1}-ste5ΔN-CTM (= Snc2 TM domain)	this study
pPP1270	pIH-G11ΔN.S7	integrating HIS3 P_{GAL1}-STE11ΔN-STE7 fusion	this study
pPP1340	pS4GA-WT	CEN URA3 P_{STE4}-STE4-GPA1 fusion	this study
pPP1341	pS4GA-K126E	CEN URA3 P_{STE4}-STE4(K126E)-GPA1 fusion	this study
pPP1342	pS4GA-L117R	CEN URA3 P_{STE4}-STE4(L117R)-GPA1 fusion	this study
pPP1343	pS4GA-WL/RF	CEN URA3 P_{STE4}-STE4(W136R,L138F)-GPA1 fusion	this study
pPP1344	pS4GA-LN/RK	CEN URA3 P_{STE4}-STE4(L154R,N156K)-GPA1 fusion	this study
pPP1377	pS4-K126E	CEN URA3 P_{STE4}-STE4(K126E)	this study
pPP1378	pS4-L117R	CEN URA3 P_{STE4}-STE4(L117R)	this study
pPP1379	pS4-WL/RF	CEN URA3 P_{STE4}-STE4(W136R,L138F)	this study
pPP1380	pS4-LN/RK	CEN URA3 P_{STE4}-STE4(L154R,N156K)	this study
pPP1501	YCpGPA1-E28K	CEN LEU2 GPA1(E28K)	this study
pPP1502	pBTM-GPA1-E28K	2μm TRP1 lexA-DBD-GPA1(E28K)	this study
pPP1503	YCpGPA1-E28A	CEN LEU2 GPA1(E28A)	this study
pPP1505	pBTM-GPA1-E28A	2μm TRP1 lexA-DBD-GPA1(E28A)	this study
pPP1621	YCplac22-GPA1-WT	CEN TRP1 GPA1	10
pPP1859	pS4GA-Q323L	CEN URA3 P_{STE4}-STE4-GPA1(Q323L) fusion	this study
pPP2711	p314-GPA1-WT	CEN TRP1 GPA1	this study
pPP2743	p314-GPA1-K21ER22E	CEN TRP1 GPA1(K21E,R22E)	this study
pPP2773	pRS314-G7	CEN TRP1 P_{GAL1}-STE7	this study
pPP2801	pS4GA-WL/RF+Q323L	CEN URA3 P_{STE4}-STE4(W136R,L138F)-GPA1(Q323L) fusion	this study
pPP2802	p314-GPA1-Q323L	CEN TRP1 GPA1(Q323L)	this study
pPP2806	pGT4GA-Q323L	CEN URA3 P_{GAL1}-STE4-GPA1(Q323L) fusion	this study
pPP2807	pGT4GA-WL/RF+Q323L	CEN URA3 P_{GAL1}-STE4(W136R,L138F)-GPA1(Q323L) fusion	this study

pPP2865	pGm3-C7	2µm LEU2 GAL4-AD-STE4(K126E)	this study
pPP2866	pGm5-E73	2µm LEU2 GAL4-AD-STE4(L117R)	this study
pPP2867	pGm4-J38	2µm LEU2 GAL4-AD-STE4(D224E)	this study
pPP2868	pGm4-I22	2µm LEU2 GAL4-AD-STE4(D272A)	this study

§ Source: (1) (Neiman and Herskowitz, 1994); (2) (Stone and Reed, 1990); (3) (Pryciak and Hartwell, 1996); (4) (Bartel and Fields, 1995); (5) (Pryciak and Huntress, 1998); (6) (Moskow et al., 2000); (7) (Butty et al., 1998) ; (8) (Sikorski and Hieter, 1989); (9) (Klein et al., 2000); (10) (Stratton et al., 1996).

Materials and Methods Chapter III

Strains and Plasmids

Yeast strains are listed in Table A-3. P_{GAL1}-*CLN2* or P_{GPD1}-*CLN2* were integrated at the *HIS3* locus by transformation with *Nhe*I digested pPP1949 or pPP1948, respectively. P_{GAL1}-*CLB5* or P_{GPD1}-*CLB5* were integrated at the *HIS3* locus by transformation with *NheI* digested pPP2656 or pPP2655, respectively. P_{GAL1}-*CLN3* or P_{GAL1}-*CLB2* were integrated at the *LEU2* locus by transformation with *BstEII* digested pPP2665 or pPP2666, respectively. Replacement of the genomic *STE5* locus with the *STE5-8A* allele used a pop-in/pop-out strategy. Cells were first transformed with *Xba*I digested pPP2330 and selected for uracil prototrophy. Then, spontaneous 5-fluoro-orotic acid-resistant colonies were screened by PCR, restriction digestion, and sequencing to identify clones that retained the *STE5-8A* allele.

Plasmids are listed in Table A-4.

Signaling Assays

FUS1-lacZ induction and β-galactosidase assays were performed as described (Pryciak and Huntress, 1998; Lamson et al., 2002). Activation of *FUS1-lacZ* by galactose-inducible constructs in the presence and absence of P_{GAL1}-*CLN2* was measured 3 hrs after addition of 2% galactose to cultures grown in 2% raffinose media. To measure effects of P_{GAL1}-*CLN2* on *FUS1-lacZ* induction by pheromone, cells were grown in 2% raffinose

media, then induced with 2% galactose for 1 hr, followed by 5 μM α factor for an additional 2 hr. For *FUS1-lacZ* experiments not involving P_{GAL1}-*CLN2*, cells grown in glucose media were treated with 5 μM α factor for 2 hr.

For signaling in synchronous cultures, *cdc15* strains AA2596 and PPY1761 harbored either pPP1044 (*FUS1-lacZ*) or pPP1513 (Fus3-myc$_{13}$). Cultures in selective media were diluted into YPD and grown overnight at 25° C, shifted to 36° C for 3 hrs, then pelleted and resuspended in YPD at 25° C to release the mitotic block. To measure *FUS1-lacZ* induction, every 15 min aliquots were treated with 10 μM α factor for 22 min. Induction was stopped by transfer to an ice water bath. To measure Fus3 activation, every 30 min aliquots were treated with 5 μM α factor for 8 min. Cells were then pelleted, frozen in dry ice, and stored at -80° C. Fus3-myc$_{13}$ was immunoprecipitated from cell extracts, and phospho-Fus3 was detected by rabbit anti-phospho-p44/42 blots (#9101; Cell Signaling Technology), quantified by densitometry, normalized to Fus3-myc$_{13}$ levels measured in separate anti-myc blots, and expressed relative to time 0 for each experiment.

Halo assays (Lamson et al., 2002) used 20 μl of 1 mM (Figures 3-8E, 3-11A), 200 μM (Figure 3-11A), 100 μM (Figures 3-8D, 3-8H, 3-3C, 3-11B) or 20 μM (Figure 3-3C) α factor. Unless indicated otherwise, growth arrest was monitored after incubation for 2 days at 30˚C.

FACS analysis

For FACS experiments, *bar1*Δ strains were treated with 1 μM α factor in order to minimize the possibility of leaky arrest. Results were similar using 0.1 μM α factor (data not shown). Cells were grown to OD_{660} = 0.2-0.3 in YPD, and incubated ± α factor at 30°C. For experiments involving plasmids, cells grown overnight in selective media were transferred to YPD for 1.5 hrs prior to α factor addition. Cells were analyzed by FACS as described (Haase and Reed, 2002); instead of pepsin, cells were treated with 0.2 ml Proteinase K solution (1 mg/ml in 50 mM Tris, pH 8.0) for 1 hr at 36°C.

Immunoblotting

Immunoprecipitation and yeast extract preparation used published methods (Lamson et al., 2002). Immunoprecipitation of Ste5-myc_{13}, Fus3-myc_{13}, Ste5-HA_3, and GFP-Ste4 used mouse anti-myc (9E10; Santa Cruz Biotech), anti-HA (HA.11; Covance), and anti-GFP (clones 7.1 and 13.1; Roche) antibodies. Blots were probed with rabbit anti-myc (A-14; Santa Cruz Biotech), rabbit anti-HA (Y-11; Santa Cruz Biotech), or mouse anti-GFP (B34; Covance).

Analysis of phosphorylation-dependent mobility of Ste5-HA_3

Immunoprecipitation and yeast extract preparation used published methods (Lamson et al., 2002), except the immunoprecipitation used a lysis buffer with high salt and phosphatase inhibitors (50 mM Tris-HCl, pH 7.5, 700 mM NaCl, 150 mM NaF, 150 mM β-glycerophosphate, 1 mM EGTA, 5% glycerol, 0.25% Tween-20, and 2mM PMSF)

(Harvey et al., 2005). The immunoprecipation used 2 μl of mouse anti-HA (HA.11; Covance) and 45 μl of a 50% slurry of protein G beads that had been washed and resuspended in the high salt and high phosphatase inhibitors lysis buffer. After immunoprecipitation, samples were resuspended in 30 μl sample buffer with 50 mM NaF and 100 mM β-glycerophosphate added.

Samples were run on 10% polyacrylamide (30:1 acryl:bis) gels (see below for recipe). No SDS was added to the gel. Before loading the samples, the bottom of the gel and the wells were rinsed with running buffer to remove bubbles. 10 μl of sample was loaded onto gel and the gel was run at 4°C in a stepwise fashion. Running conditions were as follows: 20V for 10 min, then 50V for 15 min, then 100V for 45 min, and finally 200V for 2 hr and 50 min.

Gels were washed in 1X transfer buffer for 30 – 60 min and transferred to PVDF membranes at 15V for 15 min using a semi-dry transfer unit. Membranes were washed, blocked for 1 hr at room temperature in 5% milk/TTBS, and then probed overnight at 4°C with rabbit anti-HA (Y-11; Santa Cruz Biotech) diluted 1:250 in 5% milk/TTBS. Then membranes were washed and probed for 1hr at room temperature with the secondary goat anti-rabbit AP (Bio-Rad) diluted 1:3000 in 5% milk/TTBS.

Phosphatase treatment of Ste5-HA_3 was performed as described (Chang and Herskowitz, 1992).

Kellogg lab gel recipes (S. Harvey, personal communication).

Resolving Gel Mix

Percentage of gel	10.0
30% w/v acrylamide	3.34 ml
1% w/v bisacrylamide	1.3 ml
1.5 M Tris-Cl pH 8.8	2.5 ml
Water	2.8 ml

Makes 10 ml. Add 50 µl 10% w/v ammonium persulphate and 5 µl TEMED per 10 ml of this mix.

Stacking Gel Mix

30% w/v acrylamide	0.83 ml	5% final
1% w/v bisacrylamide	0.66 ml	0.13% final
0.5 M Tris-Cl (**pH 6.8!!**)	1.25 ml	125 mM final
Water	2.25 ml	

Makes 5 ml. Add 50 µl 10% w/v ammonium persulphate and 5 µl TEMED per 5 ml of this mix.

30% Acrylamide/1% Bisacrylamide.
Make stocks at the required percentage.

Kinase assays

GST-Ste5$^{1-125}$ fusions (WT, 8A and 8E) were purified from *E. coli* strain BL21-Codon Plus (Stratagene) using glutathione-Sepharose beads. The Cln2/Cdc28 complex was purified from Sf9 insect cells infected with recombinant baculoviruses (Nash et al., 2001). Cln2/Cdc28 (100 ng) was mixed with GST-Ste5$^{1-125}$ (30 µg) or histone H1 (1 µg) in 10 µl of reaction buffer (50 mM Hepes pH 7.5, 10 mM $MgCl_2$, 1 mM DTT, 10 µCi [^{32}P]-γ-ATP, 100 µM cold ATP), and incubated for 30 min at 30°C. Products were

resolved by SDS-PAGE and stained with coomassie blue. Gels were then dried and analyzed by autoradiography.

Microscopy

GFP fusions to Ste5 (full-length or fragments) were visualized without fixation, after induction from the *GAL1* promoter with 2% galactose for 2-4 hr (Pryciak and Huntress, 1998; Winters et al., 2005). Results representative of multiple repeated experiments are shown.

Elutriation

Small G1 cells were purified by centrifugal elutriation following published methods (Lew and Reed, 1993; Futcher, 1999). Briefly, large cultures (approx. 1 liter) were grown in synthetic complete medium with raffinose as a carbon source (SC+Raff) overnight at 30˚C. Cells were collected by centrifugation, resuspended in approximately 100 ml of supernatant, and sonicated (6x 30 sec.) to separate mother-daughter clumps. Cells were loaded at 60 ml/min into a 40-ml elutriation chamber at a rotor speed of 4000 rpm (Beckman JE-5.0 rotor), and then collected by increasing pump flow speed by 5-10 ml/min increments. Fractions with desired density and purity of small G1 cells were pooled. Cells were collected by centrifugation, resuspended in YPD growth medium, and incubated at 30˚C for subsequent experimental manipulations.

Strain and plasmid combinations

Combinations of strains and plasmids used for experiments in each figure are as follows.

Figure 3-1. (C) Strains PPY889 and PPY1704 harbored pPP135, pPP2063, pPP461, pPP1951, or pPP575. (D) Strains PPY890, PPY1337, PPY1849, PPY1702 harbored *STE11* plasmids (pPP1405 or pPP1407). (E) PPY858 and PPY1695 harbored pPP2128 or pPP2105. (F) Strains: PPY858, PPY1695. Plasmids: pPP1969, pPP2206, pPP2208, pPP2273, pPP1704, pPP1914, pPP2279.

Figure 3-2. (B) Strains PPY858 and PPY1695 harbored *STE5* plasmids (pPP2128 or pPP2176). Strains PPY913 and PPY1755 harbored *STE20* plasmids (pPP2370 or pPP2371). (C) Strains: PPY886 and PPY1705. Plasmids: pPP2063 and pPP2240. (D) Strains AA2596 and PPY1761 harbored a *FUS1-lacZ* reporter plasmid (pPP1044) or a Fus3-myc plasmid (pPP1513). (E) Strains PPY858 and PPY1695 harbored a *STE5-WT* (pPP2128) or a *STE5-Ala* mutant plasmid (pPP2156, pPP2175, pPP2158, pPP2124, pPP2161, pPP2162, pPP2171, pPP2172, pPP2157, pPP2159, pPP2126, pPP2173, pPP2002, pPP2160, pPP2174, pPP2176.)

Figure 3-3. (B) Strains PPY858 and PPY1696 harbored *STE5* plasmids (pPP1275, pPP1350, pPP1857, pPP1738, pPP1779, pPP1471, pPP1780, pPP1477). (C) Strains: DK186, PPY1748, PPY1877, PPY1879. (D) Strains: AA2596 and PPY1761. Plasmid: pPP1044.

Figure 3-4. (B) Strains PPY858 and PPY1695 harbored *STE5* plasmids (pPP2128, pPP2176, pPP2160, pPP2174, pPP2245, pPP2337, pPP2336, pPP2339, pPP2476, pPP2475). (C) Strain PPY858 harbored plasmids (pPP2128, pPP2176,

pPP2160, pPP2174, pPP2245, pPP2337, pPP2336, pPP2339, pPP2476, pPP2475, pPP2338). (D) Strain PPY886 harbored pPP650 or pPP449 and a *STE5* plasmid (pPP681, pPP2128, pPP2339, pPP2108). (E) Strain PPY866 harbored pPP633 and a *STE5* plasmid (pPP1134, pPP2128, pPP2245, pPP2337, pPP2336, pPP2476, pPP2339). (F) Strain: PPY886. Plasmids: pPP681, pPP2023, pPP2605, pPP2063, pPP2604, pPP2141, pPP2609. (G) Strain PPY886 harbored pPP1532 and a *STE5* plasmid (pPP1134, pPP2128, pPP2245, pPP2476, pPP2339, pPP2176, pPP2475). (H) Strain PPY657 harbored a *STE4* plasmid (pPP620, pPP857, pPP858) and a *STE5* plasmid (pPP2128, pPP2176, pPP2125, pPP2127, pPP2001, pPP2244, pPP2245).

Figure 3-5. (A) Strains PPY1215 and PPY1706 harbored pPP2063 or pPP2240. (B) Strains PPY886 and PPY1215 harbored P_{GAL1}-*GFP*-*STE5* plasmids (pPP2063, pPP2604, pPP2141, pPP2609). (C) Strain: PPY1215. Plasmids: pPP1658, pPP2331, pPP2268, pPP2255, pPP2333, pPP2270, pPP2614, pPP2616, pPP2615.

Figure 3-6. (A) Strains: PPY858 and PPY1695. Plasmids: pPP1968 and pPP2613. (B) Strains PPY1830, PPY1832, PPY842, PPY1826 harbored P_{GAL1}-*GFP*-*STE5* plasmids (pPP2063 or pPP2240).

Figure 3-7. (A) Plasmids: pPP1955, pPP2328, pPP2329. (B) Strains: PPY858, PPY1695, PPY1830, PPY1832. Plasmids: pPP2467, pPP2468, pPP2523. (C) Strains PPY858 and PPY1695 harbored pPP2467. (D) Strains: PPY858, PPY1695, PPY1896, PPY1895, PPY1897. Plasmids: pPP2467, pPP2468, pPP2663, pPP2701. (E) Strains PPY858 and PPY1695 harbored *STE5* plasmids (pPP2467, pPP2468, pPP2663, pPP2701, pPP2523). (F) Strains: PPY858, PPY1766, BOY743, PPY1753, PPY1769, CWY231,

CWY465, CWY910. Plasmids: pPP2663 and pPP2701. (G) Strains PPY1762 and BOY743 harbored pPP2663 or pPP2701.

Figure 3-8. (A) Strains: DK186, PPY1748. (B) Strain DK186 harbored *STE5* plasmids (pPP1134, pPP2128, pPP2161, pPP2156, pPP2126, pPP2002, pPP2160, pPP2174, pPP2176, pPP2245). (C) Strain: PPY1748. (D) Strains: DK186, PPY1913, PPY1748, PPY1918. (E) Strain PPY663 harbored pPP1134. Strain PPY817 harbored pPP1134. Strain PPY814 harbored pPP2176. (F) Strain PPY1855 harbored *STE5* plasmids (pPP1134, pPP2128, pPP2161, pPP2126, pPP2160, pPP2176). Strain DK186 harbored pPP1134. (G) Strains: PPY856, PPY1846, PPY1662. Plasmids: pPP681, pPP135, pPP2063, pPP2240, pPP2141. (H) Strains: PPY1778, PPY1921.

Figure 3-9. (A) Strains: DK186, PPY1748. (B) Strain: PPY1748.

Figure 3-10. Strains: DK186, PPY1748.

Figure 3-11. (A) Strain PPY814 harbored *STE5* plasmids pPP1134, pPP2128, pPP2156, pPP2175, pPP2158, pPP2124, pPP2161, pPP2162, pPP2171, pPP2172, pPP2157, pPP2159, pPP2126, pPP2173, pPP2002, pPP2160, pPP2174, pPP2176. (B) Strains: DK186, PPY1748, PPY1777, PPY1778, PPY1881, PPY1853, PPY1789. (C) Strains: DK186, PPY1748, PPY1777, PPY1778, PPY1789, PPY1853.

Table A-3. Yeast strains used in Chapter III

strain bkgnd*	strain name	genotype	source §
(a)	PPY657	*MAT***a** *FUS1::FUS1-lacZ::LYS2 ste4::ura3^{FOA} ste5::LYS2*	6
(a)	PPY663	*MAT***a** *FUS1::FUS1-lacZ::LYS2*	this study
(a)	PPY814	*MAT***a** *FUS1::FUS1-lacZ::LYS2 ste5::LYS2 far1::ADE2*	this study
(a)	PPY817	*MAT***a** *FUS1::FUS1-lacZ::LYS2 far1::ADE2*	this study
(b)	AA2596	*MAT***a** *ade1 cdc15-2*	A. Amon
(b)	DK186	*MAT***a** *bar1*	3
(b)	PPY842	*MAT***a** *ste4::ura3^{FOA} ste5::ADE2 ste20-1::TRP1*	6
(b)	PPY856	*MAT***a** *FUS1::FUS1-lacZ::LEU2 ste4::ura3^{FOA}*	6
(b)	PPY858	*MAT***a** *FUS1::FUS1-lacZ::LEU2 ste5::ADE2*	2
(b)	PPY866	*MAT*α *FUS1::FUS1-lacZ::LEU2 ste4::ura3^{FOA} ste5::ADE2 ste20-1::TRP1*	2
(b)	PPY886	*MAT***a** *FUS1::FUS1-lacZ::LEU2 ste4::ura3^{FOA} ste5::ADE2*	2
(b)	PPY889	*MAT***a** *FUS1::FUS1-lacZ::LEU2 ste4::ADE2*	2
(b)	PPY890	*MAT***a** *FUS1::FUS1-lacZ::LEU2 ste11::ADE2*	2
(b)	PPY913	*MAT***a** *FUS1::FUS1-lacZ::LEU2 ste20-3Δ::TRP1*	4
(b)	PPY1215	*MAT***a** *ste4::ura3^{FOA} ste7::ADE2*	6
(b)	PPY1337	*MAT***a** *FUS1::FUS1-lacZ::LEU2 ste20-1::TRP1 ste11::ADE2*	7
(b)	PPY1662	*MAT***a** *FUS1::FUS1-lacZ::LEU2 ste4::ura3^{FOA} ste7::ADE2*	this study
(b)	PPY1695	*MAT***a** *FUS1::FUS1-lacZ::LEU2 ste5::ADE2 HIS3::P$_{GAL1}$-CLN2*	this study
(b)	PPY1696	*MAT***a** *FUS1::FUS1-lacZ::LEU2 ste5::ADE2 HIS3::P$_{GPD1}$-CLN2*	this study
(b)	PPY1702	*MAT***a** *FUS1::FUS1-lacZ::LEU2 ste20-1::TRP1 ste11::ADE2 HIS3::P$_{GAL1}$-CLN2*	this study
(b)	PPY1704	*MAT***a** *FUS1::FUS1-lacZ::LEU2 ste4::ADE2 HIS3::P$_{GAL1}$-CLN2*	this study
(b)	PPY1705	*MAT***a** *FUS1::FUS1-lacZ::LEU2 ste4::ura3^{FOA} ste5::ADE2 HIS3::P$_{GAL1}$-CLN2*	this study
(b)	PPY1706	*MAT***a** *ste4::ura3^{FOA} ste7::ADE2 HIS3::P$_{GAL1}$-CLN2*	this study
(b)	PPY1748	*MAT***a** *bar1 STE5-8A*	this study
(b)	PPY1753	*MAT***a** *cdc4-1 ste5::ADE2*	this study
(b)	PPY1755	*MAT***a** *FUS1::FUS1-lacZ::LEU2 ste20-3Δ::TRP1 HIS3::P$_{GAL1}$-CLN2*	this study
(b)	PPY1761	*MAT***a** *ade1 cdc15-2 STE5-8A*	this study
(b)	PPY1762	*MAT***a** *ade1 cdc15-2 ste5::ADE2*	this study
(b)	PPY1766	*MAT***a** *cdc28-4 ste5::ADE2*	this study
(b)	PPY1769	*MAT***a** *cdc53-1 ste5::ADE2*	this study
(b)	PPY1777	*MAT***a** *bar1 far1::ADE2*	this study
(b)	PPY1778	*MAT***a** *bar1 far1::ADE2 STE5-8A*	this study
(b)	PPY1789	*MAT***a** *bar1 far1::ADE2 cln2::kan^{R}*	this study
(b)	PPY1826	*MAT***a** *ste4::ura3^{FOA} ste5::ADE2 ste20-1::TRP1 HIS3::P$_{GAL1}$-CLN2*	this study
(b)	PPY1830	*MAT***a** *FUS1::FUS1-lacZ::LEU2 fus3::LEU2 kss1::ura3^{FOA} ste4::ADE2*	this study
(b)	PPY1832	*MAT***a** *FUS1::FUS1-lacZ::LEU2 fus3::LEU2 kss1::ura3^{FOA} ste4::ADE2 HIS3::P$_{GAL1}$-CLN2*	this study
(b)	PPY1846	*MAT***a** *FUS1::FUS1-lacZ::LEU2 ste4::ura3^{FOA} far1::ADE2*	this study
(b)	PPY1849	*MAT***a** *FUS1::FUS1-lacZ::LEU2 ste11::ADE2 HIS3::P$_{GAL1}$-CLN2*	this study
(b)	PPY1853	*MAT***a** *bar1 far1::ADE2 cln2::kan^{R} STE5-8A*	this study
(b)	PPY1855	*MAT***a** *bar1 far1::ADE2 ste5::ura3^{FOA}*	this study
(b)	PPY1877	*MAT***a** *bar1 HIS3::P$_{GPD1}$-CLN2*	this study
(b)	PPY1879	*MAT***a** *bar1 HIS3::P$_{GPD1}$-CLN2 STE5-8A*	this study
(b)	PPY1881	*MAT***a** *bar1 HIS3::P$_{GPD1}$-CLN2 far1::ADE2 STE5-8A*	this study
(b)	PPY1895	*MAT***a** *FUS1::FUS1-lacZ::LEU2 ste5::ADE2 HIS3::P$_{GAL1}$-CLB5*	this study
(b)	PPY1896	*MAT***a** *ste5::ADE2 LEU2::P$_{GAL1}$-CLN3*	this study
(b)	PPY1897	*MAT***a** *ste5::ADE2 LEU2::P$_{GAL1}$-CLB2*	this study
(b)	PPY1913	*MAT***a** *bar1 HIS3::P$_{GPD1}$-CLB5*	this study
(b)	PPY1918	*MAT***a** *bar1 STE5-8A HIS3::P$_{GPD1}$-CLB5*	this study
(b)	PPY1921	*MAT***a** *bar1 far1::ADE2 STE5-8A HIS3::P$_{GPD1}$-CLB5*	this study
(c)	BOY743	*MAT***a** *bar1::LEU2 cdc28-13*	1
(c)	CWY231	*MAT***a** *bar1*	5
(c)	CWY465	*MAT*α *bar1 TRP1 cdc34-3*	C. Wittenberg
(c)	CWY910	*MAT*α *bar1 TRP1::P$_{GAL1}$-CLN3 cdc34-3 cln1Δ cln2xs*	C. Wittenberg

* Strain background: (a) 381G (*cry1 ade2-1^{oc} ade3 his4-580^{am} leu2-3,112 lys2^{oc} trp1^{am} ura3-52 SUP4-3^{ts}*) (b) W303 (*ade2 his3 leu2 trp1 ura3 can1*) (c) 15Dau (*ade1 his2 leu2 trp1 ura3*).

§ Source: (1) (Oehlen and Cross, 1998); (2) (Pryciak and Huntress, 1998); (3) (Zimmerman and Kellogg, 2001); (4) (Lamson et al., 2002); (5) (de Bruin et al., 2004); (6) (Winters et al., 2005); (7) (Lamson et al., 2006).

Table A-4. Plasmids used in Chapter III

Name	Alias	Description**	Source §
pPP135	pL19	CEN URA3 P_{GAL1}-STE4	2
pPP449	pRS314-Galp	CEN TRP1 P_{GAL1} vector	5
pPP461	pGS5-CTM	CEN TRP1 P_{GAL1}-STE5-CTM	5
pPP575	pGS11ΔN-T	CEN TRP1 P_{GAL1}-GST-STE11ΔN	6
pPP620	pAS4-WT	2μm LEU2 GAL4-AD-STE4	8
pPP633	pSTE11-4/HIS3	CEN HIS3 STE11-4 (T596I)	4
pPP650	pGFP-GS4	CEN TRP1 P_{GAL1}-GFP-STE4	5
pPP681	pRS316	CEN URA3 vector	1
pPP857	pAS4-K55E	2μm LEU2 GAL4-AD-STE4(K55E)	8
pPP858	pAS4-N157H,S175P	2μm LEU2 GAL4-AD-STE4(N157H,S175P)	this study
pPP1044	pH-CFL	CEN HIS3 FUS1-lacZ reporter	9
pPP1134	p316P*	CEN URA3 vector	this study
pPP1275	p316P*-CYC1ter	CEN URA3 T_{CYC1} vector	8
pPP1350	pS5ET	CEN URA3 STE5 T_{CYC1}	8
pPP1405	pFD53-STE11-WT	CEN URA3 STE11 wt	7
pPP1407	pFD53-STE11-Asp3	CEN URA3 STE11-Asp3 (=S281D, S285D, T286D)	7
pPP1471	pS5ET/Δ117-122	CEN URA3 STE5(Δ117-122) T_{CYC1}	8
pPP1477	pS5ET/Δ152-159	CEN URA3 STE5(Δ152-159) T_{CYC1}	8
pPP1513	pF3-myc	CEN URA3 FUS3-myc_{13} T_{CYC1}	9
pPP1532	pH-G11-Cpr	CEN HIS3 P_{GAL1}-STE11-Cpr	8
pPP1658	pHGF5N-F	CEN HIS3 P_{GAL1}-GFP-ste5(1-214)	8
pPP1704	pS5-GFPx3	CEN URA3 STE5-GFP_{x3} T_{CYC1}	8
pPP1738	pS5ET/Δ69-93	CEN URA3 STE5(Δ69-93) T_{CYC1}	8
pPP1779	pS5ET/Δ94-123	CEN URA3 STE5(Δ94-123) T_{CYC1}	8
pPP1780	pS5ET/Δ124-151	CEN URA3 STE5(Δ124-151) T_{CYC1}	8
pPP1857	pS5ET/Δ3-36	CEN URA3 STE5(Δ3-36) T_{CYC1}	8
pPP1914	p5ΔBFX-PLC	CEN URA3 STE5[(Δ48-67) + $PLC\delta^{11-140}$]-GFP_{x3} T_{CYC1}	8
pPP1947	pGEX-6P-1	E. coli GST fusion vector (Amersham)	3
pPP1948	pIH-GPD-CLN2	integrating HIS3 P_{GPD1}-CLN2	this study
pPP1949	pIH-GAL-CLN2	integrating HIS3 P_{GAL1}-CLN2	this study
pPP1951	pT-G11-Cpr	CEN TRP1 P_{GAL1}-STE11-Cpr	this study
pPP1955	pGEX-S5-D	ste5(1-125) in pGEX-6P-1	this study
pPP1968	pS5k-GFPx3	CEN URA3 STE5-GFP_{x3} T_{CYC1}	8
pPP1969	pS5kmyc	CEN URA3 STE5-myc_{13} T_{CYC1}	8
pPP2001	pS5kmyc-EEE	CEN URA3 STE5(S43E,S69E,S71E)-myc_{13} T_{CYC1}	this study
pPP2002	pS5kmyc-AAA	CEN URA3 STE5(S43A,S69A,S71A)-myc_{13} T_{CYC1}	this study
pPP2023	pCUGF-S5-WT	CEN URA3 P_{GAL1}-GFP-STE5	8
pPP2063	pCUGF-S5-Q59L	CEN URA3 P_{GAL1}-GFP-STE5(Q59L)	8
pPP2105	pS5kmyc/NLSm	CEN URA3 STE5(NLSm)-myc_{13} T_{CYC1}	8
pPP2108	pS5kmyc/C180A	CEN URA3 STE5(C180A)-myc_{13} T_{CYC1}	8
pPP2124	pS5kmyc-S43A	CEN URA3 STE5(S43A)-myc_{13} T_{CYC1}	this study
pPP2125	pS5kmyc-S43E	CEN URA3 STE5(S43E)-myc_{13} T_{CYC1}	this study
pPP2126	pS5kmyc-6971AA	CEN URA3 STE5(S69A,S71A)-myc_{13} T_{CYC1}	this study
pPP2127	pS5kmyc-6971EE	CEN URA3 STE5(S69E,S71E)-myc_{13} T_{CYC1}	this study
pPP2128	pS5kBmyc	CEN URA3 STE5-myc_{13} T_{CYC1} (w/ BssHII at STE5 codons 56-57)	this study
pPP2141	pCUGF-S5-CTM	CEN URA3 P_{GAL1}-GFP-STE5-CTM	9
pPP2156	pS5kmyc-T4A	CEN URA3 STE5(T4A)-myc_{13} T_{CYC1}	this study
pPP2157	pS5kmyc-411AA	CEN URA3 STE5(T4A,S11A)-myc_{13} T_{CYC1}	this study
pPP2158	pS5kmyc-T29A	CEN URA3 STE5(T29A)-myc_{13} T_{CYC1}	this study
pPP2159	pS5kmyc-2943AA	CEN URA3 STE5(T29A,S43A)-myc_{13} T_{CYC1}	this study
pPP2160	pS5kmyc-up4A	CEN URA3 STE5(T4A,S11A,T29A,S43A)-myc_{13} T_{CYC1}	this study
pPP2161	pS5kmyc-S69A	CEN URA3 STE5(S69A)-myc_{13} T_{CYC1}	this study
pPP2162	pS5kmyc-S71A	CEN URA3 STE5(S71A)-myc_{13} T_{CYC1}	this study
pPP2171	pS5kmyc-S81A	CEN URA3 STE5(S81A)-myc_{13} T_{CYC1}	this study
pPP2172	pS5kmyc-T102A	CEN URA3 STE5(T102A)-myc_{13} T_{CYC1}	this study
pPP2173	pS5kmyc-81102AA	CEN URA3 STE5(S81A,T102A)-myc_{13} T_{CYC1}	this study
pPP2174	pS5kmyc-dn4A	CEN URA3 STE5(S69A,S71A,S81A,T102A)-myc_{13} T_{CYC1}	this study
pPP2175	pS5kmyc-S11A	CEN URA3 STE5(S11A)-myc_{13} T_{CYC1}	this study
pPP2176	pS5kmyc-A8	CEN URA3 STE5(8A)-myc_{13} T_{CYC1}	this study
pPP2206	pS5kmyc/T52L	CEN URA3 STE5(T52L)-myc_{13} T_{CYC1}	8
pPP2208	pS5kmyc/Q59L	CEN URA3 STE5(Q59L)-myc_{13} T_{CYC1}	8

pPP2240	pCUGF-S5-Q59L+A8	CEN URA3 P_{GAL1}-GFP-STE5(Q59L+8A)	this study
pPP2244	pS5kmyc-dn4E	CEN URA3 STE5(S69E,S71E,S81E,T102E)-myc_{13} T_{CYC1}	this study
pPP2245	pS5kmyc-8E	CEN URA3 STE5(8E)-myc_{13} T_{CYC1}	this study
pPP2255	pHG-GST-F5N-D	CEN HIS3 P_{GAL1}-GST-GFP-ste5(1-125)	8
pPP2268	pHGF5N-F-8E	CEN HIS3 P_{GAL1}-GFP-ste5(1-214)/8E	this study
pPP2270	pHG-GST-F5N-D-8E	CEN HIS3 P_{GAL1}-GST-GFP-ste5(1-125)/8E	this study
pPP2273	pS5kmyc/T52L,Q59L	CEN URA3 STE5(T52L,Q59L)-myc_{13} T_{CYC1}	this study
pPP2279	p5ΔBFX-PLCx2	CEN URA3 STE5[(Δ48-67)+2x $PLC\delta^{11-140}$]-GFP_{x3} T_{CYC1}	this study
pPP2328	pGEX-S5-D-A8	ste5(1-125)/8A in pGEX-6P-1	this study
pPP2329	pGEX-S5-D-8E	ste5(1-125)/8E in pGEX-6P-1	this study
pPP2330	p306-S5-A8	integrating URA3 STE5-8A	this study
pPP2331	pHGF5N-F-A8	CEN HIS3 P_{GAL1}-GFP-ste5(1-214)/8A	this study
pPP2333	pHG-GST-F5N-D-A8	CEN HIS3 P_{GAL1}-GST-GFP-ste5(1-125)/8A	this study
pPP2336	pS5kmyc-dn8E	CEN URA3 STE5(dn8E)-myc_{13} T_{CYC1}	this study
pPP2337	pS5kmyc-up8E	CEN URA3 STE5(up8E)-myc_{13} T_{CYC1}	this study
pPP2338	pS5kmyc-16A	CEN URA3 STE5(16A)-myc_{13} T_{CYC1}	this study
pPP2339	pS5kmyc-16E	CEN URA3 STE5(16E)-myc_{13} T_{CYC1}	this study
pPP2370	p316-S20XK-WT	CEN URA3 STE20-WT (STE20 seq: -1210 to +3075)	this study
pPP2371	p316-S20XK-13A	CEN URA3 STE20(13A) (STE20 seq: -1210 to +3075)	this study
pPP2465	pS5kmyc-up1AA,2AA	CEN URA3 STE5(T4A,P5A,S11A,P12A)-myc_{13} T_{CYC1}	this study
pPP2466	pS5kmyc-up3AA,4AA	CEN URA3 STE5(T29A,P30A,S43A,P44A)-myc_{13} T_{CYC1}	this study
pPP2467	pS5kB-HA	CEN URA3 STE5-HA_3 T_{CYC1}	this study
pPP2468	pS5kHA-A8	CEN URA3 STE5(8A)-HA_3 T_{CYC1}	this study
pPP2475	pS5kmyc-14A#2	CEN URA3 STE5(14A)-myc_{13} T_{CYC1}	this study
pPP2476	pS5kmyc-14E#2	CEN URA3 STE5(14E)-myc_{13} T_{CYC1}	this study
pPP2523	pS5kHA-16E	CEN URA3 STE5(16E)-HA_3 T_{CYC1}	this study
pPP2604	pCUGF-S5-Q59L+16E	CEN URA3 P_{GAL1}-GFP-STE5(Q59L+16E)	this study
pPP2605	pCUGF-S5-16E	CEN URA3 P_{GAL1}-GFP-STE5(16E)	this study
pPP2609	pCUGF-S5-CTM+16E	CEN URA3 P_{GAL1}-GFP-STE5-CTM+16E	this study
pPP2613	pS5k-A8-GFPx3	CEN URA3 STE5(8A)-GFP_{x3} T_{CYC1}	this study
pPP2614	pHG-GST-F5N-D-Q59L	CEN HIS3 P_{GAL1}-GST-GFP-ste5(1-125)/Q59L	this study
pPP2615	pHG-GST-F5N-D-Q59L+16E	CEN HIS3 P_{GAL1}-GST-GFP-ste5(1-125)/Q59L+16E	this study
pPP2616	pHG-GST-F5N-D-Q59L+8E	CEN HIS3 P_{GAL1}-GST-GFP-ste5(1-125)/Q59L+8E	this study
pPP2655	pIH-GPD-CLB5	integrating HIS3 P_{GPD1}-CLB5	this study
pPP2656	pIH-GAL-CLB5	integrating HIS3 P_{GAL1}-CLB5	this study
pPP2663	pS5kHA-ΔNLS	CEN URA3 STE5(Δ48-67)- HA_3 T_{CYC1}	this study
pPP2665	YIpG2-CLN3	integrating LEU2 P_{GAL1}-CLN3	D. Lew
pPP2666	YIpG2-CLB2	integrating LEU2 P_{GAL1}-CLB2	D. Lew
pPP2701	pS5kHA-ΔNLS+8A	CEN URA3 STE5(Δ48-67/8A)- HA_3 T_{CYC1}	this study

§ Source: (1) (Sikorski and Hieter, 1989); (2) (Whiteway et al., 1990); (3) Amersham, Inc.; (4) (Madhani et al., 1997); (5) (Pryciak and Huntress, 1998); (6) (Moskow et al., 2000); (7) (van Drogen et al., 2000); (8) (Winters et al., 2005) (9) (Lamson et al., 2006).

** STE5-8A = T4A,S11A,T29A,S43A,S69A,S71A,S81A,T102A
STE5-14A = T4A,P5A,S11A,P12A,T29A,S43A,S69A,P70A,S71A,P72A,S81A,P82A,T102A,P103A
STE5-16A = T4A,P5A,S11A,P12A,T29A,P30A,S43A,P44A,S69A,P70A,S71A,P72A,S81A,P82A,T102A,P103A
STE5-8E = T4E,S11E,T29E,S43E,S69E,S71E,S81E,T102E
STE5-up8E = T4E,P5E,S11E,P12E,T29E,P30E,S43E,P44E
STE5-dn8E = S69E,P70E,S71E,P72E,S81E,P82E,T102E,P103E
STE5-14E = T4E,P5E,S11E,P12E,T29E,S43E,S69E,P70E,S71E,P72E,S81E,P82E,T102E,P103E
STE5-16E = T4E,P5E,S11E,P12E,T29E,P30E,S43E,P44E,S69E,P70E,S71E,P72E,S81E,P82E,T102E,P103E

APPENDIX B

REFERENCES

Apanovitch, D. M., Iiri, T., Karasawa, T., Bourne, H. R., and Dohlman, H. G. (1998). Second site suppressor mutations of a GTPase-deficient G-protein alpha-subunit. Selective inhibition of Gbeta gamma-mediated signaling. J Biol Chem *273*, 28597-28602.

Arkowitz, R. A. (1999). Responding to attraction: chemotaxis and chemotropism in Dictyostelium and yeast. Trends Cell Biol *9*, 20-27.

Ayscough, K. R., and Drubin, D. G. (1998). A role for the yeast actin cytoskeleton in pheromone receptor clustering and signalling. Curr Biol *8*, 927-930.

Bagorda, A., Mihaylov, V. A., and Parent, C. A. (2006). Chemotaxis: moving forward and holding on to the past. Thromb Haemost *95*, 12-21.

Barale, S., McCusker, D., and Arkowitz, R. A. (2006). Cdc42p GDP/GTP cycling is necessary for efficient cell fusion during yeast mating. Mol Biol Cell *17*, 2824-2838.

Bardwell, L. (2005). A walk-through of the yeast mating pheromone response pathway. Peptides *26*, 339-350.

Bartel, P. L., and Fields, S. (1995). Analyzing protein-protein interactions using two-hybrid system. Methods Enzymol *254*, 241-263.

Bender, A., and Pringle, J. R. (1989). Multicopy suppression of the *cdc24* budding defect in yeast by *CDC42* and three newly identified genes including the *ras*-related gene *RSR1*. Proceedings of the National Academy of Sciences USA *86*, 9976-9980.

Bender, A., and Sprague, G. F., Jr. (1986). Yeast peptide pheromones, a-factor and alpha-factor, activate a common response mechanism in their target cells. Cell *47*, 929-937.

Bhattacharyya, R. P., Remenyi, A., Good, M. C., Bashor, C. J., Falick, A. M., and Lim, W. A. (2006). The Ste5 scaffold allosterically modulates signaling output of the yeast mating pathway. Science *311*, 822-826.

Bigay, J., Faurobert, E., Franco, M., and Chabre, M. (1994). Roles of lipid modifications of transducin subunits in their GDP- dependent association and membrane binding. Biochemistry *33*, 14081-14090.

Blagosklonny, M. V., and Pardee, A. B. (2002). The restriction point of the cell cycle. Cell Cycle *1*, 103-110.

Blinder, D., Bouvier, S., and Jenness, D. D. (1989). Constitutive mutants in the yeast pheromone response: ordered function of the gene products. Cell *56*, 479-486.

Blondel, M., Alepuz, P. M., Huang, L. S., Shaham, S., Ammerer, G., and Peter, M. (1999). Nuclear export of Far1p in response to pheromones requires the export receptor Msn5p/Ste21p. Genes Dev *13*, 2284-2300.

Bloom, J., and Cross, F. R. (2007). Multiple levels of cyclin specificity in cell-cycle control. Nat Rev Mol Cell Biol *8*, 149-160.

Blumer, K. J., Reneke, J. E., and Thorner, J. (1988). The STE2 gene product is the ligand-binding component of the alpha-factor receptor of Saccharomyces cerevisiae. J Biol Chem *263*, 10836-10842.

Bourne, H. R. (1997). How receptors talk to trimeric G proteins. Curr Opin Cell Biol *9*, 134-142.

Brandman, O., Ferrell, J. E., Jr., Li, R., and Meyer, T. (2005). Interlinked fast and slow positive feedback loops drive reliable cell decisions. Science *310*, 496-498.

Breitkreutz, A., Boucher, L., and Tyers, M. (2001). MAPK specificity in the yeast pheromone response independent of transcriptional activation. Curr Biol *11*, 1266-1271.

Bunemann, M., Frank, M., and Lohse, M. J. (2003). Gi protein activation in intact cells involves subunit rearrangement rather than dissociation. Proc Natl Acad Sci U S A *100*, 16077-16082.

Burack, W. R., and Shaw, A. S. (2000). Signal transduction: hanging on a scaffold. Curr Opin Cell Biol *12*, 211-216.

Burkholder, A. C., and Hartwell, L. H. (1985). The yeast alpha-factor receptor: structural properties deduced from the sequence of the STE2 gene. Nucleic Acids Res *13*, 8463-8475.

Butty, A. C., Perrinjaquet, N., Petit, A., Jaquenoud, M., Segall, J. E., Hofmann, K., Zwahlen, C., and Peter, M. (2002). A positive feedback loop stabilizes the guanine-nucleotide exchange factor Cdc24 at sites of polarization. Embo J *21*, 1565-1576.

Butty, A. C., Pryciak, P. M., Huang, L. S., Herskowitz, I., and Peter, M. (1998). The role of Far1p in linking the heterotrimeric G protein to polarity establishment proteins during yeast mating. Science *282*, 1511-1516.

Cabrera-Vera, T. M., Vanhauwe, J., Thomas, T. O., Medkova, M., Preininger, A., Mazzoni, M. R., and Hamm, H. E. (2003). Insights into G protein structure, function, and regulation. Endocr Rev *24*, 765-781.

Casamayor, A., and Snyder, M. (2002). Bud-site selection and cell polarity in budding yeast. Curr Opin Microbiol *5*, 179-186.

Celic, A., Martin, N. P., Son, C. D., Becker, J. M., Naider, F., and Dumont, M. E. (2003). Sequences in the intracellular loops of the yeast pheromone receptor Ste2p required for G protein activation. Biochemistry *42*, 3004-3017.

Chang, F., and Herskowitz, I. (1990). Identification of a gene necessary for cell cycle arrest by a negative growth factor of yeast: FAR1 is an inhibitor of a G1 cyclin, CLN2. Cell *63*, 999-1011.

Chang, F., and Herskowitz, I. (1992). Phosphorylation of FAR1 in response to alpha-factor: a possible requirement for cell-cycle arrest. Mol Biol Cell *3*, 445-450.

Chant, J. (1999). Cell polarity in yeast. Annu Rev Cell Dev Biol *15*, 365-391.

Chant, J., Corrado, K., Pringle, J. R., and Herskowitz, I. (1991). Yeast BUD5, encoding a putative GDP-GTP exchange factor, is necessary for bud site selection and interacts with bud formation gene BEM1. Cell *65*, 1213-1224.

Chant, J., and Herskowitz, I. (1991). Genetic control of bud site selection in yeast by a set of gene products that constitute a morphogenetic pathway. Cell *65*, 1203-1212.

Chen, C. A., and Manning, D. R. (2001). Regulation of G proteins by covalent modification. Oncogene *20*, 1643-1652.

Cherkasova, V., Lyons, D. M., and Elion, E. A. (1999). Fus3p and Kss1p control G1 arrest in Saccharomyces cerevisiae through a balance of distinct arrest and proliferative functions that operate in parallel with Far1p. Genetics *151*, 989-1004.

Choi, K. Y., Satterberg, B., Lyons, D. M., and Elion, E. A. (1994). Ste5 tethers multiple protein kinases in the MAP kinase cascade required for mating in S. cerevisiae. Cell *78*, 499-512.

Cole, G. M., Stone, D. E., and Reed, S. I. (1990). Stoichiometry of G protein subunits affects the *Saccharomyces cerevisiae* mating pheromone signal transduction pathway. Molecular and Cellular Biology *10*, 510-517.

Colman-Lerner, A., Gordon, A., Serra, E., Chin, T., Resnekov, O., Endy, D., Pesce, C. G., and Brent, R. (2005). Regulated cell-to-cell variation in a cell-fate decision system. Nature *437*, 699-706.

Costanzo, M., Nishikawa, J. L., Tang, X., Millman, J. S., Schub, O., Breitkreuz, K., Dewar, D., Rupes, I., Andrews, B., and Tyers, M. (2004). CDK activity antagonizes Whi5, an inhibitor of G1/S transcription in yeast. Cell *117*, 899-913.

Cowan, C. R., and Hyman, A. A. (2004). Asymmetric cell division in C. elegans: cortical polarity and spindle positioning. Annu Rev Cell Dev Biol *20*, 427-453.

Cross, F. R. (1990). Cell cycle arrest caused by CLN gene deficiency in Saccharomyces cerevisiae resembles START-I arrest and is independent of the mating-pheromone signalling pathway. Mol Cell Biol *10*, 6482-6490.

Cross, F. R. (1995). Starting the cell cycle: what's the point? Curr Opin Cell Biol *7*, 790-797.

de Bruin, R. A., McDonald, W. H., Kalashnikova, T. I., Yates, J., 3rd, and Wittenberg, C. (2004). Cln3 activates G1-specific transcription via phosphorylation of the SBF bound repressor Whi5. Cell *117*, 887-898.

Dietzel, C., and Kurjan, J. (1987). The yeast SCG1 gene: a G alpha-like protein implicated in the a- and alpha-factor response pathway. Cell *50*, 1001-1010.

Dirick, L., Bohm, T., and Nasmyth, K. (1995). Roles and regulation of Cln-Cdc28 kinases at the start of the cell cycle of Saccharomyces cerevisiae. Embo J *14*, 4803-4813.

Dohlman, H. G., Song, J., Ma, D., Courchesne, W. E., and Thorner, J. (1996). Sst2, a negative regulator of pheromone signaling in the yeast Saccharomyces cerevisiae: expression, localization, and genetic interaction and physical association with Gpa1 (the G-protein alpha subunit). Mol Cell Biol *16*, 5194-5209.

Dohlman, H. G., and Thorner, J. W. (2001). Regulation of G protein-initiated signal transduction in yeast: paradigms and principles. Annu Rev Biochem *70*, 703-754.

Dolan, J. W., and Fields, S. (1990). Overproduction of the yeast STE12 protein leads to constitutive transcriptional induction. Genes and Development *4*, 492-502.

Dorer, R., Pryciak, P. M., and Hartwell, L. H. (1995). Saccharomyces cerevisiae cells execute a default pathway to select a mate in the absence of pheromone gradients. Journal of Cell Biology *131*, 845-861.

Elion, E. A. (2000). Pheromone response, mating and cell biology. Curr Opin Microbiol *3*, 573-581.

Elion, E. A. (2001). The Ste5p scaffold. J Cell Sci *114*, 3967-3978.

Etienne-Manneville, S. (2004). Cdc42--the centre of polarity. J Cell Sci *117*, 1291-1300.

Feng, Y., Song, L. Y., Kincaid, E., Mahanty, S. K., and Elion, E. A. (1998). Functional binding between Gβ and the LIM domain of Ste5 is required to activate the MEKK Ste11. Curr Biol *8*, 267-278.

Flotho, A., Simpson, D. M., Qi, M., and Elion, E. A. (2004). Localized feedback phosphorylation of Ste5p scaffold by associated MAPK cascade. J Biol Chem *279*, 47391-47401.

Franca-Koh, J., Kamimura, Y., and Devreotes, P. (2006). Navigating signaling networks: chemotaxis in Dictyostelium discoideum. Curr Opin Genet Dev *16*, 333-338.

Futcher, B. (1999). Cell cycle synchronization. Methods Cell Sci *21*, 79-86.

Gales, C., Van Durm, J. J., Schaak, S., Pontier, S., Percherancier, Y., Audet, M., Paris, H., and Bouvier, M. (2006). Probing the activation-promoted structural rearrangements in preassembled receptor-G protein complexes. Nat Struct Mol Biol *13*, 778-786.

Gartner, A., Jovanovic, A., Jeoung, D. I., Bourlat, S., Cross, F. R., and Ammerer, G. (1998). Pheromone-dependent G1 cell cycle arrest requires Far1 phosphorylation, but may not involve inhibition of Cdc28-Cln2 kinase, in vivo. Mol Cell Biol *18*, 3681-3691.

Gaudet, R., Bohm, A., and Sigler, P. B. (1996). Crystal structure at 2.4 angstroms resolution of the complex of transducin betagamma and its regulator, phosducin. Cell *87*, 577-588.

Gilman, A. G. (1987). G proteins: transducers of receptor-generated signals. Annual Review of Biochemistry *56*, 615-649.

Gulli, M., Jaquenoud, M., Shimada, Y., Niederhauser, G., Wiget, P., and Peter, M. (2000). Phosphorylation of the Cdc42 exchange factor Cdc24 by the PAK-like kinase Cla4 may regulate polarized growth in yeast. Mol Cell *6*, 1155-1167.

Gustin, M. C., Albertyn, J., Alexander, M., and Davenport, K. (1998). MAP kinase pathways in the yeast *Saccharomyces cerevisiae*. Microbiol Mol Biol Rev *62*, 1264-1300.

Gutkind, J. S. (2000). Regulation of mitogen-activated protein kinase signaling networks by G protein-coupled receptors. Sci STKE *2000*, RE1.

Haase, S. B., and Reed, S. I. (2002). Improved flow cytometric analysis of the budding yeast cell cycle. Cell Cycle *1*, 132-136.

Hagen, D. C., McCaffrey, G., and Sprague, G. F., Jr. (1986). Evidence the yeast STE3 gene encodes a receptor for the peptide pheromone a factor: gene sequence and implications for the structure of the presumed receptor. Proc Natl Acad Sci U S A *83*, 1418-1422.

Hamm, H. E. (1998). The many faces of G protein signaling. J Biol Chem *273*, 669-672.

Hamm, H. E. (2001). How activated receptors couple to G proteins. Proc Natl Acad Sci U S A *98*, 4819-4821.

Harris, K., Lamson, R. E., Nelson, B., Hughes, T. R., Marton, M. J., Roberts, C. J., Boone, C., and Pryciak, P. M. (2001). Role of scaffolds in MAP kinase pathway specificity revealed by custom design of pathway-dedicated signaling proteins. Curr Biol *11*, 1815-1824.

Hartwell, L. H., Culotti, J., Pringle, J. R., and Reid, B. J. (1974). Genetic control of the cell division cycle in yeast. Science *183*, 46-51.

Harvey, S. L., Charlet, A., Haas, W., Gygi, S. P., and Kellogg, D. R. (2005). Cdk1-dependent regulation of the mitotic inhibitor Wee1. Cell *122*, 407-420.

Henchoz, S., Chi, Y., Catarin, B., Herskowitz, I., Deshaies, R. J., and Peter, M. (1997). Phosphorylation- and ubiquitin-dependent degradation of the cyclin-dependent kinase inhibitor Far1p in budding yeast. Genes Dev *11*, 3046-3060.

Hirschman, J. E., and Jenness, D. D. (1999). Dual lipid modification of the yeast ggamma subunit Ste18p determines membrane localization of Gbetagamma. Mol Cell Biol *19*, 7705-7711.

Iijima, M., Huang, Y. E., and Devreotes, P. (2002). Temporal and spatial regulation of chemotaxis. Dev Cell *3*, 469-478.

Inouye, C., Dhillon, N., and Thorner, J. (1997). Ste5 RING-H2 domain: role in Ste4-promoted oligomerization for yeast pheromone signaling. Science *278*, 103-106.

Irazoqui, J. E., Gladfelter, A. S., and Lew, D. J. (2003). Scaffold-mediated symmetry breaking by Cdc42p. Nat Cell Biol *5*, 1062-1070.

Itoh, Y., Cai, K., and Khorana, H. G. (2001). Mapping of contact sites in complex formation between light-activated rhodopsin and transducin by covalent crosslinking: use of a chemically preactivated reagent. Proc Natl Acad Sci U S A *98*, 4883-4887.

Jackson, C. L., and Hartwell, L. H. (1990a). Courtship in S. cerevisiae: Both cell types choose mating partners by responding to the strongest pheromone signal. Cell *63*, 1039-1051.

Jackson, C. L., and Hartwell, L. H. (1990b). Courtship in *Saccharomyces cerevisiae*: an early cell-cell interaction during mating. Molecular and Cellular Biology *10*, 2202-2213.

Jackson, C. L., Konopka, J. B., and Hartwell, L. H. (1991). S. cerevisiae α pheromone receptors activate a novel signal transduction pathway for mating partner discrimination. Cell *67*, 389-402.

Jaspersen, S. L., Huneycutt, B. J., Giddings, T. H., Jr., Resing, K. A., Ahn, N. G., and Winey, M. (2004). Cdc28/Cdk1 regulates spindle pole body duplication through phosphorylation of Spc42 and Mps1. Dev Cell *7*, 263-274.

Jaspersen, S. L., and Winey, M. (2004). The budding yeast spindle pole body: structure, duplication, and function. Annu Rev Cell Dev Biol *20*, 1-28.

Jenness, D. D., Burkholder, A. C., and Hartwell, L. H. (1983). Binding of alpha-factor pheromone to yeast a cells: chemical and genetic evidence for an alpha-factor receptor. Cell *35*, 521-529.

Jenness, D. D., and Spatrick, P. (1986). Down regulation of the alpha-factor pheromone receptor in S. cerevisiae. Cell *46*, 345-353.

Jeoung, D. I., Oehlen, L. J., and Cross, F. R. (1998). Cln3-associated kinase activity in Saccharomyces cerevisiae is regulated by the mating factor pathway. Mol Cell Biol *18*, 433-441.

Johnson, G. L., and Lapadat, R. (2002). Mitogen-activated protein kinase pathways mediated by ERK, JNK, and p38 protein kinases. Science *298*, 1911-1912.

Kirschner, M., Gerhart, J., and Mitchison, T. (2000). Molecular "vitalism". Cell *100*, 79-88.

Klein, S., Reuveni, H., and Levitzki, A. (2000). Signal transduction by a nondissociable heterotrimeric yeast G protein. Proc Natl Acad Sci U S A *97*, 3219-3223.

Knoblich, J. A. (2001). Asymmetric cell division during animal development. Nat Rev Mol Cell Biol *2*, 11-20.

Kranz, J. E., Satterberg, B., and Elion, E. A. (1994). The MAP kinase Fus3 associates with and phosphorylates the upstream signaling component Ste5. Genes Dev *8*, 313-327.

Lambright, D. G., Sondek, J., Bohm, A., Skiba, N. P., Hamm, H. E., and Sigler, P. B. (1996). The 2.0 Å crystal structure of a heterotrimeric G protein. Nature *379*, 311-319.

Lamson, R. E., Takahashi, S., Winters, M. J., and Pryciak, P. M. (2006). Dual role for membrane localization in yeast MAP kinase cascade activation and its contribution to signaling fidelity. Curr Biol *16*, 618-623.

Lamson, R. E., Winters, M. J., and Pryciak, P. M. (2002). Cdc42 regulation of kinase activity and signaling by the yeast p21-activated kinase Ste20. Mol Cell Biol *22*, 2939-2951.

Leeuw, T., Wu, C., Schrag, J. D., Whiteway, M., Thomas, D. Y., and Leberer, E. (1998). Interaction of a G-protein β-subunit with a conserved sequence in Ste20/PAK family protein kinases. Nature *391*, 191-195.

Levitzki, A., and Klein, S. (2002). G-protein subunit dissociation is not an integral part of G-protein action. Chembiochem *3*, 815-818.

Lew, D. J., and Reed, S. I. (1993). Morphogenesis in the yeast cell cycle: regulation by Cdc28 and cyclins. J Cell Biol *120*, 1305-1320.

Lodowski, D. T., Pitcher, J. A., Capel, W. D., Lefkowitz, R. J., and Tesmer, J. J. (2003). Keeping G proteins at bay: a complex between G protein-coupled receptor kinase 2 and Gβγ. Science *300*, 1256-1262.

Madden, K., and Snyder, M. (1992). Specification of sites for polarized growth in Saccharomyces cerevisiae and the influence of external factors on site selection. Mol Biol Cell *3*, 1025-1035.

Madden, K., and Snyder, M. (1998). Cell polarity and morphogenesis in budding yeast. Annu Rev Microbiol *52*, 687-744.

Madhani, H. D., and Fink, G. R. (1998). The riddle of MAP kinase signaling specificity. Trends Genet *14*, 151-155.

Madhani, H. D., Styles, C. A., and Fink, G. R. (1997). MAP kinases with distinct inhibitory functions impart signaling specificity during yeast differentiation. Cell *91*, 673-684.

Mahanty, S. K., Wang, Y., Farley, F. W., and Elion, E. A. (1999). Nuclear shuttling of yeast scaffold Ste5 is required for its recruitment to the plasma membrane and activation of the mating MAPK cascade. Cell *98*, 501-512.

Manahan, C. L., Patnana, M., Blumer, K. J., and Linder, M. E. (2000). Dual lipid modification motifs in G(alpha) and G(gamma) subunits are required for full activity of the pheromone response pathway in Saccharomyces cerevisiae. Mol Biol Cell *11*, 957-968.

Marcus, S., Polverino, A., Barr, M., and Wigler, M. (1994). Complexes between STE5 and components of the pheromone-responsive mitogen-activated protein kinase module. Proc Natl Acad Sci U S A *91*, 7762-7766.

Matheos, D., Metodiev, M., Muller, E., Stone, D., and Rose, M. D. (2004). Pheromone-induced polarization is dependent on the Fus3p MAPK acting through the formin Bni1p. J Cell Biol *165*, 99-109.

Matsuura, I., Denissova, N. G., Wang, G., He, D., Long, J., and Liu, F. (2004). Cyclin-dependent kinases regulate the antiproliferative function of Smads. Nature *430*, 226-231.

McKinney, J. D., Chang, F., Heintz, N., and Cross, F. R. (1993). Negative regulation of *FAR1* at the Start of the yeast cell cycle. Genes Dev *7*, 833-843.

McKinney, J. D., and Cross, F. R. (1995). *FAR1* and the G1 phase specificity of cell cycle arrest by mating factor in *Saccharomyces cerevisiae*. Mol Cell Biol *15*, 2509-2516.

McLaughlin, S., and Aderem, A. (1995). The myristoyl-electrostatic switch: a modulator of reversible protein-membrane interactions. Trends Biochem Sci *20*, 272-276.

Medkova, M., Preininger, A. M., Yu, N. J., Hubbell, W. L., and Hamm, H. E. (2002). Conformational changes in the amino-terminal helix of the G protein alpha(i1) following dissociation from Gbetagamma subunit and activation. Biochemistry *41*, 9962-9972.

Metodiev, M. V., Matheos, D., Rose, M. D., and Stone, D. E. (2002). Regulation of MAPK function by direct interaction with the mating-specific Galpha in yeast. Science *296*, 1483-1486.

Miyajima, I., Nakafuku, M., Nakayama, N., Brenner, C., Miyajima, A., Kaibuchi, K., Arai, K., Kaziro, Y., and Matsumoto, K. (1987). GPA1, a haploid-specific essential gene, encodes a yeast homolog of mammalian G protein which may be involved in mating factor signal transduction. Cell *50*, 1011-1019.

Morrison, D. K., and Davis, R. J. (2003). Regulation of MAP kinase signaling modules by scaffold proteins in mammals. Annu Rev Cell Dev Biol *19*, 91-118.

Moskow, J. J., Gladfelter, A. S., Lamson, R. E., Pryciak, P. M., and Lew, D. J. (2000). Role of Cdc42p in pheromone-stimulated signal transduction in *Saccharomyces cerevisiae*. Mol Cell Biol *20*, 7559-7571.

Nakayama, N., Kaziro, Y., Arai, K., and Matsumoto, K. (1988). Role of STE genes in the mating factor signaling pathway mediated by GPA1 in Saccharomyces cerevisiae. Mol Cell Biol *8*, 3777-3783.

Nakayama, N., Miyajima, A., and Arai, K. (1985). Nucleotide sequences of STE2 and STE3, cell type-specific sterile genes from Saccharomyces cerevisiae. Embo J *4*, 2643-2648.

Nakayama, N., Miyajima, A., and Arai, K. (1987). Common signal transduction system shared by STE2 and STE3 in haploid cells of Saccharomyces cerevisiae: autocrine cell-cycle arrest results from forced expression of STE2. Embo J *6*, 249-254.

Nash, P., Tang, X., Orlicky, S., Chen, Q., Gertler, F. B., Mendenhall, M. D., Sicheri, F., Pawson, T., and Tyers, M. (2001). Multisite phosphorylation of a CDK inhibitor sets a threshold for the onset of DNA replication. Nature *414*, 514-521.

Nasmyth, K. (1996). At the heart of the budding yeast cell cycle. Trends Genet *12*, 405-412.

Neer, E. J. (1995). Heterotrimeric G proteins: organizers of transmembrane signals. Cell *80*, 249-257.

Neiman, A. M., and Herskowitz, I. (1994). Reconstitution of a yeast protein kinase cascade in vitro: activation of the yeast MEK homologue STE7 by STE11. Proc Natl Acad Sci U S A *91*, 3398-3402.

Nern, A., and Arkowitz, R. A. (1998). A GTP-exchange factor required for cell orientation. Nature *391*, 195-198.

Nern, A., and Arkowitz, R. A. (1999). A Cdc24p-Far1p-Gβγ protein complex required for yeast orientation during mating. J Cell Biol *144*, 1187-1202.

Nern, A., and Arkowitz, R. A. (2000a). G proteins mediate changes in cell shape by stabilizing the axis of polarity. Mol Cell *5*, 853-864.

Nern, A., and Arkowitz, R. A. (2000b). Nucleocytoplasmic shuttling of the Cdc42p exchange factor Cdc24p. J Cell Biol *148*, 1115-1122.

Neves, S. R., Ram, P. T., and Iyengar, R. (2002). G protein pathways. Science *296*, 1636-1639.

Nomoto, S., Nakayama, N., Arai, K., and Matsumoto, K. (1990). Regulation of the yeast pheromone response pathway by G protein subunits. Embo J *9*, 691-696.

Oda, Y., Huang, K., Cross, F. R., Cowburn, D., and Chait, B. T. (1999). Accurate quantitation of protein expression and site-specific phosphorylation. Proc Natl Acad Sci U S A *96*, 6591-6596.

Oehlen, L. J., and Cross, F. R. (1994). G1 cyclins CLN1 and CLN2 repress the mating factor response pathway at Start in the yeast cell cycle. Genes Dev *8*, 1058-1070.

Oehlen, L. J., and Cross, F. R. (1998). Potential regulation of Ste20 function by the Cln1-Cdc28 and Cln2-Cdc28 cyclin-dependent protein kinases. J Biol Chem *273*, 25089-25097.

Oehlen, L. J., Jeoung, D. I., and Cross, F. R. (1998). Cyclin-specific START events and the G1-phase specificity of arrest by mating factor in budding yeast. Mol Gen Genet *258*, 183-198.

Park, H. O., Bi, E., Pringle, J. R., and Herskowitz, I. (1997). Two active states of the Ras-related Bud1/Rsr1 protein bind to different effectors to determine yeast cell polarity. Proc Natl Acad Sci U S A *94*, 4463-4468.

Park, H. O., Chant, J., and Herskowitz, I. (1993). BUD2 encodes a GTPase-activating protein for Bud1/Rsr1 necessary for proper bud-site selection in yeast. Nature *365*, 269-274.

Park, H. O., Kang, P. J., and Rachfal, A. W. (2002). Localization of the Rsr1/Bud1 GTPase involved in selection of a proper growth site in yeast. J Biol Chem *277*, 26721-26724.

Park, S. H., Zarrinpar, A., and Lim, W. A. (2003). Rewiring MAP kinase pathways using alternative scaffold assembly mechanisms. Science *299*, 1061-1064.

Peter, M., Gartner, A., Horecka, J., Ammerer, G., and Herskowitz, I. (1993). FAR1 links the signal transduction pathway to the cell cycle machinery in yeast. Cell *73*, 747-760.

Peter, M., and Herskowitz, I. (1994). Direct inhibition of the yeast cyclin-dependent kinase Cdc28-Cln by Far1. Science *265*, 1228-1231.

Pierce, K. L., Premont, R. T., and Lefkowitz, R. J. (2002). Seven-transmembrane receptors. Nat Rev Mol Cell Biol *3*, 639-650.

Printen, J. A., and Sprague, G. F., Jr. (1994). Protein-protein interactions in the yeast pheromone response pathway: Ste5p interacts with all members of the MAP kinase cascade. Genetics *138*, 609-619.

Pruyne, D., and Bretscher, A. (2000a). Polarization of cell growth in yeast. J Cell Sci *113 (Pt 4)*, 571-585.

Pruyne, D., and Bretscher, A. (2000b). Polarization of cell growth in yeast. I. Establishment and maintenance of polarity states. J Cell Sci *113 (Pt 3)*, 365-375.

Pruyne, D., Legesse-Miller, A., Gao, L., Dong, Y., and Bretscher, A. (2004). Mechanisms of polarized growth and organelle segregation in yeast. Annu Rev Cell Dev Biol *20*, 559-591.

Pryciak, P. M., and Hartwell, L. H. (1996). *AKR1* encodes a candidate effector of the Gβγ complex in the *Saccharomyces cerevisiae* pheromone response pathway and contributes to control of both cell shape and signal transduction. Mol Cell Biol *16*, 2614-2626.

Pryciak, P. M., and Huntress, F. A. (1998). Membrane recruitment of the kinase cascade scaffold protein Ste5 by the Gβγ complex underlies activation of the yeast pheromone response pathway. Genes Dev *12*, 2684-2697.

Qi, M., and Elion, E. A. (2005). MAP kinase pathways. J Cell Sci *118*, 3569-3572.
Rebois, R. V., Warner, D. R., and Basi, N. S. (1997). Does subunit dissociation necessarily accompany the activation of all heterotrimeric G proteins? Cell Signal *9*, 141-151.

Richardson, H. E., Wittenberg, C., Cross, F., and Reed, S. I. (1989). An essential G1 function for cyclin-like proteins in yeast. Cell *59*, 1127-1133.

Robinson, M. J., and Cobb, M. H. (1997). Mitogen-activated protein kinase pathways. Curr Opin Cell Biol *9*, 180-186.

Schandel, K. A., and Jenness, D. D. (1994). Direct evidence for ligand-induced internalization of the yeast α-factor pheromone receptor. Molecular and Cellular Biology *14*, 7245-7255.

Schrick, K., Garvik, B., and Hartwell, L. H. (1997). Mating in Saccharomyces cerevisiae: the role of the pheromone signal transduction pathway in the chemotropic response to pheromone. Genetics *147*, 19-32.

Segall, J. E. (1993). Polarization of yeast cells in spatial gradients of alpha mating factor. Proceedings of the National Academy of Sciences USA *90*, 8332-8336.

Shimada, Y., Gulli, M. P., and Peter, M. (2000). Nuclear sequestration of the exchange factor Cdc24 by Far1 regulates cell polarity during yeast mating. Nat Cell Biol *2*, 117-124.

Sikorski, R. S., and Hieter, P. (1989). A system of shuttle vectors and yeast host strains designed for efficient manipulation of DNA in Saccharomyces cerevisiae. Genetics *122*, 19-27.

Sohrmann, M., and Peter, M. (2003). Polarizing without a c(l)ue. Trends Cell Biol *13*, 526-533.

Sondek, J., Bohm, A., Lambright, D. G., Hamm, H. E., and Sigler, P. B. (1996). Crystal structure of a G_A protein βγ dimer at 2.1 Å resolution. Nature *379*, 369-374.

Song, J., and Dohlman, H. G. (1996). Partial constitutive activation of pheromone responses by a palmitoylation-site mutant of a G protein alpha subunit in yeast. Biochemistry *35*, 14806-14817.

Song, J., Hirschman, J., Gunn, K., and Dohlman, H. G. (1996). Regulation of membrane and subunit interactions by N-myristoylation of a G protein alpha subunit in yeast. J Biol Chem *271*, 20273-20283.

Sprang, S. R. (1997). G protein mechanisms: insights from structural analysis. Annu Rev Biochem *66*, 639-678.

Stone, D. E., Cole, G. M., de Barros Lopes, M., Goebl, M., and Reed, S. I. (1991). N-myristoylation is required for function of the pheromone-responsive G alpha protein of yeast: conditional activation of the pheromone response by a temperature-sensitive N-myristoyl transferase. Genes Dev *5*, 1969-1981.

Stone, D. E., and Reed, S. I. (1990). G protein mutations that alter the pheromone response in *Saccharomyces cerevisiae*. Molecular and Cellular Biology *10*, 4439-4446.

Stratton, H. F., Zhou, J., Reed, S. I., and Stone, D. E. (1996). The mating-specific G(alpha) protein of Saccharomyces cerevisiae downregulates the mating signal by a mechanism that is dependent on pheromone and independent of G(beta)(gamma) sequestration. Mol Cell Biol *16*, 6325-6337.

Strickfaden, S. C., Winters, M. J., Ben-Ari, G., Lamson, R. E., Tyers, M., and Pryciak, P. M. (2007). A Mechanism for Cell-Cycle Regulation of MAP Kinase Signaling in a Yeast Differentiation Pathway. Cell *128*, 519-531.

Stuart, D., and Wittenberg, C. (1995). CLN3, not positive feedback, determines the timing of CLN2 transcription in cycling cells. Genes Dev *9*, 2780-2794.

Sunahara, R. K., Tesmer, J. J., Gilman, A. G., and Sprang, S. R. (1997). Crystal structure of the adenylyl cyclase activator Gsalpha. Science *278*, 1943-1947.

Taylor, J. M., Jacob-Mosier, G. G., Lawton, R. G., Remmers, A. E., and Neubig, R. R. (1994). Binding of an alpha 2 adrenergic receptor third intracellular loop peptide to G beta and the amino terminus of G alpha. J Biol Chem *269*, 27618-27624.

Tesmer, J. J., Berman, D. M., Gilman, A. G., and Sprang, S. R. (1997a). Structure of RGS4 bound to AlF4--activated G(i alpha1): stabilization of the transition state for GTP hydrolysis. Cell *89*, 251-261.

Tesmer, J. J., Sunahara, R. K., Gilman, A. G., and Sprang, S. R. (1997b). Crystal structure of the catalytic domains of adenylyl cyclase in a complex with Gsalpha.GTPgammaS. Science *278*, 1907-1916.

Tesmer, V. M., Kawano, T., Shankaranarayanan, A., Kozasa, T., and Tesmer, J. J. (2005). Snapshot of activated G proteins at the membrane: the Galphaq-GRK2-Gbetagamma complex. Science *310*, 1686-1690.

Toenjes, K. A., Sawyer, M. M., and Johnson, D. I. (1999). The guanine-nucleotide-exchange factor Cdc24p is targeted to the nucleus and polarized growth sites. Curr Biol *9*, 1183-1186.

Tyers, M. (1996). The cyclin-dependent kinase inhibitor $p40^{SIC1}$ imposes the requirement for Cln G1 cyclin function at Start. Proc Natl Acad Sci U S A *93*, 7772-7776.

Tyers, M., and Futcher, B. (1993). Far1 and Fus3 link the mating pheromone signal transduction pathway to three G1-phase Cdc28 kinase complexes. Mol Cell Biol *13*, 5659-5669.

Tyers, M., Tokiwa, G., and Futcher, B. (1993). Comparison of the Saccharomyces cerevisiae G1 cyclins: Cln3 may be an upstream activator of Cln1, Cln2 and other cyclins. Embo J *12*, 1955-1968.

Ubersax, J. A., Woodbury, E. L., Quang, P. N., Paraz, M., Blethrow, J. D., Shah, K., Shokat, K. M., and Morgan, D. O. (2003). Targets of the cyclin-dependent kinase Cdk1. Nature *425*, 859-864.

Valdivieso, M. H., Sugimoto, K., Jahng, K. Y., Fernandes, P. M., and Wittenberg, C. (1993). *FAR1* is required for posttranscriptional regulation of *CLN2* gene expression in response to mating pheromone. Mol Cell Biol *13*, 1013-1022.

Valtz, N., Peter, M., and Herskowitz, I. (1995). *FAR1* is required for oriented polarization of yeast cells in response to mating pheromones. J Cell Biol *131*, 863-873.

van Drogen, F., O'Rourke, S. M., Stucke, V. M., Jaquenoud, M., Neiman, A. M., and Peter, M. (2000). Phosphorylation of the MEKK Ste11p by the PAK-like kinase Ste20p is required for MAP kinase signaling in vivo. Curr Biol *10*, 630-639.

van Drogen, F., Stucke, V. M., Jorritsma, G., and Peter, M. (2001). MAP kinase dynamics in response to pheromones in budding yeast. Nat Cell Biol *3*, 1051-1059.

Vanni, C., Ottaviano, C., Guo, F., Puppo, M., Varesio, L., Zheng, Y., and Eva, A. (2005). Constitutively active Cdc42 mutant confers growth disadvantage in cell transformation. Cell Cycle *4*, 1675-1682.

Vidwans, S. J., and Su, T. T. (2001). Cycling through development in Drosophila and other metazoa. Nat Cell Biol *3*, E35-39.

Wall, M. A., Coleman, D. E., Lee, E., Iñiguez-Lluhi, J. A., Posner, B. A., Gilman, A. G., and Sprang, S. R. (1995). The structure of the G protein heterotrimer $G_{i\alpha 1}\beta_1\gamma_2$. Cell *83*, 1047-1058.

Wassmann, K., and Ammerer, G. (1997). Overexpression of the G1-cyclin gene *CLN2* represses the mating pathway in Saccharomyces cerevisiae at the level of the MEKK Ste11. J Biol Chem *272*, 13180-13188.

Wedegaertner, P. B., Wilson, P. T., and Bourne, H. R. (1995). Lipid modifications of trimeric G proteins. J Biol Chem *270*, 503-506.

Wedlich-Soldner, R., Altschuler, S., Wu, L., and Li, R. (2003). Spontaneous cell polarization through actomyosin-based delivery of the Cdc42 GTPase. Science *299*, 1231-1235.

Wedlich-Soldner, R., and Li, R. (2003). Spontaneous cell polarization: undermining determinism. Nat Cell Biol *5*, 267-270.

Wedlich-Soldner, R., Wai, S. C., Schmidt, T., and Li, R. (2004). Robust cell polarity is a dynamic state established by coupling transport and GTPase signaling. J Cell Biol *166*, 889-900.

Whiteway, M., Clark, K. L., Leberer, E., Dignard, D., and Thomas, D. Y. (1994). Genetic identification of residues involved in association of α and β G-protein subunits. Molecular and Cellular Biology *14*, 3223-3229.

Whiteway, M., Hougan, L., Dignard, D., Thomas, D. Y., Bell, L., Saari, G. C., Grant, F. J., O'Hara, P., and MacKay, V. L. (1989). The *STE4* and *STE18* genes of yeast encode potential β and γ subunits of the mating factor receptor-coupled G protein. Cell *56*, 467-477.

Whiteway, M., Hougan, L., and Thomas, D. Y. (1990). Overexpression of the *STE4* gene leads to mating response in haploid Saccharomyces cerevisiae. Mol Cell Biol *10*, 217-222.

Whiteway, M. S., Wu, C., Leeuw, T., Clark, K., Fourest-Lieuvin, A., Thomas, D. Y., and Leberer, E. (1995). Association of the yeast pheromone response G protein βγ subunits with the MAP kinase scaffold Ste5p. Science *269*, 1572-1575.

Whitmarsh, A. J., and Davis, R. J. (1998). Structural organization of MAP-kinase signaling modules by scaffold proteins in yeast and mammals. Trends Biochem Sci *23*, 481-485.

Wiget, P., Shimada, Y., Butty, A. C., Bi, E., and Peter, M. (2004). Site-specific regulation of the GEF Cdc24p by the scaffold protein Far1p during yeast mating. Embo J *23*, 1063-1074.

Winters, M. J., Lamson, R. E., Nakanishi, H., Neiman, A. M., and Pryciak, P. M. (2005). A membrane binding domain in the Ste5 scaffold synergizes with Gβγ binding to control localization and signaling in pheromone response. Mol Cell *20*, 21-32.

Wittenberg, C. (2005). Cell cycle: cyclin guides the way. Nature *434*, 34-35.

Wittenberg, C., Sugimoto, K., and Reed, S. I. (1990). G1-specific cyclins of S. cerevisiae: cell cycle periodicity, regulation by mating pheromone, and association with the p34CDC28 protein kinase. Cell *62*, 225-237.

Wodarz, A. (2005). Molecular control of cell polarity and asymmetric cell division in Drosophila neuroblasts. Curr Opin Cell Biol *17*, 475-481.

Wu, C., Leeuw, T., Leberer, E., Thomas, D. Y., and Whiteway, M. (1998). Cell cycle-and Cln2p-Cdc28p-dependent phosphorylation of the yeast Ste20p protein kinase. J Biol Chem *273*, 28107-28115.

Zimmerman, Z. A., and Kellogg, D. R. (2001). The Sda1 protein is required for passage through start. Mol Biol Cell *12*, 201-219.